Proceedings of

Ceres 2001 Workshop

October 9-12, 2001
Paris, France

Institut de Mécanique Céleste et de Calcul des Ephémérides
Observatoire de Paris

Dépôt légal : février 2004
ISBN : 2-91015-43-2

Foreword

You will find herewith the proceedings of the workshop Ceres 2001 organized in honour of the bicentenary of the discovery of Ceres by Piazzi and dedicated to astrometry and physics of asteroids thanks to observational networks.

We are glad to present here these proceedings : the contributions of the participants covered all the topics of the workshop. They deal with celestial mechanics and physics of the asteroids and also with theoretical and observational studies. The progress of our knowledge on asteroids needs to investigate simultaneously these topics. The efficiency of the observational networks has been put into light and the need of an improved astrometric accuracy was demonstrated as a necessary step for new discoveries. The determination of the masses of the asteroids, the interpretation of the observations of occultations, will be improved thanks to high accurate astrometric observations, together with photometric measurements. Then we will be able to reach information on what are the asteroids and what are the composition and the evolution of the solar system.

We hope that discussions have been helpful for the participants and that collaborations have started among them.

Acknowledgements

We wish to thank here all of those who contributed to the success of the workshop, and in particular the scientific organizing committee and the local organizing committee : Mrs Baron, Derouazi, Martinez, Raoult, Simon, MM. Mulo, Renaudineau, Vaubaillon for the organization of the meeting and Mrs S. Lemaître-Pottier for the making of the proceedings.

We also wish to thanks the chairperson of the sessions and of the discussions who allowed the workshop to be fruitful and interesting.

We are indebted to the members of the organizing committee who read carefully all the submitted papers before publication and we thank all the participants for their contribution.

Special thanks are for the organisms which help us for the meeting: scientific council of Paris observatory for a financial support, Institut d'Astrophysique de Paris for their welcome in their building, Museum National d'Histoire Naturelle for their kind invitation and the DFI Group for the loan of computer terminals.

J.-E. Arlot and W. Thuillot eds

Organizing committee

J.-E. Arlot [1] (chairman), M.-A. Barucci [2], C. Blanco [6], J. Berthier (1), F. Colas [1], D. Hestroffer [1], J. Lecacheux [2], J. Renaudineau [1], D. Simon [1], P. Tanga [3,5], W. Thuillot[1], A. Vienne [1,4].

1- IMCCE, Observatoire de Paris
2- LESIA, Observatoire de Paris
3- Observatoire de Turin
4- Université de Lille
5- OCA
6- Institut d’astronomie de l’université de Catane

Astrometry and physics of minor planets from observational networks

Organized by *Institut de mécanique céleste et de calculs des éphémérides, observatoire de Paris*, the Ceres 2001 workshop, dedicated to the discovery of Ceres by Piazzi in 1801, gathered professional and amateur astronomers, theoreticians and observers, interested in asteroids and more generally in small bodies of the solar system, modeling motions, looking for physical properties of these objects and observing through common networks. This workshop permit also to review the techniques used at the present time for the observations of asteroids.

Topics were :

- astrometric observations of the asteroids : towards a better accuracy ;
- prediction and observation of occultations of stars by asteroids : increasing the efficiency of the networks of observers ;
- photometric observations of the asteroids : determination of rotation and poles, modeling the figure of the asteroids ;
- search for satellites of asteroids, for binary asteroids : detection of new systems ;
- observation of the other small bodies of the solar system : improvement of the dynamical models
- networks of observers.

The present proceedings provide the communications presented during the workshop.

Astrométrie et physique des petites planètes grâce aux réseaux d'observateurs

L'atelier de travail Cérès 2001, organisé par *l'Institut de mécanique céleste et de calculs des éphémérides, observatoire de Paris*, était dédié à la découverte de Cérès par Piazzi en 1801. Il a rassemblé des astronomes professionnels et amateurs, observateurs et théoriciens, intéressés par l'étude des astéroïdes et plus généralement par celle des petits objets du système solaire, la modélisation des mouvements, la détermination des paramètres physiques et utilisant les observations réalisées par les réseaux d'observateurs ou y participant. Cet atelier de travail a permis également de discuter des techniques actuellement utilisées pour ces observations.

Les sujets traités ont été :

- les observations astrométriques des astéroïdes : vers l'amélioration de la précision ;
- les prédictions et observations des occultations stellaires : comment accroître l'efficacité des réseaux d'observateurs ;
- les observations photométriques d'astéroïdes : la détermination des pôles de rotation, la morphologie des astéroïdes ;
- la recherche des satellites d'astéroïdes et des astéroïdes binaires : vers la détection de nouveaux systèmes ;
- l'observation des autres petits objets du système solaire : vers un amélioration des modèles dynamiques ;
- les réseaux d'observateurs.

Le présent volume des comptes rendus contient les communications faites pendant cet atelier de travail.

Table of contents / Table des matières

The discovery of Ceres by Piazzi in 1801 *(abstract)*

Fodera Giorgia

The discovery of Ceres by Giuseppe Piazzi on January 1st 1801 soon followed (March 28, 1802) by that of Pallas by Olbers was immediately perceived by William Herschel as a potentially fruitful field of investigation of a *new species of celestial bodies, with which hitherto we have not been acquainted.*

In the light of the fairly recent surge of studies and wealth of results on the small bodies of the solar system, Herschel's words sound prophetical.

In this paper I shall address the circumstances of the discovery of Ceres, the reaction of the astronomical community at the announcement of the discovery, and the evolution (if any) of thought about the nature of these bodies after the discovery of Pallas, Juno and Vesta.

Hegel and the discovery of the asteroids

Rapaport Michel

1 . Introduction

It is probably not frequent to quote the philosopher Hegel in the frame of a scientific workshop. But since this workshop is dedicated to the bicentenary of the discovery of CERES, I will present some reasons which can justify the presence of the well known philosopher in a communication. Indeed Hegel begins his long academic carreer by the defence of his thesis *Dissertation philosophica de orbitis planetarum* at Iena University in october 1801. This diploma was for him necessary for teaching at the University, where he was invited by Schelling. The two first parts of his dissertation develop a critical analysis of the physical concepts used at this epoch and a philosophical construction of the solar system.

Before we comment the third part of this thesis, we recall that the Titius Bode formula was the main reason of the efforts devoted to the search of a missing planet between the orbits of Mars and Jupiter. The Titius Bode « law » consists in a comparison between the radii of the orbits of planets and the values of a geometric series and suggests the presence of a planet between the orbits of Mars and Jupiter. During the last years of the 18^{th} century, several surveys were made by several groups of astronomers as von Zach, and the 1/1/1801, Piazzi at Palerm Observatory discovered a new object in the sky. This object was then lost and found again after the works of Gauss which confirm that the discovered object, Ceres, is the searched planet. In the same time, Hegel in the third part of his thesis illustrates his conceptions of the solar system by a calculation on the distances between the planets and he concludes that, **if his hypothesis are right**, it is not necessary to search a planet between the orbits of Mars and Jupiter.

2 . The arguments of Hegel

In the very short last chapter (2 pages), Hegel writes that he is not pleased with the Titius Bode law concerning the distribution of the semi major axis of the planets, and particularly with the series (0, 3, 6, 12, 24, 48, 96, 192) corresponding with the expression 3*(2**n) which appears in the Titius Bode law. Hegel prefers to introduce series coming from the two « Timée » (besides the Timée of Platon, there exists another Timée believed to be by Timee de Locros). These series are made of powers of 2 (1, 2, 4, 8) and 3 (1, 3, 9, 27).

Hegel then writes « Let us consider the series 1, 2, 3, 4, 9, 8, 27. Iask permission to replace the number 8 by 16 and I consider the series 1, 2, 3, 4, 9, 16, 27 ».

Hegel continues saying « **If the series agrees better than the arithmetic progression with the true order of the nature, then it is obvious that the fourth and fifth rank are separated by a large interval and that, at this place, there is not a missing planet** ».

3 . The comments to the dissertation of Hegel

There were, of course, many reactions to the purposes of Hegel, which were published some monthes after the first observations of Ceres and most of these reactions were not in favor with the work of the philosopher.

The comments of **F.X. von Zach**, director of the Seeberg Observatory near Gotha were very violent. He considers that the thesis of Hegel is a « litterar vandalism » coming from people « who need to learn before to teach ».

Several scientists or philosophers express critical opinions on this work. K.F. Gauss writes « **The mistakes made by Hegel are a good example of errors made by philosophers** ». The French mathematician **Bourbaki** writes in *Eléments d'histoire des mathématiques* that « Hegel is behind the science of his epoch ». **F. de Gandt**, translator of the dissertation of Hegel in french is very severe. He emphazises that Hegel did not understand the main concepts of mechanics of his epoch.

However some authors are not so critical. For example, in an article published in 1992 by the german magazine *Sterne und Weltraum*, D.B. Hermann suggests some explanations to the point of view of Hegel ; he emphasizes that Hegel says that there is no planet between Mars and Jupiter only if the series considered by himself are more pertinent than the arithmetic series considered by the Titius Bode law.

4 . Conclusion

Hegel is one of the most important philosophers in the history of philosophy. Nevertheless he was clearly behind the physics of his epoch and this perhaps means that a great philosopher can simultaneously be a bad physicist. Some scientists used this example in order to criticize philosophy in general, and to minimize its part in the elaboration of the concepts of physics. But a systematic opposition between science and philosophy would be certainly dangerous for both disciplines.

References

A french translation by F. De Gandt of the original *Dissertatio Philosophica de Orbitis Planetarum* published at Iena (1801) was published by the Librairie Philosophique J. Vrin in 1979.

A german translation can be found in *G.W.F. Hegel Erste Druckschriften*, Lasson ed (1928).

K.E. Edgeworth and TNOs

McFarland John

Abstract. *An overview of Kenneth Essex Edgeworth's theory of the origin and development of the solar system is presented. Particular reference is made to his pre-Second World War writings on the trans-Neptunian region.*

1 . Introduction

The independent economist and theoretical astronomer Kenneth Essex Edgeworth (1880–1972) was born in Streete, Co. Westmeath, Ireland, a son of Thomas Newcomen and Elizabeth Dupré Edgeworth. His mother was the sister of the gentleman astronomer, William Edward Wilson (1851–1908) who had established a well-equipped private observatory at Daramona House in Streete in the late nineteenth century (Wilson 1900; Warner 1977; McNally and Hoskin 1988). It was W.E. Wilson who aroused an interest in astronomy in his young nephew, Kenneth (Edgeworth 1965).

Edgeworth won a mathematical scholarship to and the Jones prize of Marlborough School in England, and the Pollock Medal at the Royal Military Academy, Woolwich (McFarland 1996). Embarking on a military career, as a commissioner in the Royal Engineers he was transferred to South Africa in 1900 and saw service in the Boer War. On his return to England, he was elected a Fellow of the Royal Astronomical Society in 1903. He served in many countries until the outbreak of the First World War in 1914 when he was sent to France as head of a Signal communications unit. Edgeworth retired from the Army in 1926 shortly after being nominated to the rank of Colonel.

Around this time, Edgeworth published papers on electrical engineering on topics such as his pitch scheme for frequency measurements and wireless transmitters (Edgeworth and Cobbold 1925, Edgeworth 1926). Following his retirement from the Army, Edgeworth was appointed chief engineer for the Department of Posts and Telegraphs in Sudan, a post he resigned in 1931 to return to reside at Booterstown, Co. Dublin. From Booterstown, Edgeworth published a series of four books on global economics (Edgeworth no date, Edgeworth 1932, Edgeworth 1933, Edgeworth 1944).

2 . 1943 Paper : The Evolution of our Planetary System

In 1943, Edgeworth published a paper concerning the origin and development of the planetary system in which he postulated the existence of a reservoir of potential comets beyond the orbit of Pluto. He states « It may be inferred that the outer region of the solar system ... is occupied by a very large number of comparatively small bodies ... From time to time a member of this swarm of potential comets wanders from its own sphere and appears as an occasional visitor to the inner regions of the solar system. » (Edgeworth 1943a).

The first sentence of the Introduction of this paper reads : « This paper was originally written at considerably greater length, but it has been cut down owing to the shortage of paper ». The paper shortage resulted from the constraints imposed as a consequence of the Second World War. Revd. Martin Davidson, editor of the *Journal of the British Astronomical Association* wrote to Edgeworth about the need to reduce the size of his original paper as the quota of paper allocated to the British Astronomical Association was already almost exhausted. Edgeworth's original intention was that the paper should have been published as a series of individual contributions in a number of issues of the *BAA Journal*.

3 . 1943 Manuscript : Astronomical Evolution

In the spring of 2000, the author's attention was drawn to a recently held exhibition of some of Edgeworth's photographs. Through inquiries concerning this exhibition, the author was eventually directed to Edgeworth's manuscripts. Among these manuscripts was the full-length version of the 1943 *JBAA* paper. The printed version of the paper was entitled *The Evolution of our Planetary System*. However, this was not Edgeworth's original title, it was changed without his approval, or indeed knowledge. The original title was *Astronomical Evolution* (Edgeworth 1943b). The printed title was too restrictive, he had wanted an all-embracing title to indicate the similarity of the processes involved in the formation of the planet-satellite systems, the planetary system, and the Galactic system of stars.

There is very little difference between the sections on comets in the manuscript and printed versions. However, Edgeworth does elaborate a little more on the difference in structure between the main-belt asteroids and the potential comets orbiting beyond Neptune and Pluto. The material from which the asteroids formed was located in a region of higher temperature and, consequently, presence of solvents, thus assisting the bonding process during asteroid formation. However, in the outer cometary region, the condensing material was at much lower temperatures and hence there was much weaker bonding of the material and only loose assemblages could form.

This gives the situation regarding Edgeworth's 1943 prediction of trans-Neptunian objects, but the story really begins at least five years earlier, for in the spring of 1938, Edgeworth completed a manuscript entitled *The Evolution of the Solar System* (Edgeworth 1938).

4 . 1938 Manuscript : The Evolution of the Solar System

In Chapter 8 of the 1938 manuscript, *Meteors and Comets*, Edgeworth wrote in much greater depth on the trans-Neptunian region. He mentioned various theories of the origin of comets, and stated that the theory that comets are « ordinary and permanent members of the solar system » is the « only theory that was not open to immediate and fatal objections ». Edgeworth then considered this theory from a dynamical point of view and in a sub-section entitled *Evolution of the Comets from the Interplanetary Fluid* states that « it is reasonable to assume that the proposed swarm of meteorites extended far beyond the present planetary orbits, and it may further be postulated that, for some reason at present unexplained, the conditions at the periphery of the disc were unsuited to the formation of large single planets ».

Edgeworth begins this work by stating that each new theory begins with a rebuttal of the theory in vogue, and this new theory then suffers the same fate. For example, Laplace (fluid of immense extent) replaced Buffon (Earth formed by the collision of a comet with the Sun). Laplace was displaced by Chamberlin and Moulton (planetesimal theory – the planetesimals resulting from an encounter of the Sun with another star). Jeans and Jeffreys improved on Chamberlin and Moulton by introducing some changes regarding the nature of the collision and the after events. Jeans and Jeffreys were then replaced by Lyttleton (planets formed as the result of the collision of a star with a binary system, one member of which was the Sun). Edgeworth felt that Lyttleton had left a theory really no better that its predecessors.

Edgeworth then constructed his own theory regarding the formation of the solar system and Galaxy by retaining those portions of earlier theories which seemed plausible, and rejecting those parts which he felt were unworkable. His initial postulates were : 1) the regularities of the motions of the various solar system members are not due to chance but have some general cause (after Laplace), 2) the only general cause is a « fluid of immense extent » (Laplace), and 3) the fluid was not supported by internal pressure, but every part of it must have been revolving about the Sun with a velocity appropriate to its position (Chamberlin). Planetary formation was a process of condensation, driven by gravitation. According to Laplace, the extension of the fluid was due to internal pressure, and contraction was due to loss of heat. In Edgeworth's theory, the fluid was extended by rotation, and contraction was due to loss of angular momentum. Edgeworth postulated that the members of the planetary system developed from a vast cloud of scattered material (gas, dust, and small solid particles of average diameter 0.5 cm and average mass 0.2 gm).

Edgeworth began with the assumption that the Sun was already formed, and in a state similar to its present condition. The Sun was surrounded by the vast cloud, and if it was rotating sufficiently rapidly it eventually assumed the form of a disc, the thickness of which depended on the random velocities of the particles. The smaller the random velocities, the thinner the disc. As the disc became thinner, it became denser and unstable causing turbulence. Eddies then began to form rotating upon themselves and becoming denser than the rest of the disc. Viscous friction between these condensations slowed down their rotation causing their central densities to increase further.

Certain scenarios were now possible : 1) the condensations could continue condensing upon themselves, 2) the condensations could break up into smaller condensations, or 3) the condensations could coalesce until only one condensation remained in each particular region of the disc. If either 1 or 2 occurred then a solar system of minor planets would have developed. In our solar system of a number of planets and a small mass fraction of minor planets, Edgeworth concluded that the condensations attracted one another gravitationally causing close approaches or collisions resulting in fewer and fewer condensations until only one remained in each region of the disc, later forming the planet-satellite systems. Edgeworth commented that the cloud of scattered material must have extended from 10^{10} km to three or four times this distance, or more, from the Sun, *i.e.* up to $200 - 300$ AU. However, the opacity of the material was too low to allow the formation of single large planets so that a large number of bodies would still exist in this region today, individually orbiting the Sun. He then calculated the expected average size and number of bodies populating the outer solar system. For a total disc mass in this region of one third of an Earth mass, he derived an order of magnitude figure of 200 millions objects of average mass 2×10^{-9} Earth masses. For a total of one tenth of an Earth mass in the disc, he estimated a population of 2000 millions bodies with an average mass of 5×10^{-11} Earth masses.

A copy of a manuscript by Edgeworth on the origin of the solar system was sent to Dr W.J. Luyten by Prof. F.J.M. Stratton, apparently in early 1938, at the suggestion of Dr R.A. Lyttleton. This may have been the manuscript of *The Evolution of the Solar System*. On the whole, Luyten was sympathetic with the views of Edgeworth regarding his theory on the formation of the solar system, and felt that the solution to the problem was to be found in the direction of Edgeworth's ideas (Luyten 1938). Edgeworth approached a number of publishing houses to have his 1938 manuscript published as a book. However, all the publishers were sceptical about the prospects for the book's commercial success because of the nature of the topic. Methuen & Co. Ltd., for example, suggested that Edgeworth should publish the book on commission, but for a print run of 1000 copies (binding 250), the cost would have been £ 137.10s, which Edgeworth could not justify. Thus, sadly, the book was never published, but it was used extensively in his 1961 book *The Earth, The Planets and The Stars*.

5 . Conclusion

Edgeworth's main contributions to solar system studies were his prediction that the trans-Neptunian region contains thousands of millions of potential comets which replenish those comets which are continually consumed, and his recognition that the distribution and dissipation of the angular momentum in the solar system resulted from viscous and tidal friction. Edgeworth was developing his ideas on the origin and evolution of the solar system and the origin of comets at a pivotal time (c. 1935–1950) in solar system cosmogony, especially so far as comets are concerned (*cf.* Bailey, Clube and Napier 1990). Publication of these two manuscripts by Edgeworth would be extremely valuable not only to help complete the historical record of theories on the origin and development of the solar system, but also to explore the avenues of research and the possible personal contacts that are suggested in them. These results serve to reinforce the notion that Edgeworth's name should be associated with the reservoir of comets in the trans-Neptunian region (Brück 1996, McFarland 1996).

References

Bailey, M.E., Clube, S.V.M., Napier, W.M., 1990, *The Origin of Comets*. Pergamon Press.

Brück, M.T., 1996, The Edgeworth–Kuiper Belt?, *The Irish Astron. J.*, **23**, 3.

Edgeworth, K.E., 1926, Frequency Variations in Thermionic Generators, J. *Institution of Electrical Engineers*, **64**, 349-366.

Edgeworth, K.E., no date, *The Industrial Crisis*, Cherbury, Booterstown, Co. Dublin.

Edgeworth, K.E., 1932, *The Trade Balance*, Cherbury, Booterstown, Co. Dublin.

Edgeworth, K.E., 1933, *The Price Level*, Cherbury, Booterstown, Co. Dublin.

Edgeworth, K.E., 1938, The Evolution of the Solar System, Unpublished manuscript, 226pp, Trustees of the National Library of Ireland, Ms. No. 16869/47 &/48.

Edgeworth, K.E., 1943a, The Evolution of our Planetary System, *J. British Astronomical Association*, **53**, 181-188.

Edgeworth, K.E., 1943b, Astronomical Evolution, Unpublished manuscript, 88pp, Trustees of the National Library of Ireland, Ms. No. 16862.

Edgeworth, K.E., 1944, *Unemployment Can be Cured*, Cherbury, Booterstown, Co. Dublin.

Edgeworth, K.E., 1961, *The Earth, The Planets and The Stars, Their Birth and Evolution*, The Macmillan Company, New York.

Edgeworth, K.E., 1965, *Jack of All Trades – The Story of My Life*, Allen Figgis, Dublin.

Edgeworth, K.E., Cobbold, G.W.N., 1925, The measurement of frequency and allied quantities in wireless telegraphy, *J. Institution of Electrical Engineers*, **63**, 919-922.

Luyten, W.J., 1938, Letter to K.E. Edgeworth, dated 6 June 1938. 2pp, Trustees of the National Library of Ireland, Ms. No. 16869/45.

McFarland, J., 1996, Kenneth Essex Edgeworth – Victorian Polymath and Founder of the Kuiper belt? *Vistas in Astronomy*, **40**, 343–354.

McNally, D., Hoskin, M., 1988, William E. Wilson's Observatory at Daramona House, *J. Hist. Astron.*, **19**, 146-153.

Methuen & Co. Ltd., 1938, Letter to K.E. Edgeworth, dated 31 December 1938, 2pp., Trustees of the National Library of Ireland, Ms. No. 16869/10.

Warner, B., 1977, W.E. Wilson and the Daramona Observatory, *Sky & Telescope*, **53**, 108-110.

Wilson, W.E., 1900, *Astronomical and Physical Researches made at Mr Wilson's Observatory, Daramona, Westmeath,* being a privately published collection of Wilson's papers.

Asteroid models from disk-integrated photometry

Kaasalainen Mikko

Abstract. *Advanced optimization techniques allow the deduction of the macroscopic shapes, rotational states, and scattering parameters of asteroids from photometric measurements of total brightnesses in different viewing/illumination geometries. Shape classes comprise convex, nonconvex, and binary objects, while rotational states include relaxed rotation, precessing motion, and mutually orbiting configurations.*

1 . Introduction

Disk-resolved images can be obtained only of a limited number of the small atmosphereless bodies of our solar system. This is why disk-integrated photometry is and will remain a major source of information on these objects; consequently, efficient methods are needed for interpreting such data.

Traditional methods are mostly based on the epochs of some lightcurve features, lightcurve amplitudes, and triaxial ellipsoids or their modifications (Magnusson *et al.* 1989, 1996; Barucci *et al.* 1992; Kwiatkowski 1995 and Binzel *et al.* 1993). These methods are practical if the data are very limited; they are especially suitable for getting the first pole direction estimate for an asteroid not yet well observed.

Advanced methods, with which this presentation is concerned, solve the lightcurve inversion problem with general deconvolution methods and optimization techniques. The model is not based on a shape given a priori, and all available data is used in the analysis (Kaasalainen and Torppa 2001; Kaasalainen *et al.* 2001). Recent observations of precessing and binary systems have also led to new inversion schemes (Kaasalainen 2001; Mottola and Lahulla 2000; Pravec and Hahn 1997).

2 . General considerations

Lightcurves produced by arbitrary objects can be computed numerically using a ray-tracing code. Once it is known that a surface patch d*s* is both visible and illuminated, its contribution d*L* to the total brightness *L* is given by (omitting irrelevant scale factors such as the squares of distances)

$$\mathrm{d}L = S(\mu, \mu_0, \alpha)\varpi \mathrm{d}s \qquad (1)$$

where ϖ and S are albedo and the scattering law (in a simple form here; more arguments can naturally be included); α is the solar phase angle; $\mu = E \cdot n$ and $\mu_0 = (E_0 \cdot n)$, where **E** and

$\mathbf{E}_0$ are, respectively, unit vectors towards the observer (Earth) and the Sun, and **n** is the surface unit normal.

A general solution for the inverse problem can only be found when all parameters are determined simultaneously. Our aim is thus to minimize

$$\chi^2 = \left\| \mathrm{L}_{\mathrm{obs}} - \mathrm{L} \right\|^2 \tag{2}$$

where $\mathbf{L}_{\mathrm{obs}}$ and **L** are, respectively, vectors containing the observed and modelled brightnesses at the observation epochs. Since absolute brightnesses of observations are often not known accurately enough, and the scattering model may be insufficient as well, the practical approach is usually to regard some or all of the photometric data as relative. In this case we minimize

$$\chi^2_{\mathrm{rel}} = \sum_i \left\| \frac{\mathrm{L}^2_{\mathrm{obs}}}{\bar{L}^{(i)}_{\mathrm{obs}}} - \frac{\mathrm{L}^{(i)}}{\bar{L}^{(i)}} \right\|^2 \tag{3}$$

where, through the average brightnesses $\bar{L}^{(i)}$ of each lightcurve sequence *i*, both the observed and the model lightcurves are renormalized to mean brightnesses of unity.

Using (3) reflects a natural phenomenon: it is primarily the shapes of the lightcurves that are strongly connected with the pole, the period, and the shape of the asteroid. The absolute brightnesses are principally connected with the scattering properties; thus one can actually decouple one set of parameters from the rest to some extent.

3 . Convex modelling

The inverse problem can be robustly analyzed if it is assumed that the body can be modelled with a convex shape. Such a shape is computationally easiest to give in the form of a convex polyhedron; the shape parameters to be solved are the areas of the facets. Once these are known, the vertices of the facets can be straightforwardly obtained by iteratively solving the so-called Minkowski problem (Lamberg and Kaasalainen 2001).

Obviously the shape parameter may as well be taken to represent the unknown facet albedo or its product with the facet area. Shape parameters can thus be separated from those of albedo only by using suitable constraints. Probe data and simple physical considerations indicate that we have a good reason to attribute lightcurve variation to shape as much as possible, and to invoke albedo variegation only when necessary. One of the advantages of convex modelling is that the result contains a straightforward indicator of this necessity, which can then be represented as, e.g., a simple one-spot model over a freely adjustable shape.

The convex representation of the surface has strong stability properties; this is why it is much safer to attribute brightness changes to shape rather than albedo. This stability also means that the inversion result is *not* very sensitive to random noise in observations. In fact, the result is insensitive even to the (realistic) choice of the light-scattering model of the surface. Nonconvexities can be seen as deviations from the basic convex shape. The global characteristics of even quite strongly nonconvex bodies can well be recognized from the convex model.

4 . Nonconvex models

Lightcurve observations can usually be well explained with a convex model even when the data are produced by a shape known to have large concave features. Thus we can conclude that lightcurves seldom carry detailed information on nonconvex features. This is mostly due to the fact that solar phase angles have to be very large to cause striking shadowing effects. Thus the signature of nonconvex features is usually drowned in the noise at low and intermediate solar phase angles. Another significant factor is that the light-scattering properties of the surface can seldom be modelled very accurately.

Nonconvex models are technically rather straightforward to construct by combining a ray-tracing procedure with a standard optimization method. However, nonconvex models usually do not really reach lower χ^2s than convex ones. Even in theory, reliable general nonconvex inversion requires highly accurate observations, very favourable observation geometries, and an accurate scattering model. Fortunately, large flat areas on the convex solution already indicate the presence and locations of major nonconvex features.

If we happen to come across one of the very rare objects whose lightcurve data cannot be fitted well with a convex model, we can be quite certain that there must be considerable global concavities on the surface. Contact binaries having a distinctly double-lobed appearance are good candidates for such a class of objects.

5 . Light-scattering properties

The existing light-scattering models, such as those by Hapke or Lumme and Bowell (see Bowell *et al.* 1989), are still inadequate and known to produce ambiguous and unrealistic parameter values in inverse problems. A typical example of a scattering phenomenon yet to be properly modelled is the opposition effect, i.e., the brightening near zero phase angle, caused by coherent backscattering and shadowing.

For lightcurve inversion, the scattering law must be simple: too many parameters and possibilities cause instability and unrealistic results. Also, it is often easier (at least in the first analysis) simply to express the general photometric properties of the surface rather than to try to obtain detailed physical parameters. A useful scattering model for this purpose is

$$S(\mu, \mu_0, \alpha) = f(\alpha)\mu\mu_0\left(\frac{1}{\mu + \mu_0} + c\right) \quad (4)$$

which employs Lommel-Seeliger and Lambert laws to combine single and multiple scattering with a weight factor c for the latter. In this formulation $f(\alpha)$ can be determined afterwards from a set of scale factors (obtained by dividing the average observed brightness by the corresponding model brightness) for each lightcurve while it does not have to be known when solving for the other parameters. An exponential and linear model is a versatile choice for this purpose :

$$f(\alpha) = a \exp\left(-\frac{\alpha}{d}\right) + k\alpha + 1 \quad (5)$$

where a and d are the amplitude and scale length of the opposition effect, and k is the overall slope of the phase curve (with the linear part at zero phase angle normalized to unity).

The parameters of any given scattering model can be directly incorporated in the optimization procedure. Hapke, Lumme-Bowell, and the above scattering model all give quite similar results for the shape and the rotational state (Kaasalainen *et al.* 2001). Inversion should obviously be performed with at least two different scattering laws to establish a rough error estimate. Once the scattering characteristics, shape, and the rotation period and pole are known for the asteroid, one can compute proper phase curves as functions of solar phase angle in, e.g., an equatorial illumination and viewing geometry.

6 . Rotation

The great majority of asteroids are principal-axis rotators exhibiting single-period lightcurves, whereas tumbling bodies and binary systems produce multiple-period lightcurves.

6.1. Single-period lightcurves

When data over long periods of time and various observing geometries are used, the only reliable way of estimating the sidereal period P is to include it in the general pole and shape analysis. Let $\mathbf{r}_{\mathrm{ecl}}$ denote a vector in the ecliptic coordinate frame where the origin is translated to the asteroid. This vector transforms to the vector $\mathbf{r}_{\mathrm{ast}}$ in the asteroid's own frame (where z-axis is aligned with the rotation axis) by the rotation sequence

$$\mathrm{r}_{\mathrm{ast}} = R_z(\phi_0 + \omega(t - t_0))R_y(90° - \beta)R_z(\lambda)\mathrm{r}_{\mathrm{ecl}} \tag{6}$$

where β and λ are the ecliptic latitude and longitude of the rotation axis, $\omega = 2\pi/P$, t is the time, and $R_i(\alpha)$ is the rotation matrix corresponding to the rotation of the coordinate frame through angle α in the positive direction about the i-axis. The angle ϕ_0 and the epoch t_0 can be chosen at will.

The directions $\mathbf{E}$ and $\mathbf{E}_0$ of the Earth and the Sun as seen from the asteroid are now simple functions of β, λ and ω, so these parameters can readily be included in (2) or (3). Obviously there are several local minima in χ^2, so multiple initial values for the pole and the period must be applied. The case of the pole is the simplest. A standard choice is to use a few directions in each octant of the celestial sphere as starting points; such a grid will usually cover all the local minima. One can also use the pole estimates of possible previous models (for methods of obtaining simple first estimates of rotation parameters, see Magnusson *et al.* 1989, 1996).

If the lightcurve set covers many years and apparitions, the period space is filled with densely packed local minima. The smallest separation ΔP of the local minima when plotting χ^2 as a function of the trial period P is roughly given by

$$\Delta P \approx \frac{1}{2}\frac{P^2}{T} \tag{7}$$

where $T = \max(|t - t_0|)$ within the lightcurve set. One should thus use initial periods less than ΔP apart from each other covering the whole of the interval within which P can be expected to lie. Lightcurve inversion uses all apparitions and observations for the period estimate; thus, the more apparitions there are available, the more pronounced the correct local minimum of the period is.

6.2. Multiple-period lightcurves

When the effects of the relative motion between the target and the observer can be neglected or compensated for, lightcurve data can be subjected to the standard power spectrum and multidimensional Fourier analysis (Press *et al.* 1994), with which the probable underlying frequencies of the data can be singled out and given initial estimates.

A total of eight parameters are needed for a complete description of the force-free precession of an asteroid. These parameters can be included in the analysis in the same manner as in (6) (Kaasalainen 2001). The tumbling motion is governed by two periods : an exact one, P_ψ, for the rotation about an extremal axis of the inertia ellipsoid, and an average one, P_ϕ, for the precession about **M**. The (main) peaks of the power spectrum are located at frequencies that are linear combinations of f_ψ and f_ϕ, where $f = 1/P$. Prominent peaks are usually found at $2f_\varphi$ and $2(f_\phi \pm f_\psi)$; other low harmonics and combinations are typically seen as well.

The existence of binary asteroids was confirmed in the turn of the millennium with various techniques such as photometric observations, adaptive optics, and radar. Particular lightcurve features have sometimes been suggested to represent the signature of binary structures where the two bodies are in contact or are separated but in synchronous rotation with their mutual orbital motion. However, especially for contact binaries such interpretations can usually be made only indirectly (Kaasalainen *et al.* 2002a) due to the small photometric information content on nonconvexities.

The key to the identification of nonsynchronous binaries is the additive nature of the two components in the binary system. If we subtract from the lightcurve the periodic component corresponding to the rotation of the primary, and we are left with the unequivocal signature of eclipse-occultation events, then we can positively identify and consequently model the asteroid as a binary system (Mottola and Lahulla 2000; Pravec and Hahn 1997). Ellipsoidal component models are usually sufficient for deducing the dynamical parameters even if there are not many observations available.

7 . Comparison with probe and radar data

The disk-resolved data sets on the asteroids 951 Gaspra (Thomas *et al.* 1994), 241 Ida (Thomas *et al.* 1996), and 433 Eros (Veverka *et al.* 2000), taken during the Galileo and NEAR Shoemaker missions, represent the ground truth that allows us to test the performance of the adopted inversion methods. All these objects have been well observed photometrically; the corresponding detailed inversion results are discussed in Kaasalainen *et al.* (2001). The global triaxial dimensions of the lightcurve inversion and probe models agree within 5-10% for each of the three bodies, and the global-scale details of the two shape models resemble each other closely. The spin vector directions and rotation rates also completely agree (within a few degrees) with the spacecraft data for Eros and Gaspra; the restricted observation geometries for Ida allow two possible pole solutions, one of which closely agrees with the correct pole. Lightcurve inversion results also closely agree (Kaasalainen *et al.* 2001) with the radar-based models for 1620 Geographos (Hudson and Ostro 1999) and 6489 Golevka (Hudson *et al.* 2000).

Traditional pole determination methods and their variants have also produced good estimates of the pole directions and rotation periods for most of the «test-case» asteroids above (see the corresponding references above and references therein). These estimates are particularly useful as initial values that can be refined with the more detailed techniques. Traditional pole determination schemes are often unable to resolve pole ambiguities, and irregularly shaped asteroids may confuse such methods.

8 . Conclusion

The lightcurve inversion model is detailed and stable if accurate measurements made at various observing geometries are available; the key principle is thus to conduct well-planned observation campaigns. Well-equipped amateur observers and the development of automatic telescopes should be of considerable assistance in this. Near-Earth asteroids are particularly rewarding targets, since a comprehensive model of an NEA can often be constructed after one suitable apparition, i.e., an observation span of only a few months.

The requirement of various observing geometries is not very hard: almost all asteroids to which traditional triaxial ellipsoid methods can be applied can be analyzed with the general method as well. The main objective is to observe the target at as many ecliptic longitudes (and latitudes) and solar phase angles as possible. Thus, a preliminary model of a main-belt asteroid can be built even from two suitable apparitions, while three to four apparitions are usually already sufficient for the construction of a good model (Kaasalainen *et al.* 2002b). While accuracy is desired, even substantial random noise in lightcurves does not preclude their use for modelling purposes; also, relative photometry is sufficient for shape and rotation analysis.

There are several aspects of photometric analysis that should be investigated further. Theoretical models of light scattering are still not adequate; neither is it clear how well the physical scattering parameters of the surface can really be determined from disk-integrated photometric data. Such parameters include not only the characteristics of the surface regolith particles, but also statistical topographic variations on small size scales. Lightcurve observations are not restricted only to brightness measurements at visual wavelengths. Observations in the infrared, together with theoretical models of thermal emission, can be particularly valuable in deducing the albedo variegation and composition of the surface.

Perhaps the most interesting future prospect is the use of complementary data simultaneously with photometry in asteroid modelling. Examples of such data are interferometric observations (speckle or other types), timings of stellar occultations, and precise astrometric measurements (from orbiting instruments) for which the photocentre of the target does not coincide with its centre of mass. Polarimetric observations may also prove to be a useful source of data.

References

Barucci, M. A., Cellino, A., De Sanctis, C., Fulchignoni, M., Lumme, K., Zappalà, V., Magnusson, P., 1992, Ground-based Gaspra Modelling : comparison with the first Galileo image, *Astron. Astrophys*., **266**, 385-394.

Binzel, R. P., and 18 colleagues, 1993, Asteroid 243 Ida : Groundbased Photometry and a Pre-Galileo Physical Model, *Icarus*, **105**, 310-325.

Bowell, E., Hapke, B., Domingue, D., Lumme, K., Peltoniemi, J., Harris, A. W., 1989, Application of photometric models to asteroids. In *Asteroids II* (R. Binzel *et al*., eds.), 524-556. University of Arizona Press, Tucson.

Hudson, R.S., Ostro, S.J., 1999, Physical Model of Asteroid 1620 Geographos from Radar and Optical Data, *Icarus*, **140**, 369-378.

Hudson, R.S., and 26 colleagues, 2000, Radar Observations and Physical Model of Asteroid 6489 Golevka, *Icarus,* **148**, 37-51.

Kaasalainen, M., Torppa, J., 2001, Optimization methods for asteroid lightcurve inversion. I. Shape determination, *Icarus*, **153**, 24-36.

Kaasalainen, M., Torppa, J., Muinonen, K., 2001, Optimization methods for asteroid lightcurve inversion. II. The complete inverse problem, *Icarus,* **153**, 37-51.

Kaasalainen, M., 2001, Interpretation of lightcurves of precessing asteroids, *Astron. Astrophys*., **376**, 302-309.

Kaasalainen, M., Torppa, J., Piironen, J., 2002a, Binary structures among large asteroids, *Astron. Astrophys*., in press.

Kaasalainen, M., Torppa, J., Piironen, J., 2002b, Physical models of twenty asteroids from photometric data, *Icarus*, (Asteroids 2001 issue), submitted.

Kwiatkowski, T., 1995, Sidereal period, pole and shape of asteroid 1620 Geographos, A*stron.Astrophys.,* **294**, 274-277.

Lamberg, L., Kaasalainen, M., 2001, Numerical solution of the Minkowski problem, *J. Comp. Appl. Math.,* **137**, 213-227.

Magnusson, P., Barucci, M. A., Drummond, J., Lumme, K., Ostro, S. J., Surdej, J., Taylor, R. C., Zappalà, V., 1989, Determination of pole orientations and shapes of asteroids, in *Asteroids II* (R. Binzel et al., eds.), 67-97. University of Arizona Press, Tucson.

Magnusson, P., and 46 colleagues, 1996, Photometric Observations and Modeling of Asteroid 1620 Geographos, *Icarus*, **123**, 227-244.

Mottola, S., Lahulla, F., 2000, Mutual Eclipse Events in Asteroidal Binary System 1996FG3: Observations and a Numerical Model, *Icarus*, **146**, 556-567.

Pravec, P., Hahn, G., 1997, Two-period lightcurve of 1994 AW1 : Indication of a binary asteroid?, *Icarus*, **127**, 431-440.

Press, W. H., Flannery, B. P., Teukolsky, S. A., Vetterling, W. T., 1994, *Numerical Recipes in Fortran*, Cambridge University Press, Cambridge.

Thomas, P.C., Veverka, J., Simonelli, D., Helfenstein, P., Carcich, B., Belton, M.J.S., Davies, M.E., Chapman, C., 1994, The Shape of Gaspra, *Icarus*, **107**, 23-36.

Thomas, P.C., Belton, M.J.S., Carcich, B., Chapman, C., Davies, M.E., Sullivan, R., Veverka, J., 1996, The Shape of Ida, *Icarus*, **120**, 20-32.

Veverka, J., and 32 colleagues, 2000, NEAR at Eros : Imaging and Spectral Results, *Science,* **289**, 2088-2097.

Photometric observations of asteroids : rotational period, lightcurves, spin axis and shape determination

Blanco C., Cigna M., Riccioli D.

Abstract. *Numerous observational campaigns of asteroids have been made, since 1980, at the Physics and Astronomy Department of Catania University. The study of the B and V lightcurves allowed us to determine, depending on their phase coverage and longitude distribution, the most important rotational and physical parameters. A list of the observed asteroids with the related month and year of observation and the values of the rotational period, amplitude of V light variation, B-V mean colour index, coordinates of the spin axis direction and semiaxes ratios is presented.*

Keywords *: asteroids, lightcurves, B-V colour, spin axis, shape.*

1 . Introduction

At the Physics and Astronomy Department of Catania University (in the past known as Astronomy Institute of Catania University) photometric observational campaigns of asteroids have been made since 1980, mainly by using photoelectric photometry acquisition. Their main aim was to built lightcurves to determine, at different solar phase angles and longitudes, the rotational parameters of main belt asteroids : rotational period, rotational axis direction, shape, constancy of the B-V mean colour index, etc. Particular attention was devoted to the asteroids with observational constraints, like the objects with diameters smaller than 100 km or of low negative latitude, and to the asteroids with almost two known lightcurves to obtain the elements needed for applying the computational methods of the pole coordinates and shape. Since the Near-Earth Objects revealed the importance of their knowledge, relevant observing attention was addressed to them, as to the participation in the most relevant international campaigns : the Galileo target 951 *Gaspra*, the targets of Hubble Space Telescope, 4179 *Toutatis*, 1620 *Geographos* and 153 *Hilda*. Since 1990 the observational campaigns have been carried out in collaboration with Turin Astronomical Observatory.

2 . Observational characteristics

All the observations were carried out by means of the 91-cm Cassegrain telescope at the M.G. Fracastoro station of Catania Astrophysical Observatory (longitude $0^h 59^m 55^s$ E; latitude $+37^\circ 41' 30''$; altitude 1725 m a.s.l.). A cooled photon-counting single-head photometer equipped with an EMI 9863 QA-350 photomultiplier was used. The observations were performed through B (BG12 - 1mm + GG13 - 2mm; $\lambda = 4370 \pm 350$ Å) and V (GG14 - 2 mm; $\lambda = 5440 \pm 350$ Å) Schott filters and using a 2-mm diameter diaphragm, limiting the telescope field to about 28 arcsec. The timing was obtained by connecting with the Physikalisch

Technische Bundesanstalt in Mainflingen, Frankfurt (Germany) and by setting the computer clock according to the received signal. Every measurement lasted 1 min and consisted of six counts (three each alternatively in B and V) with integration times of 10 sec. A typical cycle of observations was as follows : sky, comparison star, asteroid, asteroid, comparison star, sky. Almost all used comparison stars, suitably chosen along the minor planet path, are not catalogue stars. Their non variability was checked by observing all of them and suitable check stars during each night of the related campaign and then by computing their lightcurves. To the observations, made only under clear sky conditions, collaborated M. Di Martino, G. De Sanctis, P. Tanga (Turin Astronomical Observatory), D. Lupishko (Kharkow Astronomical Observatory) and J. Piironen (Helsinki Astronomical Observatory).

3 . Reduction procedure

The reduction of the collected data was made by using a computer program suitable to the observational characteristics of the campaigns. The program estimates the differential extinction between the target object and the comparison stars and, by using these stars, nightly determines the extinction coefficients. Their values are not affected by relevant seasonal variations and agree with the mean proper ones of M.G. Fracastoro station ($K_B = 0.387 \pm 0.02$; $K_V = 0.247 \pm 0.02$). The reduction to the Johnson standard system of the asteroids and of the comparison stars measurements was made by means of standard stars included in *Blanco et al.* (1968) and in *Landolt* (1973) and normally observed each night within about 1 hour before and after the passage to the meridian. The lightcurve standard deviation was determined by introducing a fictitious rectification, to take into account the light variations due to the rotation of the asteroid. The mean error, computed by dividing the standard deviation values by the square root of the number of measurements, is of the order of 0.005 mag. The resulting uncertainty in the composite lightcurves is ±0.01 mag, hence the determination of the amplitude values suffers the same error. The values of the synodic rotational periods and the composite lightcurves were obtained by using a Fourier analysis method (Harris *et al.* 1989).

4 . Pole and shape determination

The values of the pole coordinates and of the axes ratios of all asteroids reported in Table 1 were determined by using the Amplitude-Magnitude (AM) method (Zappalà *et al.* 1983). This method gives only a preliminary indication of the rotational properties of the asteroid, but, for its simple and fast application it is particularly suitable for the cases of a very large number of rotation axis direction and shape determinations. The method is based on the assumed ellipsoidal shape of the asteroid (with semiaxes a > b > c) and on the relationship between the aspect angle, the lightcurve amplitude and the magnitude V of the asteroid at the lightcurve maximum. The knowledge of these parameters is required at least in three oppositions, well distributed in longitude. By assuming the smaller axis c to be the asteroid rotation axis, the two other axes ratio and subsequentely their single values, can be obtained from the amplitude-longitude plot. At every given orbital position of the asteroid, from the axes ratios it is possible to obtain the value of the aspect angle (with an uncertain definition of the north and south pole) and hence the pole longitude.

5 . Results

Table 1 shows the asteroids observed during the numerous campaigns, each of them was centered on the dark moon and, on an average, lasted ten consecutive nights. The name of the observed objects is listed together with the months and the years of the campaigns, the value of the rotational period and its error, the amplitude of the V lightcurve, the mean value of the B-V colour index, the pole ecliptical coordinates, the axes ratios and the reference. The amplitude of the lightcurves was obtained by measuring the maximum light variations of the smothed lightcurve. Except for the few objects whose B-V value is reported in italics, the B lightcurves present the same modulations, vs. the phase, of the respective V lightcurves, i.e. the B-V colours are constant. The results of the study of the greatest part of the asteroids reported in Table 1 were published. An estimate of the obtained results gives the determination of the pole coordinates and of the axes ratios of 48 minor planets and of the period value of about a hundred asteroids. Among those for which we determined the pole and the shape, namely well known objects, for about 50% of them we obtained the first determination of the rotational period or we improved considerably it. Greater indetermination was found if the amplitude, also of the objects of the remaining 50%, is analysed. The uncertainty increases from the analysis of the objects for which it was not possible to apply the (AM) method, i.e. less known because only one or two lightcurves are known. This means that the observational data are poor and often they provide undefined values not enough to allow us the study of the asteroidal population.

Table 1: Asteroids observed during the campaigns of photoelectric observations carried out at the Physics and Astronomy Department of Catania University and related months and years of observation, value of the rotational period and its error, amplitude of V lightcurve, B-V mean colour index, pole coordinates, axes ratios values and reference.

asteroid	campaign	period (hour)	ampl. (mag.)	B-V	pole $\lambda \beta$ (deg)	shape a/b b/c	reference
4 Vesta	Jun 78	5.341 ± 0.001	0.14	0.75			Blanco & Catalano 1979
5 Astraea	Jul/Aug 97	16.812 ± 0.005	> 0.17	0.81	132 ± 6 – 58 ± 3	1.44 1.30	Blanco et al. 2000b
6 Hebe	May/Jun 94	7.289 ± 0.001	> 0.30	0.83	128 ± 2 30 ± 3	1.32 1.11	Blanco et al. 2000b
8 Flora	Nov 97				122 ± 3 37 ± 3	1.10 1.06	Blanco & Riccioli 1998
10 Hygiea	Dec/Jan 93	13.820 ± 0.002	0.13	0.85	118 ± 1 44 ± 1	1.34 1.14	Blanco & Riccioli 1998
11 Parthenope	May 92	13.700 ± 0.005	0.14		73 ± 7 – 51 ± 5	1.23 1.21	Blanco & Riccioli 1998
12 Victoria	Jan 88	8.650 ± 0.001	0.20				Blanco et al. 1989
12 Victoria	Aug 96	8.686 ± 0.009	0.35	0.88			Riccioli et al. 2001
13 Egeria	Apr/May 97	6.991 ± 0.006	0.47	0.72	103 ± 4 13 ± 10	1.43 1.26	Blanco et al. 2000b
14 Irene	Apr/May 80	18.710 ± 0.001	0.03	0.87	90 ± 3 – 34 ± 2	1.15 1.08	Blanco & Riccioli 1998
19 Fortuna	Sep 93	7.433 ± 0.001	0.28	0.73	65 ± 17 49±9	1.44 1.10	Blanco et al. 1996a
26 Proserpina	Feb 95	6.668 ± 0.001	0.08	0.87	47 ± 1 – 4 ± 7	1.16 1.40	Blanco et al. 2000b
27 Euterpe	Nov 93	8.490 ± 0.005	> 0.13	0.81			work in progress
34 Circe	May 96	12.225 ± 0.006	> 0.30	0.70	113 ± 5 17 ± 22	1.32 1.00	Blanco et al. 2000b
44 Nysa	Sep/Dec 79	6.422 ± 0.001	0.60				Birch et al. 1983
53 Kalypso	May/Jun 94	19.308 ± 0.010	> 0.70	0.75			work in progress
53 Kalypso	Dec 96						work in progress

Table 1: Asteroids observed during the campaigns of photoelectric observations carried out at the Physics and Astronomy Department of Catania University and related months and years of observation, value of the rotational period and its error, amplitude of V lightcurve, B-V mean colour index, pole coordinates, axes ratios values and reference.

asteroid	campaign	period (hour)	ampl. (mag.)	B-V	pole λβ (deg)	shape a/b b/c	reference
56 Melete	Aug 95	6.974 ± 0.005	> 0.10	0.36	90± 50 20± 50	1.17 1.09	work in progress
63 Ausonia	Apr 98	9.282 ± 0.003	0.27	0.63	125± 2 -36± 3	2.39 1.00	Blanco et al. 2000b
66 Maja	Mar 90	9.733 ± 0.005	0.25				Blanco et al. 1990
66 Maja	Mar 94	9.761 ± 0.003	0.29	0.54	156± 6 62± 1	1.66 1.40	Blanco et al. 2000b
87 Sylvia	Jan 88	5.183 ± 0.001	0.40				Blanco et al. 1989
92 Undina	May 97	15.961 ± 0.005	> 0.64	0.77			work in progress
95 Arethusa	Jul/Aug 95	8.651 ± 0.009	0.40	0.60			Blanco & Riccioli 1999
96 Aegle	Apr 96						work in progress
96 Aegle	May 96	10.470 ± 0.004	> 0.40	0.75			Blanco et al. 2000a
97 Klotho	Aug 96	8.028 ± 0.010	> 0.34	0.71			work in progress
102 Miriam	Oct/Nov 94	15.853 ± 0.002	0.08	0.82			Riccioli et al. 2001
103 Hera	Nov 97						work in progress
108 Hecuba	Mar 90	14.460 ± 0.001	0.18	0.88	259± 7 -6± 7	1.80 1.10	Blanco & Riccioli 1998
108 Hecuba	Aug 93	14.460 ± 0.001	> 0.14	0.88	259± 7 -6± 7	1.80 1.10	Blanco & Riccioli 1998
108 Hecuba	Nov 93	14.460 ± 0.001	> 0.08	0.88	259± 7 -6± 7	1.80 1.10	Blanco & Riccioli 1998
121 Hermione	Mar 92	9.238 ± 0.010	0.28	0.73	60± 12 -42± 18	1.29 1.39	Blanco & Riccioli 1998
122 Gerda	Mar 91	10.332 ± 0.004	0.25	0.82			Di Martino et al. 1994
136 Austria	Ju92/No93	11.500 ± 0.010	> 0.08	0.60			work in progress
137 Meliboea	Sept/Oct 91	15.280 ± 0.020	0.11		149± 3 8± 3	1.18 1.11	Blanco et al. 2000b
138 Tolosa	Jan 95	12.585 ± 0.009	0.68	0.90			Blanco & Riccioli 1999
138 Tolosa	Feb 95	12.585 ± 0.009	> 0.80	0.90			Blanco & Riccioli 1999
140 Siwa	Mar 94	18.917 ± 0.003	> 0.12	0.78			Riccioli et al. 2001
140 Siwa	Jun 95	18.917 ± 0.002	0.10	0.80			Riccioli et al. 2001
150 Nuwa	Jul/Sep 93	8.140 ± 0.005	> 0.10	0.72	257± 13 1± 13	1.10 1.02	Blanco & Riccioli 1998
153 Hilda	Aug 92	5.110 ± 0.001	0.05	0.65			Lagerkvist et al. 1995
159 Aemilia	Dec 96	12.068 ± 0.005	> 0.23	0.70			work in progress
160 Una	Oct 91	5.610 ± 0.010	0.14				Di Martino et al. 1994
168 Sibylla	Mar 91	23.820 ± 0.004	> 0.30	0.71			Di Martino et al. 1994
168 Sibylla	Feb 96						work in progress
170 Maria	Jul/Sep 96	5.510 ± 0.004	0.20	0.83			Blanco et al. 2000a
173 Ino	Dec 96	5.890 ± 0.015	> 0.17	0.70	189± 4 -10± 4	1.18 1.04	work in progress
175 Andromache	Nov 93	7.109 ± 0.005	0.21	0.65			Blanco et al. 2000a
176 Iduna	May/Jun 94	5.630 ± 0.006	> 0.14	0.74			work in progress
176 Iduna	Jul/Aug 95	5.630 ± 0.006	> 0.23	0.74	85± 1 36± 1	1.39 1.28	Blanco et al. 2000b
176 Iduna	Dec 96	5.630 ± 0.006	0.30	0.74	85± 1 36± 1	1.39 1.28	Blanco et al. 2000b
181 Eucaris	Jun 95	8.024 ± 0.002	0.10	0.82			Riccioli et al. 2001
185 Eunike	Jul/Aug 97	10.690 ± 0.008	> 0.32	0.67			work in progress
188 Menippe	Jul 93	8.450 ± 0.003	> 0.18	0.75			work in progress

Table 1: Asteroids observed during the campaigns of photoelectric observations carried out at the Physics and Astronomy Department of Catania University and related months and years of observation, value of the rotational period and its error, amplitude of V lightcurve, B-V mean colour index, pole coordinates, axes ratios values and reference.

asteroid	campaign	period (hour)	ampl. (mag.)	B-V	pole λβ (deg)	shape a/b b/c	reference
189 Phthia	Sep/Oct 97						work in progress
189 Phthia	Nov 97						work in progress
198 Ampella	Aug 95	5.701 ± 0.002	0.12	0.85			Blanco & Riccioli 1999
198 Ampella	Sep 95	5.701 ± 0.002	> 0.08	0.85			work in progress
212 Medea	Feb 95	18.175 ± 0.009	0.83	0.68			Blanco & Riccioli 1999
218 Bianca	Jul/Aug 97	6.070 ± 0.006	> 0.15	0.86	118± 8 42± 7	1.25 1.15	work in progress
220 Stephania	Sep 93	8.040 ± 0.006	> 0.21	0.98			work in progress
225 Henrietta	May/Jun 94	9.173 ± 0.009	> 0.26	0.67	59± 21 51± 7	1.31 1.00	work in progress
226 Weringia	Apr 93						work in progress
231 Vindobona	Sep/Oct 97	5.547 ± 0.005	0.81	0.95			Blanco et al. 2000a
236 Honoria	Sep 93	12.333 ± 0.006	> 0.09	0.89	178± 14 - 66± 14	1.23 1.14	Blanco et al. 1996b
238 Hypatia	Jun 92	8.840 ± 0.010	0.17				Riccioli et al. 1995
241 Germania	Nov/Dec 91	15.570 ± 0.003	0.16	0.66			Riccioli et al. 2001
250 Bettina	Sep/Oct 97	5.065 ± 0.005	0.42	0.74	95± 5 -1± 30	1.74 1.58	Blanco et al. 2000b
258 Tyche	Jul/Aug 97	9.983 ± 0.006	0.43	0.86	252± 15 -20± 15	1.51 1.25	Blanco et al. 2000b
259 Aletheia	Apr 96						work in progress
286 Iclea	Feb 95	9.359 ± 0.002	0.18	0.68			Blanco & Riccioli 1999
287 Nephthys	May 93	7.580 ± 0.004	> 0.28	0.90	99± 1 54± 1	1.31 1.21	Blanco et al. 1996b
306 Unitas	Jul/Aug 97	8.750 ± 0.005	> 0.11	0.85			work in progress
313 Chaldaea	May 96	10.130 ± 0.007	> 0.16	0.71	209± 24 -55± 24	1.29 2.08	work in progress
313 Chaldaea	Jul/Aug 97	10.130 ± 0.007	> 0.24	0.71	209± 24 -55± 24	1.29 2.08	work in progress
324 Bamberga	Sep/Nov 78	29.420 ± 0.008	0.08	0.69			Scaltriti et al. 1980
333 Badenia	Sep/Oct 97	8.160 ± 0.006	0.20	0.77			Blanco et al. 2000a
335 Roberta	Sep/Oct 97	4.349 ± 0.009	0.78	0.62	258± 4 25± 9	2.09 1.14	Blanco et al. 2000b
338 Budrosa	Mar 94	9.814 ± 0.048	> 0.40	0.70			work in progress
352 Gisela	Aug 92	5.560 ± 0.009	0.42	0.92	213± 5 53± 5	1.47 1.38	Blanco et al. 2000b
352 Gisela	Mar 94	5.560 ± 0.005	> 0.25	0.92			work in progress
371 Bohemia	Nov 93	12.480 ± 0.010	> 0.16	0.91			Riccioli et al. 1995
371 Bohemia	Set/Oct 97	6.931 ± 0.009	> 0.44	0.91			work in progress
372 Palma	May 96						work in progress
377 Campania	Sep 90	8.507 ± 0.003	0.27	0.68			Di Martino et al. 1994
377 Campania	Aug 92	8.480 ± 0.010	> 0.17	0.69	266± 7 0± 7	1.32 0.90	Blanco et al. 1996b
379 Huenna	Jul 97	6.660 ± 0.005	> 0.10	0.68			work in progress
389 Industria	Sep/Oct 97						work in progress
407 Arachne	Nov 97						work in progress
409 Aspasia	Jul/Aug 97	9.090 ± 0.006	> 0.22	0.71	216± 43 16± 43	1.26 0.97	work in progress
411 Xante	May 93	7.480 ± 0.010	> 0.23	0.76			Riccioli et al. 1995
419 Aurelia	Aug 92	16.630 ± 0.010	0.18	0.62			Riccioli et al. 1995
419 Aurelia	Aug 96	16.630 ± 0.006	> 0.27	0.64	13± 2 -34± 2	1.28 1.16	Blanco et al. 2000b

Table 1: Asteroids observed during the campaigns of photoelectric observations carried out at the Physics and Astronomy Department of Catania University and related months and years of observation, value of the rotational period and its error, amplitude of V lightcurve, B-V mean colour index, pole coordinates, axes ratios values and reference.

asteroid	campaign	period (hour)	ampl. (mag.)	B-V	pole λ β (deg)	shape a/b b/c	reference
432 Pythia	May/Jun 94	8.341 ± 0.003	> 0.27	0.83	121± 9 65± 6	1.37 1.27	Blanco et al. 2000b
444 Gyptis	Jul 97						work in progress
454 Mathesis	Oct 91	7.075 ± 0.025	0.28				Di Martino et al. 1994
455 Bruchsalia	Dec 96	10.645 ± 0.003	0.40	0.72			Blanco et al. 2000a
471 Papagena	Dec 96	6.327 ± 0.004	> 0.22	0.68	21± 3 31± 3	1.25 1.38	Blanco et al. 2000b
485 Genua	Jul 94	18.055 ± 0.006	> 0.52	0.83			work in progress
488 Kreusa	May 97	6.457 ± 0.009	0.30	0.70			Blanco et al. 2000a
500 Selinur	Sep 90		> 0.10				Di Martino et al. 1994
500 Selinur	Sep 94	9.590 ± 0.003	0.18	0.69			Blanco et al. 2000a
509 Iolanda	Jul 95	16.592 ± 0.003	0.39	0.75			Blanco et al. 2000a
537 Pauly	Jun 95	6.450 ± 0.002	> 0.12	0.88	290± 31 40± 31	1.25 1.88	Blanco et al. 2000b
550 Senta	Sep/Oct 91	20.555 ± 0.010	> 0.20				Di Martino et al. 1994
550 Senta	Sep 95	20.555 ± 0.004	> 0.16	0.85			work in progress
566 Stereoskopia	Jan 90	9.685 ± 0.006	> 0.12				work in progress
566 Stereoskopia	Oct/Nov 94	9.685 ± 0.006	0.25	0.80			Blanco et al. 2000a
568 Cheruskia	Jan 95	14.654 ± 0.005	0.44	0.70			Blanco et al. 2000a
568 Cheruskia	Feb 95	14.654 ± 0.005	> 0.30	0.70			work in progress
570 Kythera	Sep 94	6.919 ± 0.006	0.15	0.70			Blanco et al. 2000a
639 Latona	Mar 94	6.170 ± 0.004	> 0.32	0.85			Riccioli et al. 2001
639 Latona	Aug 96	6.170 ± 0.004	0.35	0.85			Riccioli et al. 2001
654 Zelinda	Sep/Oct 97						work in progress
660 Crescentia	Jul 94	7.990 ± 0.004	> 0.30	0.88			work in progress
665 Sabine	Aug 92	3.932 ± 0.008	0.35	0.67			Riccioli et al. 1995
674 Rachele	Sep 93	30.940 ± 0.040	> 0.15	0.85			Blanco & Riccioli 1999
674 Rachele	Nov 93	30.940 ± 0.040	0.09	0.83			Blanco & Riccioli 1999
700 Auravictrix	Apr 93	5.940 ± 0.004	> 0.30	0.98			work in progress
712 Boliviana	Aug 96	11.852 ± 0.004	> 0.15	0.72			work in progress
713 Luscinia	Oct 95	9.274 ± 0.002	0.12	0.68			Blanco et al. 2000a
735 Marghanna	Nov 93	6.664 ± 0.003	> 0.07	0.60			work in progress
783 Nora	Apr 93						work in progress
860 Ursina	Sep 94	9.330 ± 0.015	0.50	0.65			Blanco & Riccioli 1999
905 Universitas	Sep/Oct 97						work in progress
912 Maritima	May 96	6.066 ± 0.004	0.14	0.72			Blanco et al. 2000a
914 Palisana	Jun 92	15.620 ± 0.010	0.18	0.72			Riccioli et al.1995
937 Bethgea	Sep 90	8.356 ± 0.006	0.16	0.89			Di Martino et al. 1994
951 Gaspra	Jan 90	7.042 ± 0.001	0.46	0.80			Blanco et al. 1991
984 Gretia	Jul/Ago 97	5.560 ± 0.018	> 0.80	0.95	228± 9 - 12± 9	2.25 1.00	Blanco et al. 2000b
1021 Flammario	Feb 96						work in progress
1069 Planckia	Mar 94	5.050 ± 0.004	> 0.87	0.80			work in progress

Table 1: Asteroids observed during the campaigns of photoelectric observations carried out at the Physics and Astronomy Department of Catania University and related months and years of observation, value of the rotational period and its error, amplitude of V lightcurve, B-V mean colour index, pole coordinates, axes ratios values and reference.

asteroid	campaign	period (hour)	ampl. (mag.)	B-V	pole λβ (deg)	shape a/b b/c	reference
1369 Ostanina	Aug 95	6.145 ± 0.005	0.80	0.58			Blanco & Riccioli 1999
1469 Linzia	Oct/Nov 94	6.067 ± 0.009	0.42	0.81			Blanco & Riccioli 1999
1620 Geographos	Sep 94	5.220 ± 0.009	0.20	0.86	56± 6 -47± 4	2.58 1.00	Magnusson et al. 1996
3578 Carestia	Aug 96	7.082 ± 0.002	0.25				Blanco et al. 2000a
4179 Toutatis	De 93/Ja 94	29.980 ± 0.009	0.40				Spencer et al. 1995

References

Birch, P.V., Tedesco, E.F., Taylor, R.C., Binzel, R.P., Blanco, C., Catalano, S., Hartigan, P., Scaltriti, F., Tholen, D.J., Zappalà, V., 1983, *Icarus*, **54**, 1.

Blanco, C., Catalano, S., 1979, *Icarus*, **40**, 359.

Blanco, C., Cigna, M., Riccioli, D., 2000b, *Planet. Space Sci.,* **48**, 973.

Blanco, C., Di Martino, M., De Sanctis, G., Riccioli, D., 1996b, *Planet. Space Sci.,* **44**, 93.

Blanco, C., Di Martino, M., Dotto, E., Gilmore, A.C., Kilmartin, P.M., Riccioli, D., 1996a, *Planet. Space Sci.*, **44**, 87.

Blanco, C., Di Martino, M., Ferreri, W., Gonano, M., Mottola, S., Neukum, G., 1990, 12° *Europ. Reg.* Meeting of the IAU. Davos, Switzerland, 8-11 October.

Blanco, C., Di Martino, M., Ferreri, W., Gonano, M., Mottola, S., Neukum, G., 1991, *Adv. Space Rev.*, **11**, (12)193.

Blanco, C., Di Martino, M., Gonano, M., Jauman, R., Mottola, S., Nagel, E., Neukum, G., Zappalà, V., 1989, *Mem. Soc. Astr. It.*, **60**, 195.

Blanco, C., Di Martino, M., Riccioli, D., 2000a, *Planet. Space Sci.,* **48**, 271.

Blanco, C., Riccioli, D., 1998, *Astron. Astrophys. Suppl. Ser.,* **131**, 385.

Blanco, C., Riccioli, D., 1999, *Proc. IAU Coll.,* **173**, 175.

Blanco, V.M., Demers, S., Douglass, G.G., Fitzgeralg, M.P., Publ. U.S. Naval Observatory 21.

Di Martino, M., Blanco, C., Riccioli, D., De Sanctis, G., 1994, *Icarus*, **107**, 269.

Harris, A.W., Young, J.W., Bowell, E., Martin, R.L., Poutanen, M., Scaltriti, F., Zappalà, V., Schober, H.J., Debehogne, H., Zeigler, K.W., 1989, *Icarus*, **77**, 171.

Lagerkvist, C-I., Di Martino, M., Blanco, C., Dahlgren, M., Erikson, A., Lahulla, J.F., Lazzarin, M., Lumme, K., Pohjolainen, S., Riccioli, D., 1995, *Earth, Moon and Planets,* **71**, 189.

Landolt, A.U., 1973, *Astron J.*, **78**, 959.

Magnusson, P., Dahlgren, M., Barucci, M.A., Jorda, L., Binzel, R.P., Slivan, S.M., Blanco, C., Riccioli, D., Buratti, B.J., Colas, F., Berthier, J., De Angelis, G., Di Martino, M., Dotto, E., Drummond, J.D., Fink, U., Hicks, M., Grundy, W., Wisniewski, W., Gaftonyuk, N.M., Geyer, E.H., Bauer, T., Hoffmann, M., Ivanova, V., Komitov, B., Donchev, Z., Denchev, P., Krugly, Yu.N., Velichko, F.P., Chiorny, V.G., Lupishko, D.F., Shevchenko, V.G., Kwiatkowski, T., Kryszczynska, A., Lahulla, J.F., Licandro, J., Mendez, O., Mottola, S., Erikson, A., Ostro, S.J., Pravec, P., Pych, W., Tholen, D.J., Whiteley, R., Wild, W.J., Wolf, M., Sarounova, L., 1996, *Icarus*, **123**, 227.

Riccioli, D., Blanco, C., Cigna, M., 2001, *Planet. Space Sci.*, **49**, 657.

Riccioli, D., Blanco, C., Di Martino, M., De Sanctis, G., 1995, *Astron. Astrophys. Suppl. Ser.*, **111**, 297.

Scaltriti, F., Zappalà, V., Schober, H.J., Hanslemeier, A., Saudy, A., Piironen, J., Blanco, C., Catalano, S., 1981, *Astron. Astrophys. Suppl. Ser.*, **100**, 326.

Scaltriti F., Zappalà, V., Stanzel, R., Blanco, C., Catalano, S., Young, J.W., 1980, *Icarus*, **43**, 391.

Spencer, J.R., Akimov, L.A., Angeli, C., Angelini, P., Barucci, M.A., Birch, P., Blanco, C., Buie, M.W., Caruso, A., Chiornij, V.G., Colas, F., Dentchev, P., Dorokhov, N.I., De Sanctis, M.C., Dotto, E., Ezhkova, O.B., Fulchignoni, M., Green, S., Harris, A.W., Howell, E.S., Hudecek, T., Kalashnikov, A.V., Kobelev, V.V., Korobova, Z.B., Koshkin, N.I., Kozhevnikov, V.P., Krugly, Y.N., Lazaro, D., Lecacheux, J., MacConnel, J., Mel'nikov, S.Y., Michalowski, T., Mueller, B.E.A., Nakamura, T., Neese, C., Nolan, M.C., Osborn, W., Pravec, P., Riccioli, D., Shevchenko, V.S., Shevchenko, V.G., Tholen, D.J., Velichko, F., Venditti, C., Venditti, R., Wisniewski, W.Z., Young, J., Zellner, B., 1995, *Icarus*, **117**, 71.

Flux Preserving Regularization (FPR) method of restoration

Bratsolis Emmanuel, Sigelle Marc

Abstract. *In this article we try to give a simple method of spatial regularization deriving from Richardson-Lucy (RL) algorithm in order to overcome the problem of noise amplification during the image reconstruction process. It is very important in astronomy to regularize images while controlling their photometric behavior. We propose a new reconstruction method preserving both the global photometry and local photometric aspects.*

Keywords *: Image processing, restoration, regularization, photometric behavior*

1 . Introduction

The Richardson-Lucy algorithm is the technique most widely used for restoring astronomical images. It can be derived very simply if we start with the blurred image equation and the equation for Poisson statistics.

There are two types of noise. The first one is not associated with the true signal and comes from backgrounds such as the read-out noise of a detector, which has a Gaussian distribution, or the sky background. The sky background noise can be removed before any other data processing, whereas the read-out noise can be modified into a Poisson distribution by a simple modification of data when its Gaussian distribution is known, provided its variance is large enough. The second type of noise is associated with the signal recording process. A regularization method has to be applied to remove this type of noise. We assume in the following that read-out and sky background noise have been corrected. Here we present a new regularization method for RL restoration, named FPR[1].

2 . Recall of the Richardson-Lucy restoration algorithm

We consider the case of ground-based optical or infrared imaging by a single aperture. Let $O(x, y)$ be the true two-dimensional intensity distribution of the object, where x, y are two orthogonal coordinates in some small region of the sky. The measured data $D(x, y)$ after «bias» and «flat-field» corrections takes the form of a convolution :

$$\begin{aligned} D(x, y) &= \iint H(x-u, y-v)\ O(u, v)\ du\ dv + N(x, y) \\ &= (H * O)(x, y) + N(x, y) \end{aligned} \tag{1}$$

where $*$ indicates two-dimensional convolution, $H(x, y)$ is the point spread function (PSF) of the imaging system and $N(x, y)$ represents the additive noise.

We shall from now on adopt a discrete representation of signals, *i.e.* work on a discrete two-dimensional lattice of sites, $S = \{s\}$. The true scene will then be noted as : $O = \{O_s\}_{s \in S}$ or equivalently: $O = O(i, j)$ with $(i, j) \in Z^2$.

The RL algorithm has the following form :

$$O^{(n+1)} = O^{(n)}\left[\frac{D}{H*O^{(n)}}\right]*H^T \quad \forall n \geq 1 \tag{2}$$

and initialization $O^{(1)}$, where H^T is the transpose of H. This iterative scheme will also be noted in the following as :

$$O^{(n+1)} = \mathrm{RL}(O^{(n)}), n \geq 1$$

Usually $O^{(1)}$ is taken as a uniform flat image having the same total flux as observation D.

3 . Flux-Preserving Regularization (FPR) method for restoration

The main problem with the RL algorithm is that in practice it doesn't converge to the global maximum because of the fact that we are dealing with an ill-posed problem and some *a priori* knowledge, not contained in the maximum likelihood model, is needed. Data instances that are not compatible with others can cause singularities in the restoration solution. So, a regularization method is needed to replace the ill-posed problem with a well-posed problem. The regularization approach overcomes this difficulty by choosing among the possible objects one «smooth» object that approximate the data. The basic underlying idea in most regularization approaches is the incorporation of *a priori* knowledge into the restoration.

Assume now that we modify the iterative scheme of Equation (2) in this sense :

$$O^{(n+1)} = (1-\lambda)\,\mathrm{RL}(O^{(n)}) + \lambda T(O^{(n)}) \quad \forall n \geq 1 \tag{3}$$

where $T()$ is some operator regularizing the pixel intensities, and λ is some positive constant lying between 0 and 1. We shall note from now on the total flux of an image O as :

$$F(O) = \sum_{s \in S} O_s$$

From what precedes, the total flux evolves as :

$$F(O^{(n+1)}) = (1-\lambda)\ F(D) + \lambda\ F(T(O^{(n)}))$$

When the operator $T()$ is chosen so that it preserves the total flux *i.e.*

$$F(T(O^{(n)})) = F(T(O^{(n-1)}))$$

then iteratively :

$$F(O^{(n+1)}) = F(O^{(n)}) \dots = F(O^{(1)}) = F(D)$$

i.e. total flux is preserved, provided that the initial guess $O^{(1)}$ has the same total flux as the observation D.

We can for example choose for the preserving total flux operator $T()$ any convolution filter associated with a normalized matrix R, for example a Gaussian filter whose standard deviation describes its spatial extension, or more simply a nearest-neighbor average filter, as will be used in the next section. The FPR algorithm takes now the form :

$$O^{(n+1)} = (1-\lambda)O^{(n)}\left[\frac{D}{H*O^{(n)}}\right]*H^T + \lambda R * O^{(n)} \tag{4}$$

Thus at each step the current pixel intensity will depend in a regularizing manner on its neighboring ones, according to the magnitude of parameter λ (for $\lambda = 0$ the FPR gives back the RL algorithm). It is also obvious that positivity is preserved when $0 \le \lambda \le 1$.

4 . Results

We have to choose the range of regularization operator $T()$. In the case of the small image of Titan we use the filter matrix R :

$$R = \begin{bmatrix} 0 & 0.25 & 0 \\ 0.25 & 0 & 0.25 \\ 0 & 0.25 & 0 \end{bmatrix}$$

The parameter λ is kept constant throughout all iterations.

The image of Titan (Fig. 1), was acquired with the adaptive optics system ADONIS installed at the ESO 3.6 m telescope in La Silla (Chile). The resolution is 0.05 arcsec/pixel. The image was acquired at 2.04 μm, where the methane is transparent, with a narrow-band filter, so it could be possible to see more details of surface. The PSF was measured by the system two minutes before the image acquisition. The image has been corrected for systematic effects.

The isophot contours correspond to 0.98, 0.95, 0.9, 0.85, 0.82 and 0.4 of the maximum intensity for the Titan image.

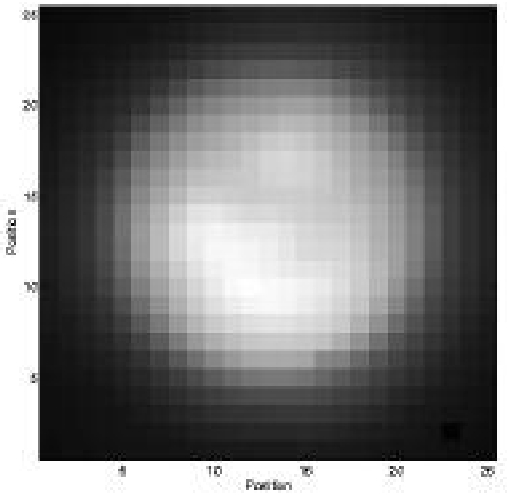

Figure 1 : Initial image of Titan 25×25

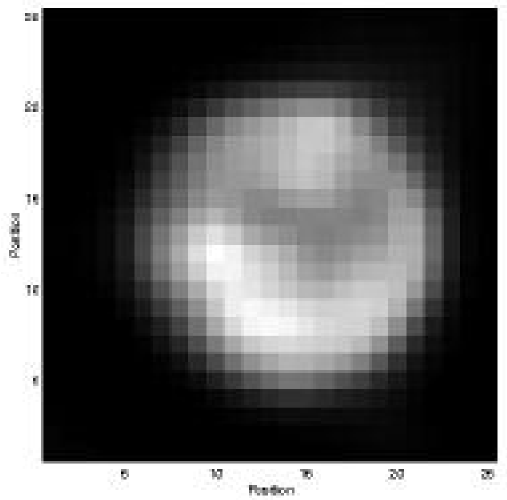

Figure 2 : Image of Titan after FPR restoration with $\lambda = 0.05$

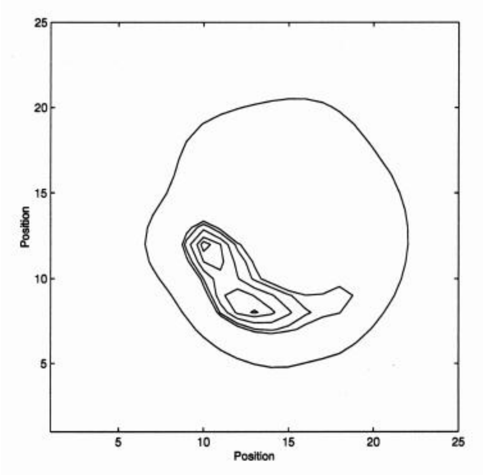

Figure 3 : Isophot contours corresponding to Figure 2

5 . Conclusion

A new method for restoration of astronomical images, named FPR, has been proposed. The mathematical presentation has been presented as well as the results for an image of Titan acquired in near infrared with the adaptive optics system ADONIS.

Acknowledgements

The authors are grateful to J.-P. Véran, A. Coustenis, M. Combes and all the people who work for the adaptive optics system ADONIS for the loan of observational material.

References

[1] Bratsolis, E., Sigelle M., A spatial regularization method preserving local photometry for Richardson-Lucy restoration, *Astronomy and Astrophysics*, **375**, no. 3, September I, 1120-1128, 2001.

CCD photometry of asteroids carried out at Poznan Observatory (Poland)

Michalowski T., Kwiatkowski T., Kryszczynska A., Hirsch R., Bartczak P., Michalowski J.

Abstract. *A small reflector with a CCD camera has been used for photometric observations of selected asteroids, with the aim of determination of their physical parameters. In the period 1997-2001, 52 asteroids were observed during 190 nights, providing 370 lightcurves of these objects.*

1 . Introduction

Ground-based observations, especially CCD photometry, provide the most abundant data on the physical properties of asteroids. Rotational periods, orientations of spin vectors and triaxial ellipsoid models can be determined from the brightness variation of the asteroids as they spin about their axes.

The photometric database contains lightcurves of about 1000 asteroids, but spin vectors have been determined only for less than 10% of them. In order to enlarge the sample of the objects with known spin vectors and shape models, we carried out CCD observations of the main belt asteroids. This observational programme was started in 1997.

2 . Instruments and data reduction

Our observational programme is carried out at the Borowiec Station of the Poznan Astronomical Observatory, 20 km south of Poznan. We use a small reflector (D = 0.4 m, F = 1.8 m) equipped with a ST-7 SBIG CCD camera placed at the newtonian focus. Its 765×510 KAF400 chip provides a field of view of $12' \times 8'$. A set of standard BVRI Bessel filters is suplemented by a «clear» filter of the same thickness, used for observations of fainter objects without refocusing the system.

This equippment allows us to do photometry of asteroids up to V=13 mag with VRI filters, and to V = 14 mag with a «clear» filter. These limiting magnitudes can be reached with 5 minute exposures, which give us a signal-to-noise ratio of 100.

Reduction of the CCD frames includes corrections for bias, dark current and flat-field. These procedures as well as the aperture photometry are performed with the CCLRC STARLINK package (http://www.starlink.rl.ac.uk). Due to rather poor weather conditions, we can observe selected asteroids during about 40 nights per year.

3 . Criteria for asteroid selection

Due to the small aperture telescope we choose asteroids brighter than V = 14 mag, which have been observed during at least one or two previous apparitions. The later means that rotational periods are known. In order to obtain a lightcurve covering most of a rotational cycle during a single night, we select objects with the periods shorter than 12 hours.

Determination of the physical parameters mentioned above is done according to the method described by Michalowski (1993). It takes as an input the magnitudes, amplitudes, and epochs of maxima of lightcurves from at least 3-4 oppositions. The output consists of sidereal periods, coordinates of spin axes and a/b and b/c parameters of asteroid shapes, obtained in a simultaneous least-square fit.

4 . Lightcurves obtained

In the period 1997-2001 we observed 52 selected asteroids during 190 nights, obtaining 370 lightcurves of these objects. Many of them did not cover the whole rotational cycle – in such case several of them where put together to form a composite lightcurve.

Full list of the observed asteroids is given below. The name of each asteroid is followed by the year of observation and the number of nights is given in parenthesis.

21	Lutetia	1998 (2)
24	Themis	1997 (5)
45	Eugenia	2000 (4) 52
52	Europa	1999 (7), 2000 (4)
73	KLytia	1999 (1), 2000 (3), 2001 (2)
85	Io	1997 (2)
90	Antiope	2000 (11) 2001 (10)
94	Aurora	1998 (3), 1999 (1)
115	Thyra	1998 (17), 2000 (3)
129	Antigone	1999 (2)
135	Hertha	1998 (6), 1999 (5)
160	Una	2000 (3), 2001 (1)
173	Ino	1997 (1), 1998 (5), 1999 (5)
174	Phaedra	1998 (2), 1999 (3), 2000 (4), 2001 (2)
184	Dejopeja	2000 (2)
192	Nausikaa	1998 (7)
193	Ambrosia	1999 (1)
218	Bianca	1997 (6), 2000 (2), 2001 (5)
225	Henrietta	2001 (2)
276	Adelheid	2000 (4)
283	Emma	1998 (3), 2000 (3), 2001 (2)
288	Glauke	1998 (15), 1999 (6), 2000 (50)
291	Alice	1999 (2)
350	Ornamenta	1999 (8)
360	Carlova	1997 (3), 1998 (4)
367	Amicitia	2000 (2)
376	Geometria	1999 (7)

377	Campania	1999 (4), 2001 (4)
378	Holmia	1999 (2), 2001 (2)
382	Dodona	1998 (4), 1999 (3), 2001 (2)
386	Siegena	1998 (4), 1999 (9)
404	Arsinoe	1999 (5)
416	Vaticana	1998 (5)
417	Suevia	2001 (3)
423	Diotima	2001 (3)
451	Patientia	1998 (4)
505	Cava	1997 (1)
556	Phyllis	2000 (2)
600	Musa	2001 (1)
665	Sabine	1998 (3), 1999 (1), 2001 (2)
690	Wratislavia	1998 (3), 2000 (1)
699	Hela	1999 (3)
771	Libera	1999 (2)
825	Tanina	1999 (8)
895	Helio	1999 (6) 2000 (2), 2001 (1)
937	Bethgea	2000 (3)
984	Gretia	1999 (3)
994	Otthild	2001 (5)
1572	Posnania	1999 (4)
2156	Kate	2001 (3)
3492	Petra-P	1998 (1)
1998	SF36	2001 (3)

5 . Conclusion

We have shown that a useful observational programme can be carried out with a small telescope equipped with an inexpensive CCD camera. Even in rather poor weather conditions, this equipment gives us valuable data for asteroid model determinations.

Acknowledgements

The observational programme presented above has been partially supported by the Polish KBN Grant 2 P03D 007 18.

Reference

Michalowski, T., 1993, Poles, shapes, senses of rotation, and sidereal periods of asteroids, *Icarus*, **106**, 563-572.

CCD lightcurves of several asteroids during their last apparitions

Apostolovska Gordana, Borisov Galin

Abstract. *CCD photometry of asteroids have been carried out since November 1993 at the Bulgarian National Astronomical Observatory - Rozhen, using 2m RCC telescope and since July 2000 using a 0.50m/ 0.70m Schmidt telescope equipped with a CCD camera ST-8E. Possibilities of further photometric investigations will be discussed.*

1 . Instrumentation

The data were obtained with CCD camera Photometrics CE200A, comprising $1024 \times 1024 px^2, 24 \mu m$ attached to 2m RCC telescope and CCD camera SBIG ST-8E Kodak KAF-1602E, comprising $1530 \times 1020 px^2, 9 \mu m$ attached to 0.50m/0.70m Schmidt telescope at the National Astronomical Observatory, Rozhen. These combinations give fields of view $5'.26 \times 5'.26$ and $18'.35 \times 27'.52$, respectively.

2 . Observations

Basic data for the observation are shown in Table 1.

Table 1: Geometrical conditions during the observations

Object	Date	Phase, Θ	m_V	Telescope	CCD
(7072) Beijindaxue	1998 12 25	00.4	17.6	2m RCC	CE200A
(1019) Strackea	2001 06 17	30.5	15.3	2m RCC	CE200A
(1019) Strackea	2001 06 26	31.5	15.4	Schmidt	ST-8E
(3443) Leetsungdao	2001 08 21	15.9	14.6	Schmidt	ST-8E
(509) Iolanda	2001 08 20	09.1	12.7	Schmidt	ST-8E

3 . Data reduction

3.1. Preliminary reduction

- Bias (dark frame) subtraction. For this purpose master biases (dark frames) are used (Howell S. B., 2000);
- Flat fielding. Twilight and dawn sky flat fields are used for the master flat which has precision < 1%;
- Cosmic rays removal. For this purpose BUIE acre procedure is used (Buie, M. W., 1998).

3.2. Aperture photometry and lightcurve analysis

For photometric measurement we use CCDPHOT software (M. W. Buie, 1998), which allows making aperture photometry. For lightcurve analysis - Asteroid Photometric Catalog Software (APC) (Lagerkvist et al, 1993), which produce composite lightcurves from several nights, calculate rotational period and also can make Fourier analysis fitting procedure of the lightcurve.

4 . Results

Lighturves are derived from on-chip differential magnitudes between asteroid and comparison stars. For asteroids Strackea (1019) and Leetsungdao (3443) the composite lightcurves and preliminary calculations of synodic period are made (Fig. 1 and Fig. 2, respectively).

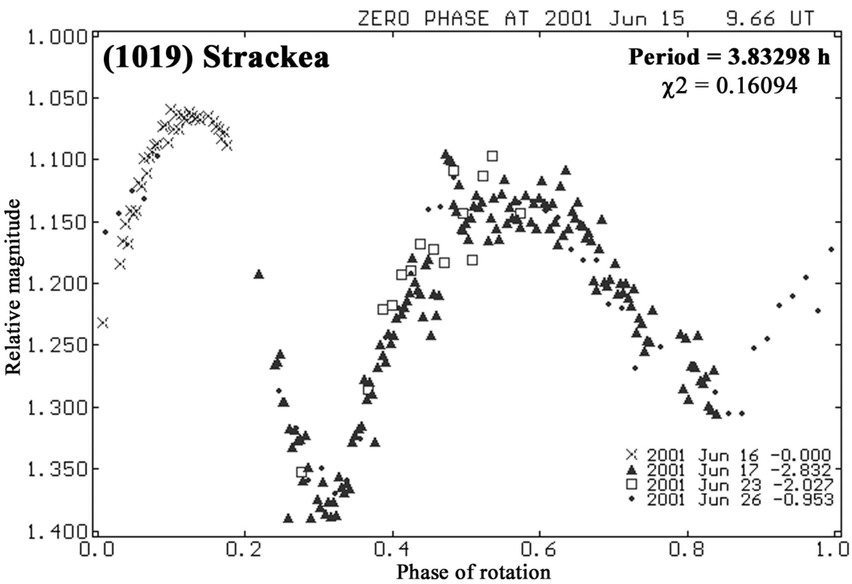

Figure 1 : Lightcurve of asteroid (1019) Strackea

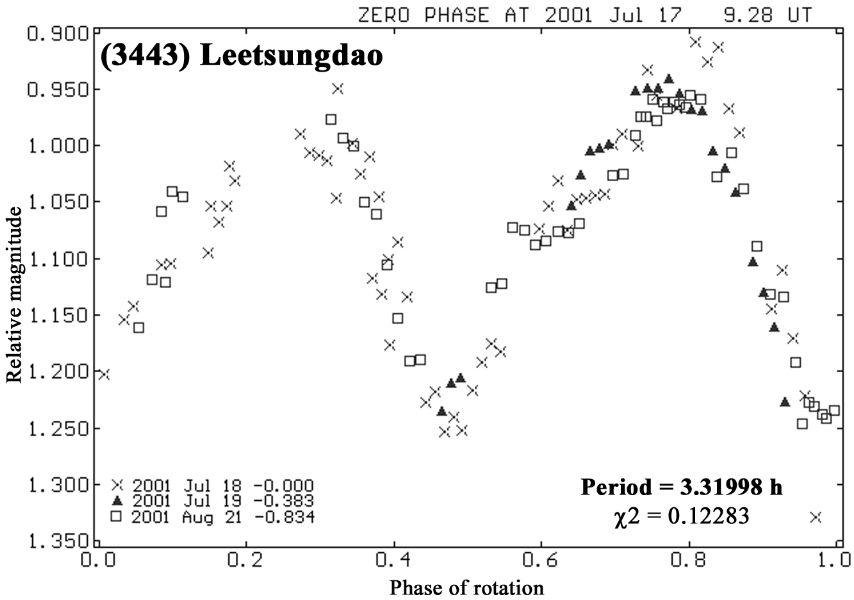

Figure 2 : Lightcurve of asteroid (3443) Leetsungdao

For one of them (1019) we have observations from four different nights with two different telescopes and these results are more reliable. The other asteroid (3443) was observed three night, but there was covered more than one period on two of them 18 July 2001 and 21 August 2001.

Single night partial lightcurve of (7072) Beijindaxue suggesting a period of ~ 10 hours. Period for (509) Iolanda was reported to be $12^h.306$ and in one night half of the rotation cycle has been covered.

All lightcurves are obtained with observations in *V* band. Also images in *B, R* and *I* filter for colour index determination are made. According to the sensitivity of the camera observing in U band is meaningful only for very bright asteroids ($m_v < 14$). In order to transform observation to a standard magnitude scale standards from the catalogue of Landolt (Landolt, A., 1992) were observed.

5 . Strategy of observations and data reduction

In the lightcurves of asteroids (509) Iolanda and (7072) Beijindaxue[1] (Fig. 3) are visible holes which appeared because during the time of observation images of standard fields were taken. As everyone can see, these holes in lightcurves are obstructions for lightcurve analysis. Because of this observing program need to be revolved very well before observations. For example standard fields need to be chosen so that the best time for their observations to be just at the beginning and at the end of observations. If we have possibility to chose such standards we can eliminate this holes in lightcurves and after this we can measure rotational period with much better accuracy. The other thing that we can do for obtaining good results is somehow to minimize errors as much as possible. The one of the most important thing for this is obtaining images with better S/N ratio. Often in asteroids observation this is impossible, because of their

1. The observations were made with the help of the other colleagues from section Solar System of Institute of Astronomy. Special thanks to Dr. Violeta Ivanova.

proper motion. For better S/N ratio we need to obtained images with long exposure, but then asteroids will look like tracks. Because of this we need to combine several images with smaller exposure, as settle them by asteroid position. For this purpose we subtract sky locally around the asteroid and then gather frames. After this procedure we have images with many tracks of all the stars and good starlike asteroid. In such a way we have good S/N ratio about photometry of asteroid. We also can make the same for the stars in the field of view and to use some of them for comparisons. This settle-procedure allow us better lightcurve analysis of faint and fast asteroids.

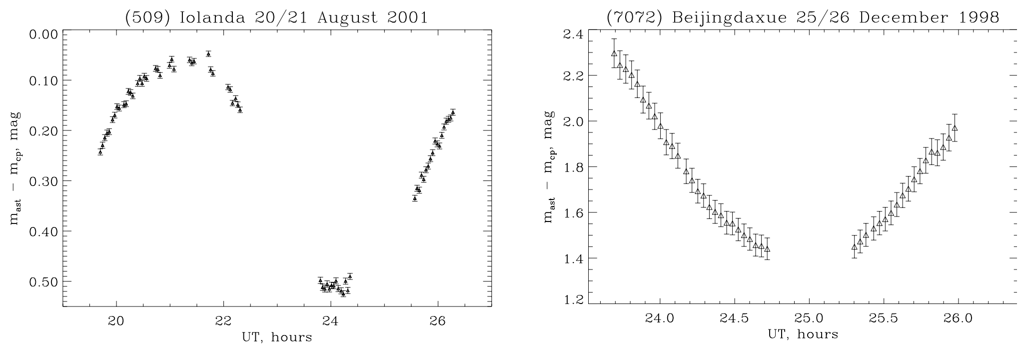

Figure 3 : Lightcurve of asteroid (509) Iolanda and (7072) Beijindaxue

6 . Conclusion

We have presented composite lightcurves and preliminary calculations of synodic period for two asteroids (1019) and (3443), as well as two partial differential lightcurves for (7072) and (509). No previous published periods of asteroids (7072) Beijindaxue, (1019) Strackea, and (3443) Leetsungdao have been found so far. The transformation to the *U BV RI* standard system will be performed with a software PDP (Photometric Data Processing) (Denchev, P., 2000). This program was used for the reduction of photoelectric data taken in a UBV photometric system and should be modified for the reduction of CCD photometric data.

Acknowledgements

We are especially grateful to Dr. Violeta Ivanova for allowing us to include her previously unpublished data on the asteroids.

References

Howell, S. B., *Handbook of CCD Astronomy*, Cambridge Univ. Press 2000.

Buie, M. W., 1998 July 21, http://www.lowell.edu/users/buie/idl/ccdphot.html.

Lagerkvist. *et al.*, 1993, *APC*, 3th Update.

Landolt, A. U., 1992, *AJ*, **104**, 340-371.

Denchev, P., Shkodrov, V., Ivanova. V., 2000, *P&SS*, 983-986.

ADAS : Asiago-DLR Asteroid Survey

Barbieri Cesare, Calvani Massimo, Claudi Riccardo, Hahn Gerhard, Hoffmann Martin, Mottola Stefano, Pignata Giuliano, Salvadori Luciano

1 . Introduction

The project to install a CCD camera on the S67/92 cm Schmidt telescope at Cima Ekar is a joint collaboration between the Department of Astronomy and the Astronomical Observatory of Padova on one side, and DLR Berlin on the other. The main scientific driver is the discovery and follow up of asteroids and comets (in particular NEOs). This paper represents a status report of the first year of operations of this project.

DLR has provided the SCAM-1 camera (see Fig.1), which can be operated both in Time-Delay Integration mode and in stare mode; the software for image acquisition and quick look; the software for astrometry and automatic detection of moving objects (Rackis). Photometry and centroiding of all stars on the frame is accomplished by using Sextractor, a public domain software package developed by E. Bertin and S. Arnouts (1996). The detector is a LORAL 2048×2048 front-illuminated CCD with a pixel size of 15×15 μm ($1''.44 \times 1''.44$ on the sky), and covers an area of 49×49 arcmin (0.67 sq deg). In TDI mode the effective exposure time for each star is of 196 s at the equator. The camera is equipped with a precision shutter, the shortest exposure time being 0.1 sec. The chip is refrigerated by a two-stage cooling device, where the primary stage is a Peltier cooler and the secondary one consists of a closed-circuit liquid refrigerator. The CCD operational temperature is –63°C.

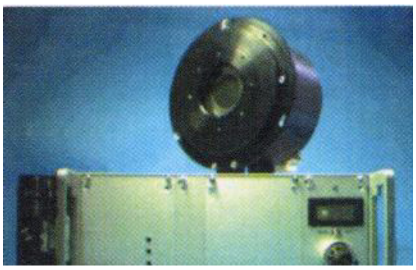

Figure 1 : The SCAM-1 camera system

Figure 2 : The SCAM camera head and its electronics attached to the NW side of the S/67-92cm telescope at Cima Ekar

2 . The First Phase, 20 Dec. 2000 – 20 Feb. 2001

During the first testing phase we used a flat metal secondary mirror in the Schmidt-Newton configuration. Although the optical quality of this mirror was not optimal we could automatically detect objects as faint as V=20.0 in 80 s exposure time. An example of an image triplet is shown in Fig. 3. In this first part of the ADAS program, we have mainly observed in guided mode. The following figures summarize the obtained data:

Total number of asteroid detections : 374
Covered field : 33.3 sq. deg.
Number of detected asteroids per sq. deg. : 11.2
Smallest detected angular rate : 3.9 arcsec/h.
Smallest detected angular displacement : 1.6 arcsec

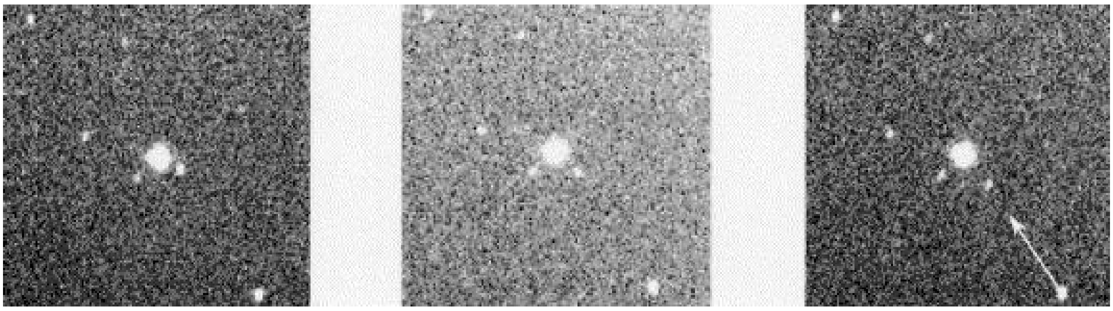

Figure 3 : Image sequence of asteroid (8965) Citrinella (V=19.03), exp. time 80 s

3 . The second phase, since 21 Feb. 2001

The second phase of ADAS started on 21 Feb 2001, with the metal flat mirror being replaced by a glass mirror, significantly improving the optical quality. The alignment of the CCD columns along the hour angle was also improved, so that the TDI scan mode could be implemented.

With the TDI technique and 30 min long scans, we cover a field of 6.15 sq. deg. 3 times in 1.7 hours, corresponding to approximately 3.6 sq. deg./h. In winter time (10h observing runs), the area covered per night would be 36 sq. deg.; in summer time (6h observing runs) the total surveyed field will be of 21.6 sq. deg.

Here are the results obtained from Feb. 21st to date (End of September 2001):
Total number of asteroid detections: 652
Covered field: 56.3 sq. deg
Number of detected asteroids per sq. deg.: 11.6
Smallest detected angular rate: 4.5 arcsec/h.
Smallest detected angular displacement: 2.5 arcsec

Table 2 and Fig. 4 provide an estimation of the astrometric precision achieved in the second phase. The residuals have been calculated only on numbered asteroids.

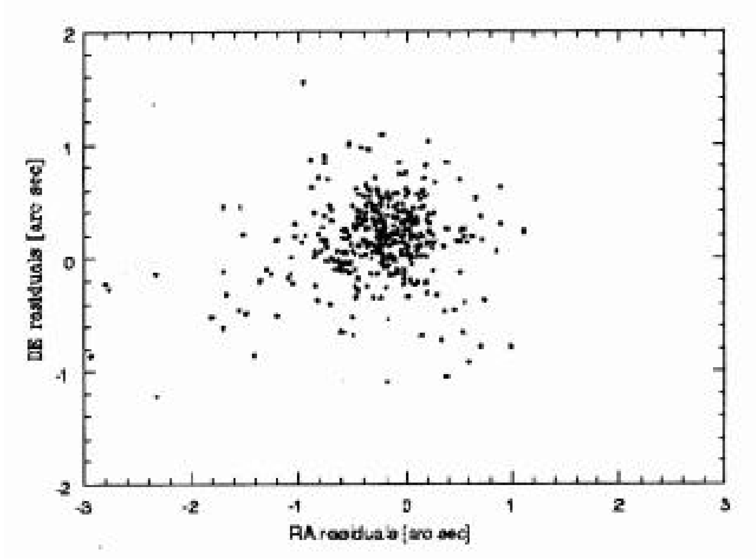

Figure 4 : The distribution of the astrometric residuals in the second phase

Table 1: The astrometric quality obtained in the second phase

Residuals (arcsec)	N° of observations	Percentage
< 0.2	52	14.3 %
< 0.5	189	52.1 %
< 1.0	319	87.9 %
< 2.0	358	98.6 %
> 2.0	5	1.4 %
All observations	363	

Table 2

Average RA residual	-0.27 ± 0.54 arcsec
Average DE residual	0.15 ± 0.35 arcsec
Average total residual	0.56 ± 0.43 arcsec

4 . Overall Results till end of September 2001

Six batches with the positions of the detected asteroids have been submitted to the Minor Planet Center, who assigned the observatory code 209 to ADAS. Thirty-eight objects have been preliminarily designated as ADAS discoveries. Table 3 provides orbital information on them.

Table 3 : Asteroids discovered by ADAS

Asteroid	Orbit	Orbital clas.	Asteroid	Orbit	Orbital clas.
2001 AC53	None	-	2001 FT167	8-day arc	MAIN BELT
2001 CF48	None	-	2001 FU167	None	-
2001 CH48	None	-	2001 FW167	None	-
2001 CJ48	None	-	2001 FN168	31-day arc	MAIN BELT
2001 CL48	None	-	2001 FP168	3-day arc	MAIN BELT
2001 CO48	None	-	2001 FR169	4 opps 1992-2001	MAIN BELT
2001 CP48	None	-	2001 FS169	None	-
2001 CA49	None	-	2001 FT169	7-day arc	MAIN BELT
2001 DN106	58-day arc	MAIN BELT	2001 FE185	None	-
2001 DP106	3 opps 1998-2001	MAIN BELT	2001 FF185	None	-
2001 DQ106	None	-	2001 FG185	None	-
2001 DW106	None	-	2001 FH185	None	-
2001 DX106	None	-	2001 FJ185	None	-
2001 DY106	None	-	2001 FH191	None	-
2001 DZ106	None	-	2001 FJ191	None	-
2001 DA107	None	-	2001 FK191	None	-
2001 DB107	None		2001 FY191	None	-
2001 FF154	24-day arc	MAIN BELT	2001 FZ191	None	-
2001 FG154	25-day arc	HILDA	2001 FA192	None	-

Fig. 5 shows the magnitude distribution of all 1161 ADAS detections. The faintest detected asteroid was 2001 FE168, V=21.0. About 23.0% of the detected asteroids have a magnitude > 19.5.

5 . Observing at small solar elongations

Several studies (Boattini and Carusi 1998, Michel *et al*. 2000) have drawn attention to the presence of an observational bias against the discovery of Aten asteroids, which spend most of their time at small solar elongations. This bias is mostly due to the fact that it is difficult to observe close to the Sun, which leads the major survey programs to concentrate on the opposition region. For this reason we have started observing at small solar elongations ($E \leq 90°$). A further motivation for this choice is the possibility to discover the postulated, but not yet detected, inner Earth objects, whose orbits are entirely lying within the Earth's orbit.

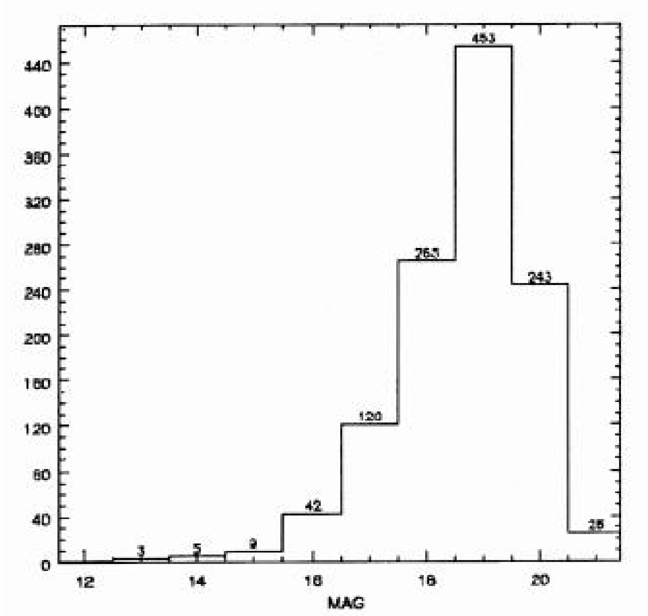

Figure 5 : The magnitude distribution of all detected asteroids

Table 4 : Small solar elongations areas observed till now

Ecliptic latitude	λ_{field}-λ_{sun} deg	Surveyed sq deg
-15° < β < 15°	[50-60]	3.9
	[70-80]	10.5
	[80-90]	4.7
β > 15°	[40-50]	0.7
	[50-60]	9.6
	[70-80]	6.7

6 . Further developments

Several improvements are being considered:
- installation of a filterwheel for color photometry
- full automatization of the telescope and dome, to improve the observing efficiency.

References

Barbieri, C., Pertile, V., Rampazzi, F., Caporali, A., Dallaporta, G.F. 1993, *A new determination of the astronomical and geodetic coordinates at Asiago and Cima Ekar Observatory*, Atti e Memorie della Accademia Patavina, **vol. CV parte II**, pag. 85.

Bertin, E., Arnouts, S. 1996, *Sextractor: Software for source extraction*, Astron. & Astrophys. Suppl. **v. 117**, pp.393-404.

Boattini, A., Carusi, A., 1998 *Aten: Importance among Near-Earth-Asteroids and search strategies,* Vistas in Astronomy **Vol. 41**, No. 4, pp. 527-541

Michel, P., Zappalà, V., Cellino, A., Tanga, P. 2000, *Estimated Abundance of Aten and asteroids evolving on orbits between Earth and Sun,* Icarus, **Volume 143**, Issue 2, pp. 421-424.

Shape Determination of the Asteroid (6053) 1993 BW1 *(abstract)*

Durech Josef

A method for determining asteroid shape from its lightcurves is presented. Asteroid shape was approximated by a polyhedral model made of 1000 triangular facets. Rotation around the axis of maximal momentum of inertia and the uniform albedo were assumed. A trial-and-error method was used to derive the shape which gives the best possible fit between observed and computed lightcurves. There are two different shapes for two pole directions (180 deg, 6 deg) and (354 deg, -14 deg) in ecliptic coordinates. An estimation of the Hapke's parameters describing the surface optical scattering properties is also given.

What can we learn from the lightcurves of freely precessing asteroids? *(abstract)*

Kryszczynska Agnieszka, Kwiatkowski T., Breiter S.

This paper presents results of modelling light variations of freely precessing asteroid, assuming its ellipsoidal shape and a geometric light scattering law. The method is based on numerical integration of Euler equations combined with the explicit expression of an asteroid's brightness as a function of Euler angles. We discuss what parameters of the asteroid rotational state can be obtained based only on their lightcurves.

Asteroid density; an overview

Birlan Mirel

Abstract : *This paper gives an overview of the present knowledges of the density of minor planets. The importance of physical properties it is underlined not only as a key to understand the origin and evolution of this population but also to constrain the initial parameters of the planetary nebula which will explain also the presence of those objects into the solar system. A synthesis of asteroid densities as well as possibles correlations of the density through the asteroid taxonomic system are also presented.*

Keywords: *asteroid, density, astrometry, taxonomy.*

1 . Introduction

Our recent studies concerning the asteroids consolidate the hypothesis of remnant planetesimals from the early solar system formation which, by mutual collisions and gravitational effects of major planets, evolved through the present population.

The density (as well as the gradients toward the nebula) remains one of the key role parameter of the primary planetary nebula. For this reason each aspect which could constrain their initial value must be taken into account. The asteroids (at least a major part of them) are objects on which the global mineralogy does not change since their formation, during the early stage of the protoplanetary nebula. The knowledge of the asteroid density will constrain the starting values of densities in the protoplanetary nebula.

2 . Mass, volume, density - what it is known ?

The three parameter are not independent. Different observation techniques could be used to obtain two of them : by gravitational perturbation we obtain the mass of the perturbed asteroid, the occultation and CCD imaging estimate the shape and volume, radar, spectroscopic observations, and comparative mineralogy are needed in order to obtain a value of asteroid density. High accuracy values of the shapes and asteroid masses are obtained through intruments embarqued on space missions, and/or space instruments: NEAR, Galileo, Hubble,…

Nowdays more than 33000 asteroids are on the astrometric database. Contrary this large number of objects, the density is not a physical parameter that can be found on each paper concerning the asteroids. This lack of papers concerning the asteroid mass (volume, density) is due to the difficulties of a good estimations of them. Moreover, following different authors, for the same object we found estimations and finally, divergent conclusions are generated. Which is the good estimation?

The error which affect the shape of the asteroid has a great importance inside the error of the density (if we assume a spherical body, the volume is proportional to the cube of the radius). For this reason, careful estimation of shapes (space missions offers an ideal instrumental support) must be taken into account.

Table 1 presents the compilation of densities of asteroids based on the masses and volumes published on the literature. Even if this table contains data obtained from both ground based observations and space experiments, only 19 asteroids could be counted. For the major part of the mass determination using ground observations, the IMPS [9] diameter values were considered in order to compute the volume. The exceptions are 1 Ceres and 4 Vesta on which Hubble observations were used to determine theirs volumes [7] and [10]. The volumes and masses used for the asteroids observed trough spacecrafts are the same published on the references. Except data obtained from space missions, all the asteroids belong to the major one (D>100 km) of the main belt.

The last column of Table 1 contains the taxonomic type [3] of each asteroid, in order to compare the density values with different mineralogy assumed to different taxonomic class. The graphic of densities versus semi-major axis is presented in Figure 1. For each asteroid, the taxonomic type was annotated on the figure, in order to distinguish possible correlations between the assumed mineralogy and the density.

Table 1 : Recent characteristics of asteroids

AST.	DIAMETER (km)	MASS (10^{18} kg)	VOLUME (10^{15} m^3)	a (u.a.)	DENSITY (10^3 kg/m^3)	REF.	TAXON
1	2a = 969.6 ± 10.2	873 ± 8.7	331.3 ± 11.9	2.7666	1.98 ± 0.09	[7];[4]	G
1	2b = 932.8 ± 11.8	946.6 ± 4.7			2.14 ± 0.09	[7];[13]	G
2	498.1 ± 18.8	316.2 ± 32	64.7 ± 7.6	2.7723	4.8 ± 1.07	[4]	B
4	468 ± 26.7	336.1 ± 50	78 ± 3	2.3614	4.3 ± 0.3	[10];[4]	V
6	185.18 ± 2.9	13.7 ± 4.4	3.32 ± 0.15	2.4252	4.28 ± 1.51	[6]	S
10	407.1 ± 6.8	93.4 ± 46	35.3 ± 1.8	3.1384	2.64 ± 1.44	[8]	C
11	153.3 ± 3.1	5.13 ± 0.25	1.88 ± 0.12	2.4530	2.72 ± 0.31	[12]	S
15	255.3 ± 15	8.35 ± 2.2	8.71 ± 1.28	2.6438	0.95 ± 0.39	[4]	S
15	255.3 ± 15	25.05 ± 5.96	8.71 ± 1.28	2.6438	2.87 ± 1.1	[6]	S
16	253.2 ± 4.0	17.3 ± 5.1	8.5 ± 0.4	2.921	2.03 ± 0.69	[14]	M
20	145.5 ± 9.3	4.77 ± 0.78	1.61 ± 0.33	2.4094	2.96 ± 1.09	[1]	S
45	214.6 ± 4.2	6.02 ± 0.3	5.17 ± ±±0.31	2.7203	1.16 ± 0.13	[5]	C
52	302.51 ± 5.4	51.88 ± 17.5	14.49 ± 0.77	3.1003	3.58 ± 1.4	[6]	C
88	200.57 ± 5.0	14.71 ± 2.58	4.22 ± 0.31	2.7724	3.48 ± 0.87	[6]	BCG
121	209.0 ± 4.7	9.35 ± 1.58	4.78 ± 0.23	3.4412	1.95 ± 0.42	[14]	C
243	SPACE MISSION ESTIMATION			2.8596	2.6 ± 0.5	[2]	S
253				2.6472	1.34 ± 0.02	[11]	C
433				1.4583	2.9 ± 0.4	[15]	S

Table 1 : Recent characteristics of asteroids

444	159.57 ± 13.1	7.16 ± 3.18	2.13 ± 0.52	2.7711	3.36 ± 2.31	[6]	C
511	326.07 ± 5.3	66.4 ± 4.77	18.14 ± 0.88	2.1902	4 ± 0.44	[6]	C
704	316.6 ± 5.2	69.6 ± 31.1	16.6 ± 0.8	3.0638	4.19 ± 2.08	[12]	C

3 . Conclusion

As it can be seen on the Table 1, it is still difficult to have a good approach on the asteroid density as long as both the mass and the shape of it are affected by large error-bars. For instance, the case of asteroid 704 Interamnia makes very difficult any conclusion that will match a carbonaceous chondrite (CI1/CM2) mineralogy with such a high density (even if it is affected by large error-bars).

Another example of divergent estimations concerns the asteroid 15 Eunomia. The density derived considering the mass proposed by Hilton [4] is a third part of those derived using the Michalak's [6] proposal of Eunomias' mass. The associate taxonomic type of this asteroid allow us to consider more realistic the mass estimation of the last mentioned author

The asteroid 16 Psyche belongs to a M–type asteroids which is associated (through spectral features and radar observations) to metallic (or chondritic entsatite) meteorites. The scientist explains the metal rich surface of Psyche by the evidence of a catastrophic collision of segregated planetesimals of the main belt. Thus, Psyche is a part of the nucleus which survived to the catastrophic collision. If we assume this hypothesis of 16 Psyche, their density two-three times lower than those of the metallic meteorites must be explained.

Another aspect which could be noted is the author-dependence of the density values. Michalak [6] compute the mass of asteroids 6, 15, 52, 88, 444, 511. On the Figure 1 it can be seen the systematic overestimation of densities derived from [6] for the C-type asteroids, comparative to densities of other C-type asteroids on the literature. Moreover, the mineralogy of a C-type asteroid (assumed to be the same as the CI1/CM2 meteorites) cannot fit to such high densities.

The small number of asteroids does not allow us a real statistic analysis. However, the density could distinguish between C and S-type asteroids. This result is important and proves that surface mineralogy could be representative in defining the sub-surface structure of an asteroid.

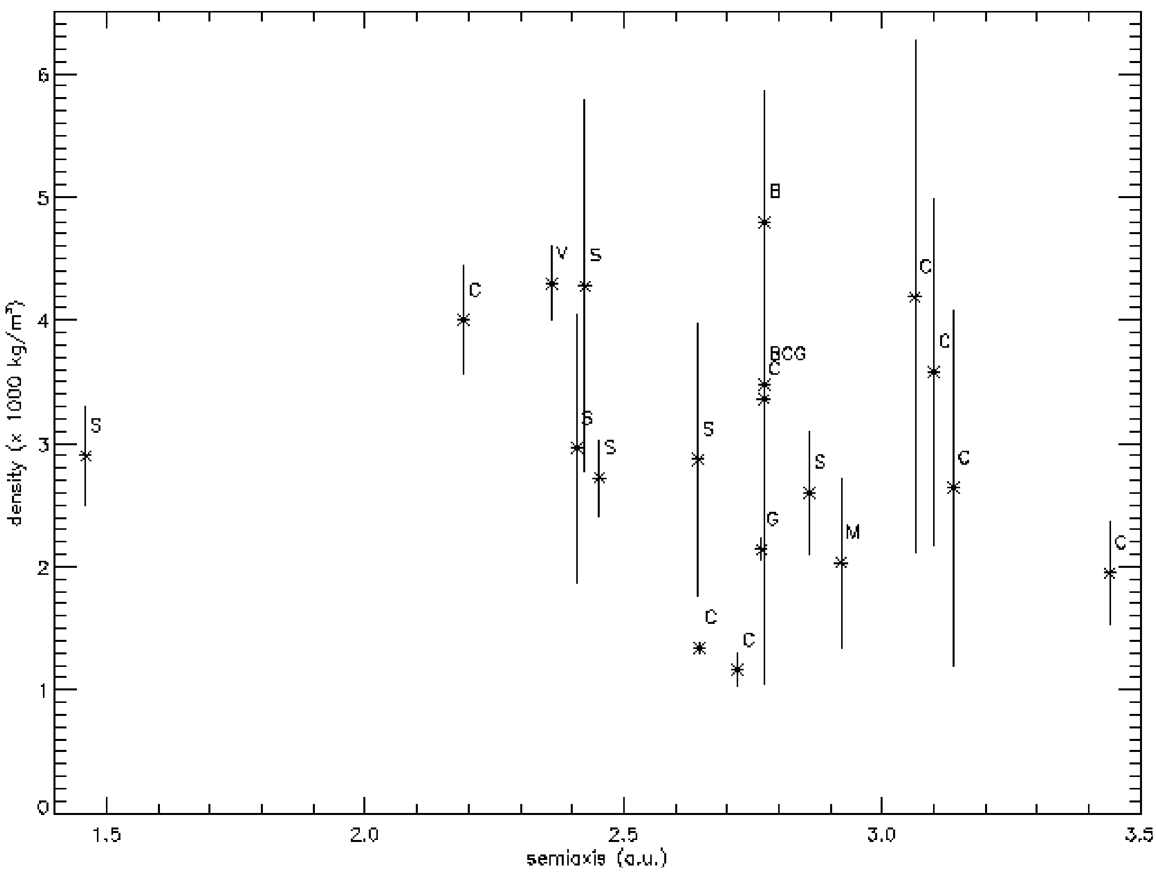

Figure 6 : Density of asteroids along the semi major axis of their orbits. For each asteroid the taxonomic type was annoted.

Acknowledgements

The author is grateful to LOC of Ceres 2001 for the successful meeting.

References

[1] Bange, J.-F., 1998, *A&A*, L1-L4.

[2] Belton, M. *et al.*, 1995, *Nature*, **374**, 785-788.

[3] Birlan, M. *et al.*, 1996, *Icarus*, 352-354.

[4] Hilton, J.L., 1999, *Astron.J.*, **117**, 1077-1086.

[5] Merline, W.J. *et al.*, 1999, *Nature*, **401**, 565-569.

[6] Michalak, G., 2001, *A&A*, **374**, 703-711.

[7] Parker, J.W. *et al.*, 2002, *Astron J.*, in press.

[8] Scholl, H. *et al.*, 1987, *A&A*, **179**, 311-316.

[9] Tedesco, E., 1992, *IMPS Technical Report*.

[10] Thomas, P.C. *et al.*, 1997, *Icarus*, **128**, 88-94.

[11] Veverka, J. *et al*., 1999 , *Icarus*, **140**, 3-16.

[12] Viateau, B., Rapaport M., 1998, *A&A*, **320**, 652-658.

[13] Viateau, B., Rapaport M., 1998, *A&A*, **334**, 729-735.

[14] Viateau, B., 2000, *A&A*, **354**, 725-731.

Eight Years Observing Asteroidal Appulses to Stars

Casas Ricard

When star occultations by asteroids are observed, there are very few occasions on which the observer actually sees the occultation. This means that at times an additional observation is needed to obtain a positive result when there is no occultation.

Eight years ago, in 1993, a bulletin of the European Asteroidal Observers Network (EAON) contained an article which caught my attention. It was about ways to determine the moment when minimum distance occurred between an asteroid and a star using visual methods, as if the parameters of a double star were being measured. At the time several kinds of CCD cameras were available on the market, all of which were accessible to amateurs and which had a software that enabled the observer to take these measurements in a simple way. After setting out observation protocol, Joaquín Vidal, of Monegrillo (Zaragoza, Spain), a member of the Grupo de Estudios Astronòmicos (GEA), carried out the first tests with a Santa Barbara Instruments ST-4 camera, which allowed him to optimize the method and prepare the necessary software for reduction.

The method consists of obtaining before and after images of the minimum distance between the asteroid and the star. The number of images to be taken depends, above all, on the reduction method that is used. If this is automatic (using IRAF), a large number of images can be taken. However, if the reduction has to be done manually, the observer should not take too many photos so as not to be overwhelmed when he has to reduce them using the camera's software: AstroArt, AVIS, etc.

Reducing the images is simple. The coordinates of the centroids of both the star and the asteroid must be determined with subpixel precision. The trajectory of the asteroid can be represented by taking the star as the centre of the coordinates, as shown in Figure 1. This trajectory can be adjusted by a regression line and on the basis of this, the minimum distance of the line at origin, at the star, can be determined. The time that this occurred can also be calculated. The astronomer thereby brings additional information to the phenomenon even though the occultation has not taken place.

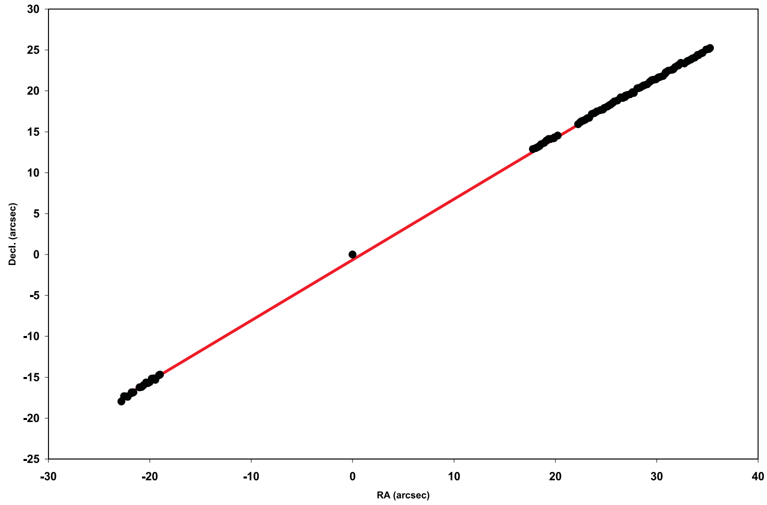

Figure 1 : Graph of the approach of 306 Unitas in August 27th, 2001.

We have been using this method for the last 8 years and we have been able to determine the minimum distance and the time this was produced on more than 140 occasions. The observations have been carried out from 5 observatories. 81 of these were done at the Teide Observatory (Tenerife), a professional observatory that depends on the Instituto de Astrof\'{i}sica de Canarias, using routine time (an hour a day for different observations) on the IAC80 telescope (http:$\backslash\backslash$www.iac.es), a telescope with 80 cm aperture and a CCD camera with a $1024 \times\ 1024$ Thomson chip cooled with liquid nitrogen. A further 42 observations were carried out at the Sabadell Observatory (Barcelona), an amateur observatory which has a telescope 50 cm in diameter and a CCD ST-6 camera of $375 \times\ 241$ pixels and a Peltier cooling system.

In order to check this method's reliability, here follows the comparison between the two positive observations made from the same installations from which the approximation observation was carried out.

The first was done on 15 December, 1999, in the Teide Observatory and involved the asteroid 814 Tauris. The occultation itself was observed using a self-guided camera in the telescope. The second one took place on 21 September, 2000, and involved the asteroid 336 Lacadiera. This occultation was observed visually at the Sabadell Observatory.

Table 1 and 2 show a comparison of the results of the two phenomena.

Table 1 : 814 Tauris – December 15th, 1999

	CCD Observation	TV Observation
Begin Occultation		21h 55m 59s72 ± 0s04
End Occultation		21h 56m 05s40 ± 0s04
Mean Time	21h 56m 02s ± 5s	21h 56m 02s56 ± 0s06
Occultation Duration		5s68 ± 0s06
Minimum Distance	0″04 ± 0″01	0″03

Table 2 : 336 Lacadiera - September 21st, 2000

	CCD Observation	Visual Observation
Begin Occultation		1h 57m 41s7 ± 0s2
End Occultation		1h 57m 49s0 ± 0s2
Mean Time	1h 58m 06s ± 4s	1h 57m 45s4 ± 0s3
Occultation Duration		7s3 ± 0s3
Minimum Distance	0″03 ± 0″02	0″02

The difference between the Mean Time obtained by the two methods is due at problems with the computer clock used to obtain the CCD images.

4 . Conclusion

• Temporal resolution. The CCD approximation method allows temporal resolutions to be reduced to a few seconds, whereas traditional methods allow for hundredths of second, whenever an occultation occurs.

• Spatial resolution. CCD enables observers to obtain arc resolutions of hundredths of second, while using traditional methods it is only possible to know the situation of the asteroid if the occultation occurs; there is added doubt concerning where the event occurs.

• The two methods – CCD and traditional – can be said to be complementary in positive events.

• In negative events, the CCD approximation method is undoubtedly superior, because, despite everything, it gives a «positive» result.

Parameters of catalogue orientations as obtained from observations of the selected minor planets at Nikolaev Astronomical Observatory

Gudkova L. A.

Abstract. *Photographic positions of 19 selected minor planets (SMP) obtained with the Zonal astrograph (F=2.04 m, D=0.12 m, field is 5°×5°) at Nikolaev Astronomical Observatory during 1961-1997 were reduced to the FK5 and ICRS systems. The average accuracy of minor planet positions is ±0.19 in FK5 and. ±0.16 in ICRS systems in both coordinates. (O-C) differences between observed and calculated positions of the 12 selected minor planets were used to calculate the mutual orientation parameters the FK5 and DE200, ICRS and DE200, ICRS and DE403 systems.*

1 . Introduction

The idea to use of bright minor planet observations for determination of the fundamental catalogue zero-point corrections was advanced by F. Dyson in 1928 and it was actively discussed in 30-th years of the last century [1]. It was supposed that star-like images of minor planets and night period of observations would be allowed to improve precision of minor planet positions as compared with observations of the big inner planets and Sun. As a result the precision of the determination of the zero-point corrections would be also improved.

It was obtained enormous number of the selected minor planet observations from 1935 up to now. These observations were used to define the orientation parameters of star catalogues $\Delta\alpha_0$ and $\Delta\delta_0$ and to study zonal periodical errors of reference catalogues. But using of the minor planet observations for this aim was not successful. Precision of the zero-point corrections by minor planet observations turned out to be worse than one of determination of the corrections by Sun and the big inner planets. Besides essential scatter of the zero-point corrections (especially for correction to origin of right ascensions) remained, both by observations of the same minor planet with different instruments, and by observations of different minor planets on the same instrument.

2 . Observations and reductions

The observations of SMP were started at Nikolaev Astronomical Observatory in 1961 when the Zonal astrograph was placed here. The photographic observations at Nikolaev were finished in 1998. Now CCD-observations are carried out on this instrument.

About 2.5 thousands of photographic observations of 19 SMP were obtained at Nikolaev from 1961 to 1997. Summery of these observations are given in Table 1. The way of observations and measuring of photoplates were kept unchanged during this entire interval. But the different reference catalogues such as Yale, AGK3, SAO, PPM and FOCAT were used during 36 years of the observations. Second, reduction algorithms and programs have been developed and modified by different authors and at different time. Therefore it was necessary all observations to reprocessed to same reference system using new reduction programs. As of 19 minor planets observed the 12 brightest SMP accounted for 95% of all observations then only the 12 SMP will be discussed below.

At the beginning all observations of the 12 SMP were reduced to the FK5/JD2000 system using reference stars from the PPM catalogue. After publicizing Hipparcos and Tycho catalogues we reduced these observations to the new International Celestial Reference System (ICRS) using dependences, obtained in previous reduction, and reference star positions from Hipparcos and Tycho catalogues (HT).

Table 1 : Observations of minor planets at Nikolaev observatory in 1961-1997

Minor planet	Observational period	Number of positions	Number of oppositions	T days	V deg
1 Ceres	1961–97	217	22	131	28
2 Pallas	1961–97	264	26	124	26
3 Juno	1961–96	245	25	119	26
4 Vesta	1961–97	241	23	122	31
5 Astraea	1983	4	1	9	3
6 Hebe	1961–97	226	23	119	31
7 Iris	1961–97	197	20	129	39
11 Parthenope	1961–97	196	20	122	32
15 Eunomia	1987–91	12	2	111	25
18 Melpomene	1962–97	212	20	115	32
25 Phocaea	1976–91	34	4	95	25
39 Laetitia	1962–93	237	24	106	23
40 Harmonia	1962–94	203	21	112	32
148 Hallia	1977	8	1	122	26
185 Eunike	1973	6	1	84	18
389 Industria	1991	4	1	34	8
433 Eros	1975	11	1	46	26
532 Herculina	1975–92	68	9	102	24
704 Interamnia	1974–90	65	7	109	20
All observation		2450	251		

Because the accuracy of the Tycho proper motions is generally too low to calculate positions at other epochs with sufficiently accuracy the proper motions were taken from ACTRC catalogue. In result we obtained two rows of the minor planet observations in FK5 and in ICRS systems. The observed positions (O) were compared with positions computed in IAA (Institute of Applied Astronomy, St.-Petersburg) by planet theories DE200 and DE403 (C) [2]. The averaged accuracy of minor planet observations at Nikolaev is ±0.19 for FK5 and. ±0.16 for ICRS systems in both coordinates [3, 4].

3 . The orientation of the catalogue and dynamical reference systems from the observations of the minor planets

The 2328 positions of the 12 selected minor planets reduced to the FK5 and ICRS systems were used to determine the mutual orientation parameters the FK5 and DE200, ICRS and DE200, ICRS and DE403 systems. We used well-known equations of two coordinate system tie where ε_x, ε_y, ε_z are the angles of rotation of the catalogue frame axes around the x, y, z–ones of the dynamical frame of reference:

$$\Delta\alpha = \varepsilon_x \, tg\delta\cos\alpha + \varepsilon_y \, tg\delta\sin\alpha - \varepsilon_z$$
$$\Delta\delta = -\varepsilon_x \sin\alpha + \varepsilon_y \cos\alpha - \Delta\delta_0$$

As the interval of the Nikolaev observations of minor planets is sufficiently long we included in equations (1) the terms depending on time ω_x, ω_y, ω_z:

$$\Delta\alpha = tg\delta\cos\alpha\,(\varepsilon_x + \omega_x (t - t_0)) + tg\delta\sin\alpha\,(\varepsilon_y + \omega_y (t - t_0)) - (\varepsilon_z + \omega_z (t - t_0)),$$
$$\Delta\delta = -\sin\alpha\,(\varepsilon_x + \omega_x (t - t_0)) + \cos\alpha\,(\varepsilon_y + \omega_y (t - t_0)) - \Delta\delta_0$$

in which $\Delta\alpha$ and $\Delta\delta$ are (O-C) differences between observed and calculated minor planet positions; ε_x, ε_y, ε_z are the initial values of rotation angles and ω_x, ω_y, ω_z, are the initial values of spin or angular velocities of rotation at the initial epoch t_0 = 1991 07 20.0 TDB (JD 2448439.5). $\Delta\delta_0$ is the constant systematic error of the catalogue declination frame and not connected to the rotation angles. The calculations have been done in each minor planet separately and on all observations together. The results are given in Tables 2, 3. The unit weight errors, σ_0 , are given in the last column of the tables. So far as the orientation parameters for ICRS and DE200, ICRS and DE403 are very similar the ones for ICRS and DE403 are presented here only.

Table 2 : Orientation parameters of FK5 and DE200/LE200 systems by observations 12 SMP at the epoch JD=2448439.5 (in mas).

Mainor planet	ε_x		ε_y		ε_z		ω_x		ω_y		ω_z		$\Delta\delta_0$		σ_0
1 Ceres	12	±21	–32	±17	–35	±13	5.6	±1.9	–2.9	±1.5	1.0	±1.2	–53	± 12	±161
2 Pallas	– 3	20	–18	18	–20	14	0.2	1.6	–0.8	1.5	–0.7	1.2	–35	12	171
3 Juno	19	20	33	21	–27	14	–0.3	1.8	1.7	1.8	0.2	1.3	–65	13	183
4 Vesta	– 2	19	8	18	–48	13	3.1	1.6	0.8	1.6	3.5	1.3	–109	12	179
6 Hebe	– 2	21	–13	22	–42	15	0	2.0	–1.8	1.9	3.0	1.3	–65	13	178
7 Iris	8	27	5	23	–46	18	8.0	2.2	–3.0	2.5	1.0	1.6	–53	15	198
11 Parthenope	16	28	– 9	25	–54	19	–0.6	3.1	0	1.7	2.3	1.5	–54	15	197
18 Melpomene	11	24	– 5	24	2	17	4.2	2.0	–1.3	2.1	0.4	1.4	–39	15	191
39 Laetitia	46	23	57	24	–46	16	4.0	1.9	–4.8	1.9	2.4	1.4	–65	14	202
40 Harmonia	20	30	16	28	–74	22	–0.4	2.4	1.6	2.1	2.3	1.7	–56	16	223

Table 2 : Orientation parameters of FK5 and DE200/LE200 systems by observations 12 SMP at the epoch JD=2448439.5 (in mas).

532 Herculina	13	40	−3	44	−65	28	−9.3	7.7	−6.0	9.0	6.1	5.7	−42	31	220
704 Interamnia	11	53	−37	48	−65	26	−2.1	8.0	−2.1	5.5	−6.7	4.2	− 8	40	190
All SMP	19	7	1	6	−39	5	2.3	0.6	0.2	0.5	1.5	0.4	−53	4	190

Table 3 : Orientation parameters of ICRS DE403/LE403 systems by observations 12 SMP at the epoch JD=2448439.5 (in mas)

Minor planet	ε_x		ε_y		ε_z		ω_x		ω_y		ω_z		$\Delta\delta_0$		σ_0
1 Ceres	21	±16	−14	±13	−36	±10	5.3	±1.5	−1.8	±1.2	0.2	±1.0	22	±9	±125
2 Pallas	−11	16	− 10	15	− 44	11	−1.8	1.3	−0.4	1.2	1.6	0.9	25	10	135
3 Juno	− 6	16	− 10	17	− 45	11	−1.6	1.5	−0.6	1.5	2.9	1.1	20	10	148
4 Vesta	− 4	14	− 12	13	− 44	10	1.5	1.4	0.5	1.2	2.5	1.0	− 24	9	133
6 Hebe	10	18	− 19	19	− 45	13	1.4	1.7	−1.8	1.6	2.7	1.2	16	11	155
7 Iris	8	23	6	20	− 49	15	2.6	1.9	−1.0	2.1	2.9	1.3	19	13	169
11 Parthenope	13	25	− 23	22	− 38	17	2.3	2.8	−1.3	1.6	1.4	1.3	40	14	175
18 Melpomene	15	21	− 2	21	− 38	15	3.1	1.7	−2.6	1.8	1.3	1.2	26	13	164
39 Laetitia	20	20	19	21	− 51	14	3.3	1.7	3.1	1.7	2.9	1.2	28	12	177
40 Harmonia	16	26	7	24	− 48	19	1.2	2.3	0.4	1.8	1.6	1.5	46	14	194
532 Herculina	5	27	− 11	30	− 42	19	−5.4	5.3	0.4	6.2	3.9	4.0	8	22	152
704 Interamnia	34	37	− 21	34	− 49	19	4.2	5.7	−3.2	3.9	1.6	3.0	34	28	136
All SMP	9	6	− 7	5	− 43	4	1.3	0.5	−0.6	0.5	2.1	0.4	22	3	158

As one can see from tables the values of orientation parameters ε_x, ε_y. ε_z are in a good agreement for ICRS−DE403 system and ones have large scatter for FK5−DE200 by the observations of the different minor planets.

4 . Influence of systematic errors of the reference catalogue on determination of the orientation parameters

To define reason of the large scatter of parameters ε_z, $\Delta\delta_o$ for FK5−DE200 we investigated star position differences between the PPM and HT catalogues for all reference stars (8060) used when the reduction of the 12 minor planet observations were made. Since systematic errors in HC and TC are believed to be negligible any difference between HT and PPM positions can be consider as errors in the PPM star positions. The mean differences (PPM−HT) (solid line) in right ascension (left) and in declination (right) averaged in the observation zone for the each minor planets and parameters ε_z and $\Delta\delta_0$, which can be considered as the corrections to zero−points of the FK5 (dotted line) and ICRS (dashed line) systems are shown on Figure 1.

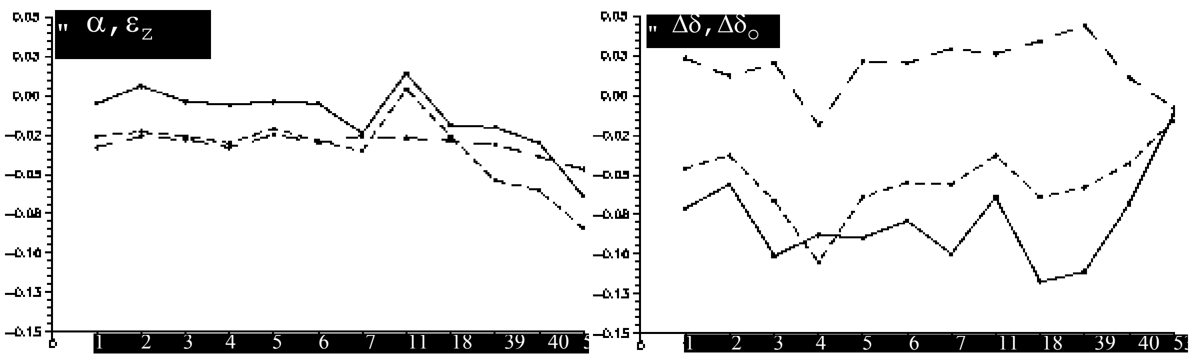

Number of minor planet   Number of minor planet

Figure 1 : Influence of the PPM catalogue systematic errors Δα, Δδ (1) on determination of orientation parameters ε_z (left) and $\Delta\delta_o$ (right) between catalogue and dynamical systems. FK5–DE200 (dotted line), ICRS–DE403 (dashed line).

As one can see on Fig.1 the scatter of the points for dashed line is insignificant. It testify about rather good taking into consideration of the systematic errors in the Nikolaev photographic observations of the selected minor planets. The solid line and the dotted line is in a good agreement on Fig.1. This fact can be considered as evidence of the influence systematic errors of the PPM catalogue on the determination of the orientation parameters between system of the PPM catalogue and dynamical system of reference given by the DE200 ephemeris. The anomalous value $\Delta\delta_o$ for Vesta possibly are caused by either irregular figure of Vesta or no taking into account of magnitude equation.

References

[1] Dyson, F. W., 1928, *Transactions IAU*, **3**, 227.

[2] Batrakov, Y. V., Chernetenko, Y. A., Gorel, G. K., Gudkova, L. A., Makarova, E. N., 1998, *Proc. of the Fourth International Workshop on positional astronomy and celestial mechanics*, Valencia, Spain, October, 7-11, 1996, Valencia, 3-10.

[3] Gorel, G. K., Gudkova, L. A., 2000, *Astron. Vestnik*, **34**, 4, 1-5.

[4] Gorel, G. K., Gudkova, L. A., 2000, Kinematics and Physics of celestial bodies, **16**, 5, 463-469.

Photographic and CCD Observations of Minor Planets from Valencia Observatory

García Alvaro López , Moraño Fernández Jose A., Yagudin Leonid, Martínez Angel Flores

Abstract. *Valencia Observatory holds a program of bright minor planets observations since 1985, in collaboration with Institute of Applied Astronomy (IAA) of St. Petersburg, Russia. Nearly 1000 film plates were taken with a 6 inches Grubb refractor (Figure 1, left) from Valencia until January 1998. Special hardware and software was developed for automatic measuring and reducing of plates. Since May 1998 a new refractor is operative at «Astronomical Centre of Alto Turia» (CAAT) and an advanced reflector telescope will be put at work in the next future.*

1 . New Observing Site (CAAT): Instruments and Observing Programs

CAAT is a joint venture of Valencia University (UV) and amateur «Asociación Valenciana de Astronomía» (AVA) to operate several telescopes at «Centro Astronómico del Alto Turia» (CAAT), an astronomical station 110 km from Valencia city. CAAT is under construction since 1996 at a high plateau 1.300 m over see level. The site is quite free of light pollution and has a very low humidity and about 280–300 clear nights per year. First telescope, a 30--20 cm. double astrograph of 3 meters focal length, constructed by Pulkovo Observatory (Kanaev et al. 1998), is operative since the beginning of 1998 (Figure 1, right). Photographic techniques have been used during the last two years, but CCD images are now obtained regularly. Automatic techniques for plate measurement, developed at OAUV since 1990, have been extended to detection and measurement of images on CCD frames. Pavilions and domes have been designed by OAUV-AVA members and have photographic and sleeping rooms and offices for telescope operation (Figure 2, left).

Figure 1 : Left : 6 inches Grubb refractor of OAUV (Valencia). **Right** : 30-20 cm double refractor of OAUV (CAAT)

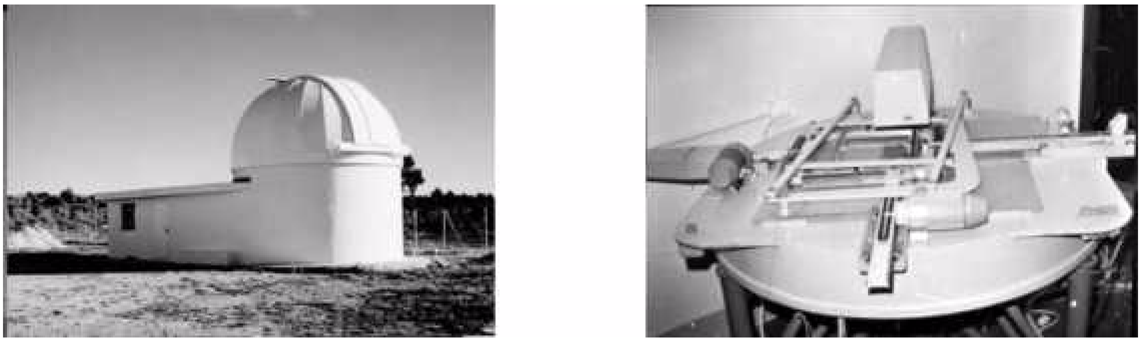

Figure 2 : Left : 6 inches Grubb refractor of OAUV (Valencia). **Right** : 30-20 cm double refractor of OAUV (CAAT)

Special mention must be done of our program of close encounters prediction and observation (Lopez *et al*. 1997, 1998). Regular observations of selected pairs of asteroids during close encounter epoch and afterward will allow to improve the knowledge of some minor planets masses not well known at present.

2 . Ephemerids for Minor Planets Observations

A regular observing session requires to obtain previously the ephemerids of one night targets. This can be done with standard software packages (CERES, STAMP, etc.) but we do it with our own software. From a list of observable Minor Planets for a full period of 400 days we get the «candidates» for any session. Osculating elements from MPC files are integrated on rectangular co-ordinates and Bulirsch-Stoer method, considering perturbations from DE403 planetary theory. Results include asteroid designation, R.A. and Dec. (J2000), time of meridian crossing and magnitude. Candidates appear ordered by time of meridian crossing for observing them in its natural order.

3 . Field Maps

Field maps and files are obtained from stellar catalogues (PPM, Hipparcos, Tycho and Tycho-2, GSC++, USNO SA1.0) in the J2000/FK5 reference system. Maps for stellar identification in 6 inches Grubb refractor (single tube) include the automatic/manual selection of a guiding star outside of central 6 by 9 cm region of plate-holder. Co-ordinates of centre of plate, asteroid and guiding star are shown. Plate-holder orientation and field of view of ocular are also presented. These maps allow to compare plate with previsions. Double astrograph fields are centred on asteroid, as the guiding star can be pointed independently with the visual tube. Centre of plate and guiding star co-ordinates are shown, as well as position of movable ocular system in the visual tube.

4 . Measuring devices and Plates

(M1). 6 by 9 cm. plates got with Grubb refractor (limit magnitude about 12; 10 to 40 reference PPM stars and one to three images of each object) are measured with two small instruments designed at OAUV. Optical head with a CCD camera is connected to a PC computer through a frame grabber. Stepping motors give X and Y values with 5 microns resolution. Plate residuals are less than 2″. Scale and tilt parameters between microscope and optical co-ordinate systems must be determined when the device is regulated.

(M2). Bigger plates (9 by 12 and 13 by 18 cm), obtained with CAAT double refractor, are measured with an Ascorecord measuring device (Figure 2, right). Both axes are moved by stepping motors with a fast rack and pinion system. Optical head can give different field size, from a few mm to several cm. Measuring process includes partial overlapping of plate fields. Scale and tilt must be determined each time the optical head is focused or moved.

(M3). Big plates can be also inspected with a scanner. This method can be useful for the search of new objects (minor planets, novae and variable stars) or for getting a preliminary list of objects to be measured with a more accurate device. Scale and tilt are not calculated in this process, but standard scanners give rather poor astrometric results.

5 . Measuring algorithms

(A1). For Grubb telescope plates, with few catalogue stars, several exposures and sidereal tracking, measuring devices (M1) and (M3) can be used. (M1) takes about 1 minute per object. Software in QuickBasic and C is applied on a PC computer. (M3) gives bigger errors but takes only a few seconds per object. Software is in VisualBasic. First step is to select two initial stars (E1, E2). After that, all catalogue stars are measured in sequence, from the asteroid (number zero) to last star of plate file. If dimmed images of one star are not identified automatically, manual measurement and/or parameter modification are applied. X and Y values of objects images centres are saved in a file.

(A2). Sidereal tracking plates with high magnitude stars and single exposures from double refractor are measured with a similar algorithm in Ascorecord (M2) and from scanner images (M3). The scanned image or each field of plate on Ascorecord is analysed and each group of images is detected and solved in individual round images. After that, plate images and reference stars are identified. Fitting gives residuals of about 1–2″ on case (M2) and about 2–4″ on case (M3).

6 . Special Algorithms

(A3). For differential tracking plates, the algorithm is similar to applied in case (A2), but image distortion and partial overlapping of images increase the difficulties of the algorithm. After image detection, the contour of each group is obtained. Images of small size are eliminated. In every contour a process of separation of objects is applied sequentially. A Gauss-like model with elongated shape is fitted to each object and subtracted (Figure 3).

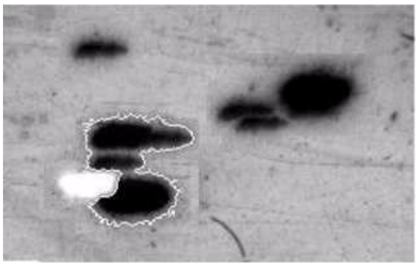

Figure 3 :

(A4). Image «spikes» produced on some telescopes and rectangular «grid» of «Carte du Ciel» plates require some special algorithms before standard measuring process (M2) or (M3) will be applied. In both cases, if not «cleaned» previously, additional images not corresponding to real objects will appear. Our algorithm for «spike» elimination gives good results.

(A5). Grid elimination on «Carte du Ciel» plates is under consideration with promising results. Other serious problems related to images distortion and «Carte du Ciel» plates quality must be considered and solved before a useful algorithm will be obtained.

7 . CCD Observations

Automatic techniques for plate's measurement, developed at OAUV since 1990, have been extended to detection and measurement of images on CCD frames.

A new Apogee AP10 CCD camera of big size is now operative at CAAT. It has a Thomson sensor of 2048 by 2048 square pixels of 14 microns. With 3 meters focal length refractor it gives a scale of nearly 1″ per pixel. The field of view is about 0.5° by 0.5°, very convenient for astrometry purposes.

7.1. Asteroids observations

Good images with magnitudes up to 17 can be obtained at CAAT without guiding in exposures of about 30 seconds, although limit magnitude for objects with high differential motions is less than expected. Diameter of faint objects is about 2–4″ when maximum resolution is applied. Regular images of faint asteroids will be obtained with the double telescope and this method will substitute at CAAT the photographic method, including big size film plates.

7.2. Satellites observation

Accurate observations of satellites of big planets when they approach to stars of well-defined position are of great interest to improve planetary ephemerides (Casas *et al*. 1998). Our CCD camera can detect these events with small exposure time intervals and high limit magnitude. As an example, we present our results with Uranus satellite Oberon that was observed on the night of September 17, 2001. Ephemerides of satellite relative to Uranus were provided by Institute of Applied Astronomy (IAA) of St. Petersburg. Six Tycho-2 stars appear on the frame field, providing the fitting of CCD parameters and satellite position. A special algorithm has been developed, in order to detect and separate satellite faint image from the planet (Figure 4). Best result were obtained with a Red filter, that dim the green light of Uranus. Other filters (Blue, Green) will be applied in other conditions.

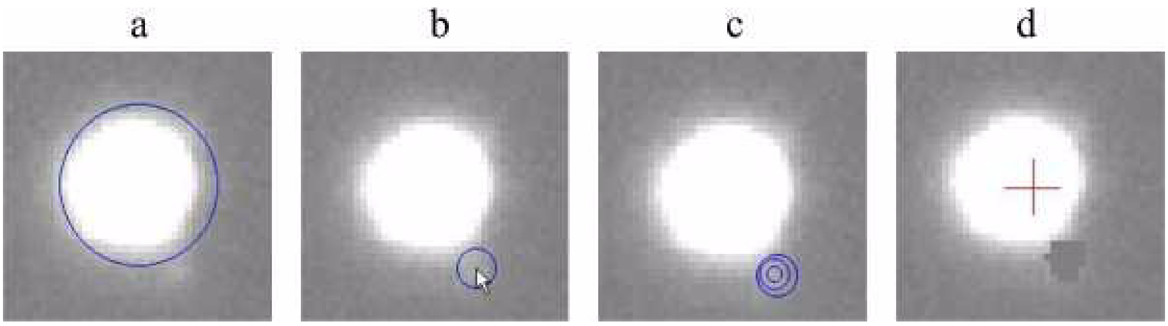

Figure 4 : Measuring process of a faint satellite. **a** : initial measuring circle; **b** : final size and position of measuring circle; **c** : result of measuring process of satellite; **d** : elimination of satellite image

8 . Considerations about CCD observations

- Higher limit magnitudes need higher time exposures. Offset guiding with 20 cm telescope will be necessary.
- Big size CCD frames make it possible to observe satellite events more frequently than before, when CCD frame fields were much smaller. The use of a denser catalogue (Tycho-2 instead of Hipparcos) provides a higher number of suitable events.
- The small separation of satellites from Uranus and Neptune makes it convenient to use full resolution of CCD frames (2048 by 2048 pixels), although the sensitivity of the camera is smaller in this case.
- A Barlow lens placed on the optical system of the telescope will increase its equivalent focal length and will allow to separate close objects.
- CCD frames can substitute photographic film in every case, if the telescope has a precise

pointing system. Overlapping of frames will provide extended fields with observing time similar to needed time for photographic work (Yershov and Lopez, 1998).

9 . Conclusions

Valencia Observatory has developed hardware and software for automatic measurement of several kinds of plates and CCD frames. They are applied to present and future observing programs with double 30–20 cm refractor. Measuring devices and algorithms can be also applied to plate digitisation. Some possible applications are shown in this paper. We offer our experience and collaboration to other groups in order to solve problems related to plate digitisation and special image identification.

References

Casas, R., Krassinsky, G. A., Yagudina, E. I., 1998, *Communications of IAA*, **117**, 2, ed. IAA, St. Petersburg, Russia, 2.

Kanaev, I.I., Yershov V., Streletsky Y., López García, A., Flores, A., Conejero, J., 1998, in *Proc. of the IV International Workshop on Positional Astronomy and Celestial Mechanics*, Peñíscola, Spain, October 1996, ed. Observatorio Astronomico de la Universidad de Valencia. Spain, 361.

López García, A., Medvedev, Yu. D., Moraño Fernández, J. A., Using close encounters of minor planets for the improvement of their masses, 1997, in *IAU Coll.165 Proc., Dynamics and Astrometry of Natural and Artificial Celestial Bodies*, ed. Kluwer Academic Publishers, 199.

López García, A., Medvedev, Yu. D., Moraño, J. A., 1998, in *Proc. of the IV International Workshop on Positional Astronomy and Celestial Mechanics*, Peñíscola, Spain, October 1996, 245.

Yershov, V.N., López García, A., Overlapping Technique for Direct CCD Astrometric Imaging, 1998, in *Proc. of the IV International Workshop on Positional Astronomy and Celestial Mechanics*, Peñíscola, Spain, October 1996.

Estimating masses of asteroids

Krasinsky G.A., Pitjeva E.V., Vasilyev M.V., Yagudina E.I.

Abstract. *The action of asteroids upon the orbits of Mars and the Earth is considered in this paper. The total mass of the asteroid belt :* $M_{belt} = (1800 \pm 100) \cdot 10^{-12} M_{\odot}$ *is estimated from analysis of the motion of major planets. This value is in a good accordance with the estimate obtained from a theoretical distribution of minor planets based on the fragmentation theory. The expression for predicting the total number of minor planets in any unit interval of absolute magnitude is derived. The comparison with the observed distribution shows that at present about 10% of the asteroids with the absolute magnitudes* $H < 14$ *are discovered.*

At present serious problems arise in construction of planetary ephemerides which could match correspond to positional observations of the highest accuracy. These problems are due to the necessity to take into account the perturbations caused by a large number of minor planets. Especially sensitive to these perturbations are the measurements of ranging to the martian landers Viking-1,2, and Pathfinder (with the typical error about 7 meters). It is easy to prove that perturbations from minor planets of the main belt with masses $m/M_{\odot} \approx 10^{-12}$ ($M_{\odot}$ is the solar mass) must be accounted for and masses of the biggest minor planets must be estimated with the same accuracy.

There are two groups of methods that allow to evaluate the masses of asteroids. The first group is astrophysical one. These methods are based on measurements of the flux of radiation from the asteroid and on spectral observations which provide its spectral class. At present 3316 radii, obtained by the astrophysical method, are published in open NASA database SBN («Small bodies node of the NASA Planetary Data System», see http://pdssbn.astro.umd.edu). This set includes both the IRAS (Infra Red Astronomical Satellite) data and results of some ground observations. For the most cases a taxonomic class of Tholen is also given. We referred the Tholen's taxonomic codes to the three compositional taxonomic types making use of the compositional interpretation of the asteroid taxonomy types after Bell 1989. These types are Carbonic (the notation C), Sillicium (S), and Metallic (M). The adopted correspondence is given by Table 1.

Table 1 : Correspondance of Tholen's classes with densities (in g/cm^3)

Tholen's classes	C, D, P, T, B, G, F	S, K, Q, V, R, A, E	M
Composition type	C	S	M
A priory density, DE405	1.8	2.4	5.0
Revised density, Standish 2000	1.29 ± 0.06	2.71 ± 0.04	5.29 ± 0.53
Revised density, Pitjeva 2001a	1.36 ± 0.03	2.67 ± 0.02	-
Revised density, this work	1.38 ± 0.02	2.71 ± 0.02	5.32 ± 0.07

The densities have been derived in the process of fitting of planetary ephemerides to radar measurements of distances to the landers and the surfaces of the inner planets. With the known radius and density, the mass of the asteroid is easily calculated.

In the methods of the second group the mass of the asteroid has to be estimated from its perturbations upon the motion of some other celestial bodies. These methods can be applied in the following cases: the perturbed body is another asteroid for which a close encounter with the perturbing body occurs, very close encounters of some asteroids took place with a space probe, several biggest asteroids affect the motion of Mars so strongly that their masses can be estimated from analysis of ranging to the Martian landers. Up to now masses of about 100 asteroids are obtained by the dynamical methods with various level of accuracies achieved. Masses of another asteroids are too small to be determined by the dynamic methods.

In the work Krasinsky *et al.* 2001 we have compared the masses obtained by a number of authors and based on the method of the close asteroid encounters with the IRAS based masses. It appears that excepting three biggest asteroids (Ceres, Pallas, and Vesta) and a few other minor planets the astrophysical method gives considerably more accurate estimates (at least by one order). So the present study is based mainly on the masses derived from IRAS data. The astrophysical method being applied to the three biggest minor planets gives wrong results because these planets have complicated internal structure, but rather accurate masses of these asteroids have been derived in the process of fitting of the planetary ephemerides to the ranging observations from perturbations upon the orbit of Mars (Standish 2000, Pitjeva 2001a).

An attempt is undertaken to extent the list of 300 perturbing asteroids accounted in the adopted DE403/DE405 ephemerides (Standish *et al.* 1995, Standish 1998). A number of experiments were tried in which the total number of perturbing asteroids and their masses varied while constructing our ephemerides of the major planets EPM and fitting those to radiometric observations of planets and spacecraft 1961–1997 (Pitjeva 2001b). We used the lunar-planetary integrator embedded in the program package ERA (Krasinsky and Vasilyev 1997). The integrator makes it possible to integrate simultaneously barycentric equations of motions of the nine major planets, Sun and Moon, equations of lunar physical libration, and reduced equations of 300-351 minor planets.

In fact the SBN database keeps two set of radii : a set derived from IRAS observations (they are referred hereafter as the radiometric radii or the system 1 of radii) and a larger set based also on ground observations (the system 2). Our analysis has shown that in most cases these two sets are in a good agreement and only a slight scaling is needed to transform SBN radii R (in km) to the radiometric ones R_r :

$$R_r = (0.966 \pm 0.001)R - (0.313 \pm 0.027) \quad (1)$$

but the radii of a number of asteroids taken in accordance with the system 2 are erroneous, too large and their accounting in the dynamical model seriously deteriorates fitting to the lander measurements. On the other hand, it appears however that the best values of radii of the 300 asteroids (perturbations from which are accounted) correspond namely to the system 2. Thus the radii given by the system 1 must be corrected making use of the relation (1) obtained by comparing the two system of radii of asteroids.

So the masses of 357 asteroids, tested by the analysis of the lander ranging data, and which we consider more plausible have been derived (Krasinsky *et al.* 2001).

There exists a large number of asteroids of the main belt which are too small to be observed from the Earth, but their summary perturbating action upon the orbit of Mars is not negligible and may be modelled by potential of a solid ring in the ecliptical plane. Mass M_{ring} of the ring as well as its radius R are considered solve-for parameters. The estimate $M_{ring} \approx (500 \pm 100) \cdot 10^{-12} M_{\odot}$ is obtained, which value is about one mass of Ceres. For the mean radius of the ring we have $R \approx 2.80$ AU with the uncertainty 3%. Then the total mass M_{belt} of the main asteroid belt (including the 300 asteroids mentioned above) may be derived: $M_{belt} \approx (1800 \pm 100) \cdot 10^{12} M_{\odot}$.

To check this estimate we can apply a theoretical distribution of the number *N(r)* of minor planets with radii exceeding r (the distribution is based on a collisional model of fragmentation described in Dohnanyi 1969, Hawkins 1959, *Minor planets* 1973). For the density *dN(r)* of this distribution the following expression holds true :

$$dN(r) = -\beta r^{-3.5} dr \text{, where } \beta > 0 \text{ is a constant.} \quad (2)$$

Let *M(r)* be the total mass of all asteroids with radii greater than *r*. Supposing that some mean density ρ may be used to calculate masses of asteroids from their volumes we obtain after integration the following expression for the distribution *M(r)* :

$$M(r) = \rho \int \frac{4}{3} \pi r^3 dN(r) = \beta_1 r^{0.5} + \beta_0 \quad (3)$$

We assume that there are no significant systematic effects of observational selection in region of changing of *r* where the asteroids are big enough. After fitting the distribution to the set of 300 asteroids whose masses and radii provide the best data for such estimating we have obtained for the value *M(r)* the following expression (*r* is in kilometers, *M* is in $10^{-12} M_{\odot}$):

$$M = 1765 - 82.9\sqrt{r} \quad (4)$$

We see from this distribution that the total mass $M(0)$ of the asteroid belt is $1765 \cdot 10^{-12} M_{\odot}$ which value is in excellent accordance with our finding based on the study of the perturbations upon the orbit of Mars. In Fig. 1 both the curve of this distribution and the experimental data (for about 2000 minor planets) are depicted.

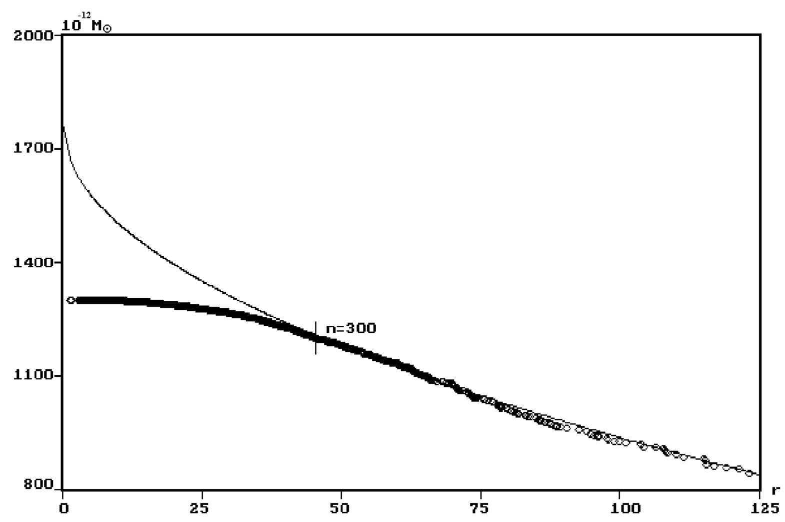

Figure 1 : Distribution of masses *M(r)* versus their radii *r*, *M(r)* is the total mass of all asteroids whose radius greater than *r* (in km).

Let's express the right part of the distribution (2) in terms of the absolute magnitude H and compare it with the all bulk of numbered asteroids. We apply the following relation (Chebotarev and Shor 1976) between radius r (in kilometers) of an asteroid and H :

$$\lg r = 3.1 - 0.2H \quad (5)$$

Then instead of (2) we obtain :

$$dN(H) \approx 0.2 \ln 10 \beta r^{-2.5} dH = 0.2 \ln 10 \beta 10^{-2.5 (3.1 - 0.2H)} dH \quad (6)$$

For the unit interval of magnitudes and in the logarithmic scale the expression (6) becomes:

$$\lg dN(H) \approx 0.5H - 1.02 \quad (7)$$

In Fig. 2 the line marked by the symbol «A» presents this relation in the plane (lg dN , H). The black circles are the values obtained after calculating the total number of minor planets at the intervals of the magnitudes $(H, H + 1)$. (The experimental data includes about 30 000 numbered asteroids). One can see that for $H < 8$ the slope of the theoretical line corresponds to the experimental dependence of lg dN on H. Supposing that there is no observational selection for $H < 8$ we can calibrate the dependence given by (7) by the experimental data in this region of the magnitudes. Then instead of (7) we obtain

$$\lg dN(H) \approx 0.5H - 1.80 \quad (8)$$

The line marked by the symbol «B» corresponds to this functional dependence. The data presented by Fig.~2 make it possible to estimate the expected number of minor planets in the asteroid belt which are not yet discovered in given intervals of absolute magnitudes (see Table 2). One can see that the expected number of asteroids of the main belt for which the magnitude $H < 14$ is about 130 000, and about 10% of such asteroids has been already discovered.

For further details the reader is referred to the paper (Krasinsky *et al.* 2001).

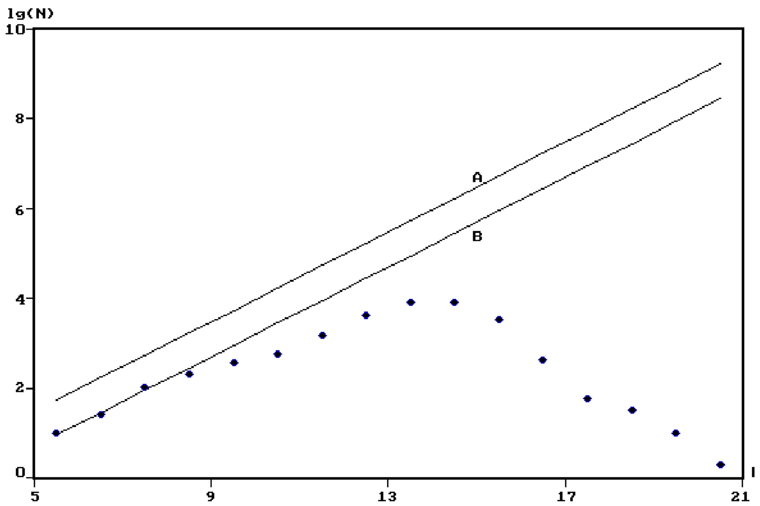

Figure 2 : Distribution of lg N versus magnitudes *H*

Table 2 : Expected (N_p) and (N_o) numbers of asteroids

H	N_o	N_p	%
5-6	10	8	100
6-7	25	28	100
7-8	101	89	100
8-9	210	280	70
9-10	363	900	40
10-11	583	3000	20
11-12	1515	9000	16
12-13	4109	28000	14
13-14	8014	90000	9
14-15	8290	280000	3

References

Bell, J. F., Davis, D.R., Hartmann, W.K., M. J. Gaffey, 1989, Asteroids : the big picture. In *Asteroids II* (R. P. Binzel, T. Gehrels., and M. S. Matthews , eds.), 921– 945. Univ. Arizona Press, Tucson.

Chebotarev, G. A., Shor, V.A., 1976, The structure of the asteroid belt, *Trudi Inst. Theoretical Astron*., **15**, 60–90 (in Russian).

Dohnanyi, J. S., 1969, Collisional model of asteroids and their debris, *J. Geophys. Res.*, **74**, 10.

Hawkins, G. S., 1959, The relation between asteroids, fireballs and meteorites, *AJ*, **64**, 450.

Krasinsky, G. A., Vasilyev, M.V., 1997, ERA: knowledge base for ephemeris and dynamical astronomy. In *Dynamics and Astrometry of Natural and Artificial Celestial Bodies*, IAU Coll. **165** (I. M. Wytrzyszczak, J. H. Lieske, and R. A. Feldman, Eds.), 239–244. Kluwer, Dordrecht.

Krasinsky, G. A., Pitjeva, E.V., Vasilyev, M.V., Yagudina, E.I., 2001, Estimating masses of asteroids, *Communication of IAA RAN*, **139**, 43.

Minor planets 1973. (N. S. Samoilova-Yachontova, ed.), 296, Nauka, Moscow, (in Russian).

Pitjeva, E. V, 2001a, Progress in the determination of some astronomical constants from radiometric observations of planets and spacecraft, *A&A*, **371**, 760–765.

Pitjeva, E. V., 2001b, Modern numerical ephemerides of planets and importance of ranging observations for their creation, *Celest. Mech. & Dyn. Astr.*, **80**, N 3/4, 249–271.

Standish, E. M., Newhall, XX, Williams, J.G., Folkner, W.M., 1995, JPL Planetary and Lunar Ephemerides, DE403/LE403, *Interoffice Memorandum*, **314.10-127**, 1–22.

Standish, E. M., 1998, JPL Planetary and Lunar Ephemerides, DE405/LE405, *Interoffice Memorandum*, **312.F-98-048**, 1–18.

Standish, E. M., 2000, Recommendation of DE405 for the 2001 Mars Surveyor mission and for Cassini, *Interoffice Memorandum*, **312.F-00-107**, 1–7.

Tholen, D. J., 1989, Asteroid taxonomic classifications, In *Asteroids II,* (R. P. Binzel, T. Gehrels, and M. S. Matthews, eds.), 1139–1150. Univ. Arizona Press, Tucson.

Accuracy of world positional CCD observations of the numbered minor planets in 1999-2000 yrs

Bykov O.P., L'vov V.N., Izmailov I.S., Sumzina N.K.

Positions of the Numbered Minor Planets (NMPs) which have been sent by observers to the Minor Planet Center in 1999 and 2000 yrs were automatically analysed by means of calculation of (O–C) values with the help of the EPOS Software Package [1] created in Pulkovo Astronomical Observatory. More then 1.2 million individual positions of the Numbered Minor Planets obtained by professional and amateur observatories were taken into consideration. Internet accessible version of Bowell's Orbital Catalogue containing more 27 thousand orbits of NMPs was used for calculations of their theoretical positions and comparisons with the observed ones. The values of «Mean error of a single observation» were calculated for the most of considered observatories during this period. These errors show the accuracy of observations and processing for each telescope in the assumption that the accuracy of the theory of motion of each Numbered Minor Planet is higher than that of its observations.

Table 1 : Observations with normal values of the «Mean error of single observation»

NMP	Code	Dynamical Time	$\alpha(gc)$	(O–C)	$\delta(gc)$	(O–C)	V
3907	761	1998 08 24.383673	3 17 44.739	0.28	+30 46 00.84	–0.08	15.8
3907	761	1998 08 24.409133	3 17 46.152	0.28	+30 46 10.85	0.12	15.8
3907	761	1998 08 25.392523	3 18 40.107	0.33	+30 52 27.69	0.04	15.4

Total mean value of 3 observations........................ 0.30+/–.02.................. 0.03+/–.06
Mean error of single observation............................ 0.03............................ 0.10

COMMENT. There are two neighbour nights of CCD observations. For any NUMBERED minor planet the (O–C) values must be zero if the errors of observations and the errors of its theory are absent. The errors of the theory for usual NUMBERED minor planet during several successive nights are very small, more less then observational errors in this conditions. Therefore, the range of these values due to observational errors may be a good characteristic of the accuracy of observational data. The real meanings of (O–C) may be different but I am investigating namely the range of these values during several close nights, or «Mean error of single observation» in this and other Tables.

Table 2 : Observations with the large values of the «Mean error of single observation»

NMP	Code	Dynamical Time	$\alpha(gc)$	(O–C)	$\delta(gc)$	(O–C)	V
3955	761	1998 10 16.163935	0 52 43.326	2.34	+ 3 26 20.94	1.62	15.4
3955	761	1998 10 16.194495	0 52 41.796	2.68	+ 3 26 17.64	1.68	15.2
3955	761	1998 10 17.165035	0 51 52.843	5.76	+ 3 24 29.44	–0.82	15.5
3955	761	1998 10 17.181125	0 51 52.129	7.22	+ 3 24 25.54	–3.00	15.2
			Total mean	4.50		–0.13	
			Mean error	2.38		2.24	

COMMENT. There are very large (O–C) ranges for RA and DEC for two close nights. Observations are only responsible for these (O–C) changings.

So, the main idea of our method of an estimation of an accuracy of the NMP observations is to use these irregularities [2] when we calculate the mean value of (O–C) and its mean error for the considered NMP with the help of the EPOS Software. The values of (O–C) may vary for various NMPs, but the mean error of these (O–C)s shows a reliability of «atmosphere + telescope + CCD camera + star catalogue + astrometric reduction» system in the mean observational conditions and is a good indicator of an accuracy of the CCD positional observations.

We get a set of such mean errors derived from all NMPs observed at a given observatory during considered observational period and then we take an average value for this set. This average value is an accuracy of the investigated NMP observations. When we calculate (O–C) residuals for one night asteroid positions we obtaine an «internal» estimation of an accuracy of observations (marked by symbol «int.» in the Tables). If our (O–C) residuals are calculated for asteroid positions obtained during several close nights of obsevations we can derive an «external» estimation of their accuracy (marked by symbol «ext.» in the Tables). As a rule, «internal» accuracy is higher than «external» one due to an influence of reference stars which are changed from night to night together with their catalogue coordinates. Of course, we must have a lot of observations of various NMPs in the set for each observatory under consideration.

The results of our analysis are given in the Tables 3-7 which represent the observatories with the same equipment. Each Table contains the number of observed Minor Planets, the number of analysed positions, the instrumental and accuracy parameters and star catalog used for reductions.

Table 3 : An accuracy of observations of the numbered minor planets observed with 0.2-m telescopes in 1999 and 2000 (*) yrs

Observatory		Teles-cope (D, F)	FOV	CCD scale, catalogue	Number of		Mean error of a single observation (in arcsec) for		«int.» or «ext.» accu-racy
code	country, name				minor planets	posi-tions	α	δ	
1	2	3	4	5	6	7	8	9	10
610	Italy,	0.25	26 x 17′	2″	413	2676	0.44	0.33	int
	Pianoro	1.0		GSC	65	878	0.49	0.47	ext
610*					40	536	0.44	0.30	int
					15	375	0.61	0.50	ext
652	Canada,	0.25	25 x 20′	2.0″	5	20	0.97	0.70	int
	Sandringham	0.8		GSC					

Table 3 : An accuracy of observations of the numbered minor planets observed with 0.2-m telescopes in 1999 and 2000 (*) yrs

715	USA,	0.25	24 x 16′	1.9»	10	36	0.51	0.60	int
	Las Cruces	1.0		USNO	4	26	0.79	0.79	ext
715*					4	18	0.30	0.48	int
739	USA,	0.25	24 x 15′	1.8″	56	178	0.44	0.50	int
	Sunflower Obs.	1.1		GSC	9	36	0.89	0.54	ext
739*					424	2452	0.56	0.38	int
					60	682	0.52	0.41	ext
740	USA,	0.25	14 x 9′	1.1″	10	77	0.44	0.50	int
	SFA Obs.	1.7		GSC	10	89	0.56	0.62	ext
744	USA, Doyan	0.25			6	21	0.25	0.08	int
	Rose Obs.	1.9		GSC					
716*	USA, Palmer	0.25	30 x 20′	2.2″	5	24	0.16	0.16	int
	Divide Obs.	1.6		Tycho	4	24	0.16	0.17	ext
670*	USA,	0.25	18 x 13′	3″	7	24	0.68	0.34	int
	Camarillo	1.2		USNO	4	25	0.30	0.21	ext
682	USA,	0.25	23 x 15′	1.8»	8	43	0.42	0.40	int
	Kanab	1.0		USNO					
682*					8	26	0.71	0.32	int
838*	USA,	0.25	14 x 18′	3″	7	30	0.39	0.44	ext
	Dayton	1.6		GSC					
849	USA,	0.25			14	48	0.82	0.77	int
	Everstar Obs.			GSC					
849*					47	156	0.74	0.90	int
852	USA,	0.25			8	48	1.13	0.72	int
	River Moss Obs.	0.50		GSC	8	54	1.05	0.77	ext
852*					5	25	0.77	0.67	int
					4	24	0.79	0.74	ext
925*	USA, Palo-	0.25			5	24	0.56	0.37	int
	minas Obs.	2.8		ACT	5	28	0.54	0.37	ext
940*	England, Wa-	0.25			6	30	0.92	0.95	int
	terlooville	1.6		GSC	6	35	0.87	1.03	ext
952	Spain,	0.25	13 x 9′	1.8″	14	46	0.35	0.24	int
	Marxuquera	1.6		GSC					
952*					4	17	0.13	0.19	int
955	Portugal,	0.25	4 x 4′	1.5″	12	159	0.66	0.60	int
	Sassoeiros	2.0		GSC	7	118	0.56	0.74	ext
153	Germany,	0.25	16 x 12′	2.8″	4	23	0.18	0.14	int
	Stuttgart	1.8		GSC	4	26	0.21	0.34	ext
169	Italy,	0.25	15 x 10′	1.1″	4	23	0.31	0.31	int
	Rosignano	1.6		GSC					
169*					6	25	0.97	1.06	int
321	Australia,	0.25			11	56	0.21	0.24	int
	Craigie			GSC	8	47	0.27	0.17	ext
322	Australia,	0.25			5	15	0.27	0.13	int
	Bickley-MCT	1.1		USNO					
322*					5	21	0.38	0.26	int
428	Australia,	0.25	14 x 9′	2.1″	6	50	0.35	0.16	int
	Reeady Creek	1.7		ACT	4	35	0.48	0.41	ext

Table 3 : An accuracy of observations of the numbered minor planets observed with 0.2-m telescopes in 1999 and 2000 (*) yrs

638	Germany, Detmold	0.25 1.6	15 x 10′	1.2″ GSC	7	24	0.92	0.71	int
164	France, St. Michel	0.21 0.8		USNO	28 16	170 137	0.62 0.64	0.67 0.72	int ext
164*					8	24	0.53	0.41	int
689	USA, USNO Flagstaff	0.2	51 x 51′	1.5″ ACT	8	35	0.18	0.22	ext
689*					649	3688	0.19	0.24	ext
517*	Switzerland, Genewa	0.20 2.0	46 x 46′	2.2″ Tycho	17	113	0.22	0.13	int
133	France, Les Tardieux	0.20 0.7	33 x 22′	2.6″ USNO	16	51	0.27	0.27	int
133*					5	15	0.42	0.44	int
642	Canada, Oak Bay	0.20 0.7		GSC	10 12	36 76	0.39 1.29	0.36 0.54	int ext
642*					10 7	162 148	0.71 0.76	0.81 0.90	int ext
958*	France, Obs. de Dax	0.20 0.6	39 x 26′	3″ USNO	12 13	67 92	0.61 0.72	0.65 0.65	int ext
138	France, Village-Neuf	0.20 0.8	36 x 24′	2.8″ GSC	4	12	0.48	0.43	int
145	Belgium,Gra-venwezel Obs.	0.20 0.7	24 x 18′	2.2″ ACT	13 5	54 25	0.64 0.48	0.40 0.54	int ext
145*					4	18	0.37	0.26	int
732	Mexico, Oaxaca	0.20 0.9	28 x 18′	2.1″ ACT	94 88	600 621	0.58 0.59	0.44 0.46	int ext
732*					51 29	273 217	0.55 0.60	0.45 0.56	int ext
628	Germany, Mulheim-Ruhr	0.20 1.2	18 x 12′	2.4″ USNO	19 5	108 48	0.31 0.46	0.30 0.48	int ext
628*					21 4	126 26	0.31 0.42	0.25 0.23	int ext
117*	Germany, Sendling	0.20 2.0	15 x 11′	2.5″ GSC	26 19	322 331	1.37 1.67	0.85 1.18	int ext
825	USA, Granville	0.20 0.7	33 x 22′	2.6″ GSC	8 7	42 44	0.34 0.71	0.52 0.72	int ext
857*	USA, Iowa Robotic Obs.	0.2 1.6	21 x 21′	1.2″ USNO	24 24	461 413	0.32 0.47	0.36 0.49	int ext
860	Brazil, Valinhos	0.20 0.7	34 x 23′	2.6″ USNO	6	24	0.32	0.49	int
860*					25 4	95 25	0.78 1.02	0.61 0.65	int ext
162*	Italy, Potenza	0.20 1.3	13 x 10′	1.1″ GSC	14	50	0.68	0.80	ext
196*	Germany, Homburg-Erbach	0.20 1.3		GSC	5 6	80 104	0.10 0.25	0.07 0.16	int ext
347*	Japan, Imaizumi	0.20 1.6	18 x 14′	3.2″ ACT	5	24	0.53	0.45	int
713	USA,	0.20	19 x 14′	3.2″	12	75	0.27	0.17	int

Table 3 : An accuracy of observations of the numbered minor planets observed with 0.2-m telescopes in 1999 and 2000 (*) yrs

	Thornton	1.6		USNO	14	93	0.34	0.24	ext
423	Australia, North Ryde	0.2 0.8	13 x 11′	4″ GSC	7	37	0.40	0.39	ext
127	Germany, Bornheim	0.19 0.8	30 x 20′	2.4″ USNO	8 12	36 61	0.14 0.37	0.08 0.48	int ext
127*					7 6	38 34	0.08 0.37	0.15 0.41	int ext
720	Mexico, Univ. de Monterrey	0.18 1.7	14 x 9′	1.1″ USNO	49 37	327 287	0.46 0.50	0.44 0.46	int ext
720*					13 9	104 92	0.53 0.54	0.66 0.64	int ext
761	USA, Zephyrhills	0.18 1.7	9 x 14′	2.2″ GSC	12 18	48 84	0.93 1.09	0.31 0.46	int ext
349*	Japan, Ageo	0.18 1.0		ACT	15 5	108 41	0.36 0.51	0.32 0.40	int ext
544	Germany, W.Foer.Obs.	0.15 2.2		HIP.	4	21	0.35	0.35	int
544*					6	33	0.57	0.46	int
631*	Germany, Hamburg	0.15 1.2	18 x 14′	2.9″ GSC	5	20	0.32	0.54	ext
727	USA, Zeno Obs.	0.15 1.0	24 x 16′	2.0″ ACT	58 11	198 65	0.23 0.31	0.25 0.36	int ext
727*					22 4	99 32	0.22 0.32	0.16 0.19	int ext

Table 4 : An accuracy of observations of the numbered minor planets observed with 0.3-m telescopes in 1999 and 2000(*) yrs

Observatory		Teles-cope (D,F)	FOV	CCD scale, catalogue	Number of		Mean error of a single observation (in arcsec) for		«int.» or «ext.» accu-racy
code	country, name				minor planets	posi-tions	α	δ	
1	2	3	4	5	6	7	8	9	10
636	Germany, Essen	0.32 1.8	15 x 15′	1.7″ USNO	20 24	87 126	0.74 0.72	0.42 0.47	int ext
170*	Spain, Obs. de Begues	0.31 1.8		GSC	4 9	12 36	0.89 0.83	1.35 1.23	int ext
649	USA, Powell Obs.	0.31		GSC	48 4	149 18	0.63 0.45	0.37 0.42	int ext
649*					42 5	166 35	0.70 0.83	0.49 0.50	int ext
426	Australia,	0.30	25 x 17′	2.0″	43	202	0.29	0.20	int

Table 4 : An accuracy of observations of the numbered minor planets observed with 0.3-m telescopes in 1999 and 2000(*) yrs

	Woomera	3.0		USNO	33	189	0.35	0.25	ext
714	USA,	0.30			17	103	0.41	0.38	int
	Bagdad	3.0		GSC	19	117	0.49	0.36	ext
620	Spain, Obs.	0.30	24 x 16′	1.9″	5	16	0.73	0.87	int
	de Mallorca	1.0		GSC					
731*	USA, Rose-	0.30	16 x 24′	1.8″	10	60	0.32	0.50	int
	Hulman Obs.	1.0		GSC	10	60	0.33	0.51	ext
734	USA,	0.30	13 x 9′	2.1″	10	60	0.39	0.33	int
	Farpoint Obs.	1.8		GSC					
734*					14	57	0.45	0.43	int
723	USA, Cotton-	0.30	26 x 17′	2.0″	10	67	0.44	0.42	ext
	wood Obs.	1.8		ACT					
723*					6	21	0.66	0.57	int
625	USA,	0.30			4	15	0.70	0.34	int
	Kihei-AMOS				6	30	0.54	0.55	ext
752	USA,	0.30	22 x 22′	2.6″	27	135	0.15	0.10	int
	Puckett Obs.	1.8		USNO	17	102	0.10	0.10	ext
758	USA, BCC Obs.,	0.30	31 x 21′	2.4″	6	23	0.31	0.25	int
	Cocoa	1.5		USNO					
858*	USA,	0.30			11	55	0.19	0.27	int
	Tebbutt Obs.	3.0		USNO	8	49	0.23	0.37	ext
843	USA, Emerald	0.30			9	39	0.68	0.34	int
	Lane Obs.	2.0		GSC	11	56	0.59	0.56	ext
843*					21	116	0.67	0.42	int
					18	113	0.71	0.52	ext
859	Brazil, Serra	0.30	26 x 17′	2″	15	90	0.26	0.17	int
	de Piedade	1.0		ACT	8	72	0.60	0.28	ext
859*					7	59	0.63	0.25	int
108	Italy,	0.30			21	76	0.89	0.84	int
	Montelupo	1.7		GSC	9	39	0.74	0.68	ext
108*					8	33	0.45	0.51	int
951	England,	0.30	25 x 25′	3″					
	Highworth	1.6		ACT	10	45	0.20	0.18	ext
951*					13	81	0.57	0.28	int
					14	95	1.03	0.35	ext
944*	Spain, Obs.	0.30	14 x 10′	2.2″	4	50	0.39	0.40	int
	Geminis	1.7		USNO	4	50	0.38	0.38	ext
166	Czech Rep.,	0.3			6	24	0.24	0.09	ext
	Upice	1.0		GSC					
540	Austria,	0.30	15 x 20′	3.5″	5	28	0.29	0.27	int
	Linz	1.5		USNO					
726	USA,	0.28	12 x 18′	2.9″	18	69	0.70	0.53	ext
	Brainerd	1.8		GSC					
627	France,	0.26	19 x 12′	3″	29	119	0.54	0.50	int
	Blauvac	1.2		USNO	8	57	0.57	0.52	ext
627*					17	72	0.38	0.36	int

Table 5 : An accuracy of observations of the numbered minor planets observed with 0.4-m telescopes in 1999 and 2000[(*)] yrs

Observatory		Teles-cope (D,F)	FOV	CCD scale, catalogue	Number of		Mean error of a single observation (in arcsec) for		«int.» or «ext.» accu-racy
code	country, name				minor planets	posi-tions	α	δ	
1	2	3	4	5	6	7	8	9	10
703	USA, Catalina	0.41	175x175′	2.6″	3406	22755	0.44	0.44	int
	Sky Survey	1.2		USNO	796	7608	0.38	0.40	ext
703*					2151	10637	0.42	0.44	int
					138	1156	0.34	0.51	ext
120	Croatia,	0.41	51 x 51′	2.8″	340	1399	0.51	0.35	int
	Visnjan	1.8		USNO	314	2008	0.58	0.40	ext
120*					257	1133	0.64	0.40	int
					188	1306	0.62	0.39	ext
294	USA,	0.41			13	59	1.17	0.88	ext
	Astroph. Obs.	2.6		GSC					
294*					8	27	0.62	0.40	int
					33	135	0.87	0.83	ext
596	Italy, Colle-	0.40	24 x 18′	4.0″	14	62	0.26	0.53	int
	verde di Guid.	1.3		GSC					
104	Italy, San	0.40	21 x 21′	2.5″	14	63	0.39	0.32	int
	Marccello	2.0		USNO	6	42	1.73	0.82	ext
104*					15	63	0.54	0.27	int
					4	26	0.66	0.47	ext
143	Switzerland,	0.40	20 x 20′	2.4″	12	57	0.49	0.30	int
	Gnosca	1.6		USNO	5	40	0.56	0.56	ext
143*					14	100	0.37	0.19	int
130	Italy,	0.4	15 x 10′	1.2″	10	40	0.35	0.27	int
	Lumezzane	2.6		USNO					
130*					19	69	0.24	0.22	int
					4	13	0.46	0.33	ext
701	USA, JunkBond	0.4	24 x 16′	1.8″	31	147	0.36	0.48	int
	Obs.,	2.5		ACT	19	113	0.37	0.36	ext
701*					11	59	0.64	0.59	int
560	Italy, Madon-	0.40	17 x 10′	2.6″	9	45	0.58	0.32	int
	na di Dossob.	2.0		GSC	6	38	0.69	0.51	ext
151	Switzerland,	0.40	24 x 16′	0.9″	41	299	0.61	0.44	int
	Eschenberg	2.3		USNO	22	214	0.62	0.52	ext
151*					39	361	0.34	0.51	int
					10	177	0.41	0.40	ext
842	USA, Gettys-	0.40			4	16	0.59	0.25	int
	burg College	4.6		ACT					
147	Italy, Osser.	0.40	16 x 16′	1.9″	5	36	0.52	0.54	int
	Astr. di Suno	1.6		USNO					
165	Spain,	0.40	58 x 39′	2.3″	4	19	0.54	0.26	ext
	Piera Obs.	0.8		USNO					
165*					4	12	0.48	0.22	ext
746	USA,	0.40	9 x 6′	1.0″	4	12	0.16	0.30	int
	Brooks Obs.	4.9		USNO					

Table 5 : An accuracy of observations of the numbered minor planets observed with 0.4-m telescopes in 1999 and 2000(*) yrs

746*					12 7	215 176	0.40 0.46	0.31 0.36	int ext
923*	USA, The Bra- dstreet Obs.	0.40 2.0		 USNO	59 12	216 72	0.39 0.29	0.29 0.23	int ext
912*	USA, Carbun- cle Hill Obs.	0.40 1.3		 ACT	4	15	0.75	0.42	int
106	Slovenia, Crni vrh	0.36 2.4	36 x 36′	2.0″ USNO	305 52	1003 231	0.48 0.53	0.45 0.48	int ext
106*					531 129	2118 717	0.40 0.37	0.35 0.38	int ext
848	Brazil, Tenagra Obs.	0.36 4.0		 ACT	5 4	24 24	0.28 0.48	0.36 0.45	int ext
683	USA, Good- ricke-Pigott	0.36 4.0	20 x 20′	2.5″ GSC	21 19	120 121	0.24 0.30	0.23 0.29	int ext
683*					4 5	15 24	0.16 0.39	0.11 0.38	int ext
719	USA, Etscorn Obs.	0.36 1.3	17 x 23′	4.0″ GSC	16 38	76 214	0.97 0.94	0.70 0.66	int ext
837*	USA, Jupiter	0.36 4.0		 USNO	5	15	0.61	0.19	int
916*	USA, Oakley Obs.	0.36	17 x 17′	2″ ACT	9	39	0.52	0.61	int
945*	Spain, Monte Deva	0.36 2.3	11 x 7′	0.6″ USNO	6	22	0.18	0.26	int
844	Uruguay, Los Molinos	0.35 2.2		 USNO	14	49	0.40	0.38	int
718	USA, Wiggins Obs.	0.35 1.4		 GSC	4 4	20 20	0.68 0.81	0.50 1.14	int ext
718*					4	43	1.07	0.82	int

Table 6 : An accuracy of observations of the numbered minor planets observed with 0.5-m telescopes in 1999 and 2000(*) yrs

Observatory code	Observatory country, name	Teles-cope (D, F)	FOV	CCD scale, catalogue	Number of minor planets	Number of posi-tions	Mean error of a single observation (in arcsec) for α	δ	«int.» or «ext.» accu-racy
1	2	3	4	5	6	7	8	9	10
159	Italy, Monte Agliale	0.51 2.3	13 x 10′	2.2″ USNO	14	66	0.76	0.40	int
619	Spain, Sabadell	0.51 2.0	14 x 11′	2.8″ GSC	16 10	71 57	0.26 0.37	0.32 0.38	int ext
747	USA, Baton Rouge Obs.	0.51 4.4	10 x 10′	1.2″ USNO	24 17	126 110	0.19 0.21	0.21 0.18	int ext
808	Argentina,	0.5	astrogr.		20	96	0.81	0.86	ext

Table 6 : An accuracy of observations of the numbered minor planets observed with 0.5-m telescopes in 1999 and 2000(*) yrs

	Carl.U.Cesco	3.8	photo.	PPM					
808*					6 65	20 351	0.75 0.62	1.79 1.30	int ext
853	USA, Biosphe- re 2 Observ.	0.5 4.0		ACT	4	16	0.06	0.09	int
853*					8 5	253 226	0.05 0.07	0.07 0.17	int ext
888*	Japan, Gekko Obs.	0.50 2.0		GSC	9	30	0.16	0.18	int
300*	Japan, Bisei Center	0.50 1.3	78 x 78′	2.3″ USNO	155 59	750 407	0.41 0.36	0.32 0.21	int ext
467	New Zealand, Auckland Obs.	0.50 3.2		USNO	7	27	0.10	0.10	int
467*					8	40	0.44	0.19	int
911*	USA, Collins Obs.	0.50 5.0		USNO	8 17	36 90	1.42 0.89	0.88 0.68	int ext
71	Bulgaria, National Obs.	0.50 1.7	28 x 18′	1.0″ GSC	6	28	0.36	0.50	int
71*					12	78	0.74	0.74	int
113	Germany, Schonbrunn	0.50 2.3	13 x 10′	2″ USNO	12 5	47 25	0.17 0.47	0.24 0.52	int ext
113*					20 7	136 59	0.53 0.31	0.28 0.28	int ext
684	USA, Prescott	0.46 2.1	23 x 15′	1.8″ GSC	7 9	24 41	0.14 0.24	0.06 0.20	int ext
684*					9 14	33 60	0.17 0.29	0.21 0.26	int ext
725	USA, Fair Oaks Ranch	0.46 2.1	24 x 16′	1.0″ ACT	5	22	0.21	0.15	ext
422	Australia, Loomberah	0.45 2.4	17 x 17′	2″ ACT	20 6	144 98	0.16 0.19	0.15 0.20	int ext
422*					11 4	52 24	0.05 0.05	0.07 0.12	int ext
552	Italy, San Vittore	0.45 1.5	15 x 20′	3.4″ GSC	5	23	0.33	0.42	int
611	Germany,	0.45	12 x 8′	2″	8	38	0.28	0.31	int
	Heppenheim	2.0		ACT					
611*					5	19	0.31	0.33	int

Table 7 : An accuracy of observations of the numbered minor planets observed with 0.6-m and more telescopes in 1999 and 2000$^{(*)}$ yrs

Observatory code	Observatory country, name	Teles-cope (D,F)	FOV	CCD scale, catalogue	Number of minor planets	Number of posi-tions	Mean error of a single observation (in arcsec) for α	Mean error of a single observation (in arcsec) for δ	«int.» or «ext.» accu-racy
1	2	3	4	5	6	7	8	9	10
807*	USA, Cerro Tololo	4.0 14.4	37 x 37′	0.3″ USNO	9	72	0.20	0.14	ext
695*	USA, Kitt Peak	3.8		 USNO	6	22	0.17	0.14	int
344*	Korea, BOAO	1.8 14.4	12 x 12′	0.3″ GSC	12	73	0.52	0.47	int
413	Australia, Siding Spring	1.2		 ACT	14	55	0.24	0.19	ext
413*					7 5	38 33	0.09 0.48	0.12 0.41	int ext
608*	USA, Haleakala-NEAT	1.2		 USNO	3498 484	16976 4033	0.21 0.74	0.26 0.85	int ext
644	USA, Palomar Mountain/NEAT	1.2			11	33	0.13	0.09	int
688*	USA, Lowell Obs.	1.07		 USNO	22	69	0.38	0.32	int
704	USA, Lincoln Lab.	1.0 2.2		 USNO	9958 6906	186649 140894	0.68 0.70	0.64 0.68	int ext
704*					14203 11794	432368 354850	0.51 0.54	0.51 0.55	int ext
49	Sweden, Kvistaberg	1.0	35 x 35′	1.0″ USNO	49 15	172 78	0.24 0.32	0.19 0.20	int ext
49*					191 53	866 368	0.20 0.47	0.22 0.29	int ext
566	USA, NEAT/GEODSS	1.0 2.2			187 4	579 24	0.25 0.52	0.18 0.47	int ext
303	Venezuela, Merida, Univ.	1.0			14	71	0.63	0.74	ext
910	France, Caussols-ODAS	0.90		 GSC	176 88	930 669	0.19 0.33	0.16 0.23	int ext
691	USA, Spacewatch	0.88 4.6	32 x 32′	1.1″ USNO	1114 458	5823 3408	0.23 0.40	0.26 0.34	int ext
691*					1898 635	10540 5261	0.20 0.34	0.21 0.31	int ext
12	Belgium, Uccle	0.85 2.1	30 x 45′	0.9″ GSC	15	69	0.23	0.13	int
12*					16 8	111 73	0.38 0.39	0.28 0.24	int ext
711	USA, McDonald Obs.	0.76 2.3	46 x 46′	1.3″ GSC	11 16	33 65	0.41 0.71	0.39 0.48	int ext
711*					12 4	45 25	0.24 0.54	0.31 0.47	int ext
121	Ukraine,	0.70	10 x 8′	2″	11	86	0.46	0.57	int

Table 7 : An accuracy of observations of the numbered minor planets observed with 0.6-m and more telescopes in 1999 and 2000(*) yrs

	Kharkov Univ.	2.8		GSC	4	69	0.61	0.72	ext
121*					9	106	0.36	0.39	int
					7	115	0.62	0.59	ext
918*	USA,	0.66			64	364	0.60	0.35	int
	Badlands Obs.	3.2		GSC	26	196	0.63	0.35	ext
557	Czech Rep.,	0.65	13 x 20′	1.6″	35	165	0.18	0.20	int
	Ondrejov	2.3		USNO	13	100	0.19	0.18	ext
557*					31	190	0.23	0.20	int
					13	136	0.25	0.26	ext
673	USA, Table	0.61	9 x 9′	0.5″	107	995	0.12	0.06	int
	Mountain	9.6		ACT	115	1468	0.16	0.22	ext
673*					77	594	0.11	0.10	int
					49	496	0.10	0.06	ext
327	China,	0.60	58 x 58′	1.7″	180	1078	0.31	0.25	int
	Peking Obs.	1.8		USNO	94	800	0.37	0.33	ext
327*					221	982	0.28	0.30	int
					61	467	0.31	0.31	ext
179*	Switzerland,	0.6			8	47	0.16	0.08	int
	Monte Generoso	4.9		USNO	7	44	0.28	0.23	ext
184*	France,	0.6	28 x 28′	0.8″	9	43	0.33	0.26	int
	Valmeca Obs.	3.6		USNO					
461*	Hungary, JATE	0.60	28 x 19′	1.1″	10	35	0.21	0.22	int
	Asteroid Serv.	1.8		USNO					
561	Hungary,	0.60	28 x 19′	1.1″	13	68	0.30	0.27	int
	Piszkesteto	1.8		USNO					
561*					11	60	0.21	0.24	int
185*	Switzerland,	0.6	23 x 15′	0.9″	5	16	0.32	0.30	int
	Jur.-Vicques	2.1		USNO					
360	Japan,	0.60	13 x 9′	1.4″	13	39	0.12	0.15	int
	Kuma Kogen	3.5		ACT					
360*					18	54	0.21	0.12	int
402	Japan,	0.60			7	28	0.14	0.11	int
	Dynic AO	3.0		GSC					
402*					15	55	0.18	0.23	int
417	Japan,	0.60			5	17	0.10	0.13	int
	Yanagida	4.8		USNO					
947	France, Sa-	0.60			11	43	0.67	0.63	ext
	int-Sulpice	3.4		USNO					
621	Germany, Ber-	0.60	11 x 10′	1.2″	17	125	0.21	0.15	int
	gisch Gladbach	3.1		USNO	17	134	0.22	0.21	ext
621*					22	152	0.14	0.12	int
					19	156	0.22	0.15	ext
750	USA,	0.60	15 x 10′	1.6″	12	56	0.41	0.38	int
	Hobbs Obs.	3.0		ACT	8	52	0.63	0.29	ext
699	USA, Lowell,	0.59	171x171′	2.5″	5849	33984	0.64	0.40	int
	LONEOS	1.1		USNO	1885	13818	1.07	0.46	ext
699*					7727	61895	0.59	0.32	int
					2169	22323	0.72	0.36	ext
118	Slovakia,	0.57	14 x 10′	0.6″	26	130	0.22	0.16	int

Table 7 : An accuracy of observations of the numbered minor planets observed with 0.6-m and more telescopes in 1999 and 2000(*) yrs

	Modra	3.3		USNO	42	262	0.37	0.30	ext
118*					14	54	0.20	0.18	int
					20	122	0.31	0.28	ext
46	Czech Rep.,	0.57	16 x 10′	1.2″	48	173	0.24	0.18	int
	Klet	3.0		USNO	6	37	0.28	0.25	ext
46*					35	142	0.22	0.19	int
					5	25	0.16	0.09	ext

Authors hope that all conclusions are obvious without of any comments. Astronomical community includes now a lot of amateur stations carring out positional CCD asteroid observations with advanced technique and high quality. Their job may be used for a decision of several scientific problems.

Our investigation seems to be the first of that kind for the MPC data and it could be continued in future.

References

[1] L'vov, V.N., Smekhacheva, R.I., Tsekmejster, S.D.,1999, EPOS - the Ephemeris Software Package for Solar System Bodies Research, *User's Guide*, Pulkovo, St. Petersburg.

[2] Bykov, O.P., On the accuracy of CCD and photo observations of asteroids and their current orbit determinations, *Proceedings of IAU Symp.,* **167** and **172**, The Hague, 1994, and Paris, 1995.

Ceres : A true Minor Planet

Christou Apostolos

1 . Introduction

Since the discovery of the first Jupiter Trojan by Max Wolf in 1906, co-orbital motion has been observed in a variety of locales in the solar system, namely the satellite system of Saturn (Dollfus 1967, Fountain & Larson 1977, Fountain & Larson 1978), the inner planet region (Bowell 1990, Mikkola *et al.* 1994, Wiegert *et al.* 1997) and, more recently, the Edgeworth-Kuiper Belt (Yu & Tremaine 1999, Nesvorny *et al.* 1999). The ubiquity of co-orbital motion is underlined by the extent of the domain in parameter space which allows this type of motion to exist. For example, on the upper limit of the mass range, Jupiter is 1/1000 the mass of the Sun, whereas in the case of Janus and Epimetheus, Saturn's mass is 10^{10} times greater than either of them.

2 . Search for main belt coorbitals

A numerical search has been carried out for known objects which are able to or currently are co-orbiting with large main-belt asteroids, and in particular (1) Ceres, (2) Pallas and (4) Vesta. The particulars of the search are described in Christou (2000b). Here we concentrate on two of the objects, (1372) Haremari and (855) Newcombia.

3 . (1372) Haremari

Minor planet (1372) Haremari has been singled out by this investigation as the object most likely to reside presently in the co-orbital resonance with a main belt asteroid, namely (1) Ceres.

The general characteristics of its motion may be demonstrated through a typical example. In the top panel of Fig. 1, we show the evolution of the relative longitude $\Delta\lambda = \lambda_{1372} - \lambda_{\mathrm{Ceres}}$ corresponding to clone -X as a function of time. There are instances where this asteroid clone executes horseshoe or tadpole librations typical of Jupiter or Mars Trojans. Its motion also exhibits other features such as transitions between different types of libration (eg near $t = 0$) and a short interval during which $\Delta\lambda$ lingers near the vicinity of Ceres. These types of dynamical behaviour are predicted in the theoretical context of eccentric and inclined Trojans (Namouni 1999) and have been observed in the short-term dynamical evolution of several near-Earth asteroids (Namouni *et al.* 1999, Christou 2000a). The situation where co-orbital dynamics are influenced by a periodic external forcing such as secular perturbations is thoroughly treated in Morais (2001). It is likely that a full quantitative treatment of the dynamics of these asteroids will require elements from both theories.

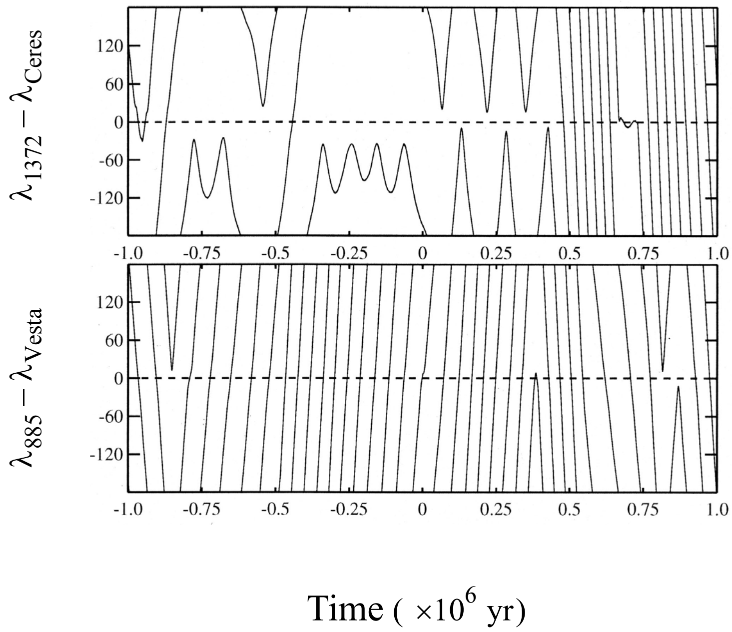

Figure 1 : Critical angle behaviour for asteroids (1372) Haremari (top) and (855) Newcombia (bottom). Due to the observational uncertainties in the initial orbital elements used in the numerical integrations the above should only be regarded as representative of their likely orbital evolution.

4 . (855) Newcombia

The motion of the transient Vesta co-orbital (855) Newcombia (bottom panel of Fig.1) is somewhat different. The average length of the libration epochs for this asteroid is noticeably reduced presumably due to Vesta's smaller mass. What appears to be a period of horseshoe libration occurs at approx. 8×10^{5} yr into the future. There is also some evidence of a modulation of the rate of precession of $\Delta\lambda$ although whether this is due to secular forcing by the planets or the result of impulsive changes in the orbit due to close encounters with Vesta remains to be seen. In view of these results we suggest that Vesta lies at the lower boundary of the mass spectrum for which co-orbital motion can exist in this challenging dynamical environment.

5 . Discussion

The ability of large asteroids to capture material in a 1:1 resonance raises some interesting possibilities concerning the smaller body population at those regions of phase space.

In the case of asteroidal dust grains ($< 10\mu m$) the narrow width of the resonant regions in semimajor axis ($\sim 10^{-3}$ AU) combined with the long libration periods for the critical argument ($\sim 10^{5}$ yr) would mean that most such particles would evolve through the resonance too fast to be captured as their orbital angular momentum is dissipated due to Poynting-Robertson drag.

On the other hand, the Yarkovsky effect operating on metre-sized fragments produces typical semimajor axis drift rates of $10^{-4}-10^{-3}$ AU/Myr (Farinella *et al.* 1998). Capture, in this case, should be possible for a non-negligible fraction of the existing population of such fragments in that region, although a dedicated study would be required to quantify, among other things, the capture efficiency. It is interesting to note that the objects discussed here lie near the upper limit (tens of km) but still within the size specturm for which the magnitude of Yarkovsky-induced drift of the semimajor axis in 100 Myr timescales is comparable to the width of the co-orbital region (Vokrouhlicky *et al.* 2001). It can thus compete favourably with collisional impulses as the cause of their current dynamical status. Such a link could be strengthened if the physical and rotational properties of these bodies, upon which the magnitude and direction of Yarkovsky dissipation are dependent, can be refined in the future.

6 . Acknowledgements

This work was supported by PPARC grant GR/L39094 and has made use of software packages available at the STARLINK network. It was carried out while the author was employed at the Astronomy Unit of Queen Mary College, University of London.

References

Bowell, E., 1990, 1990 MB, *IAU Circ.*, **5067**.

Christou, A. A., 2000a, A numerical survey of transient co-orbitals of the terrestrial planets, *Icarus*, **144**, 1–20.

Christou, A. A., 2000b, Co-orbital objects in the main asteroid belt, *Astron. Astrophys.*, **356**, L71–L74.

Dollfus, A., 1967, Un nouveau satellite de Saturne, *C. R. Acad. Sci. Paris B*, **264**, 822–824.

Farinella, P., D. Vokrouhlicky, Hartmann, W.K., 1998, Meteorite delivery through Yarkovsky orbital drift, *Icarus*, **132**, 378–387.

Fountain, J. W., Larson, S. M., 1977, A new satellite of Saturn, *Science*, **197**, 915–917.

Fountain, J. W., Larson S. M., 1978, Saturn's ring and nearby faint satellites, *Icarus*, **36**, 92–106.

Mikkola, S., Innanen, K., Muinonen, K., Bowell, E., 1994, A preliminary analysis of the orbit of the Mars Trojan asteroid (5261) Eureka, *Celest. Mech. Dynam. Astron*., **358**, 53–64.

Morais, M. H. M., 2001, Hamiltonian formulation of the secular theory for Trojan-type motion, *Astron. Astrophys*., **369**, 677–689.

Namouni, F., 1999, Secular interactions of co-orbiting objects, *Icarus*, **137**, 293–314.

Namouni, F., Christou, A.A., Murray, C.D., 1999, Co-orbital dynamics at large eccentricity and inclination, *Phys. Rev. Lett*., **83**, 2506–2509.

Nesvorny, D., Roig, F., Ferraz-Mello, S., 1999, Close approaches to trans-neptunian objects to Pluto have left observable signatures of their orbital distribution, *Astron. J.*, **119**, 953–969.

Vokrouhlicky, D., Broz, M., Farinella, P., Knezevic, Z., 1998, Yarkovsky-driven leakage of Koronis family members, *Icarus*, **150**, 78–93.

Wiegert, P. A., Innanen, K.A., Mikkola, S., 1997, An asteroidal companion to the Earth, *Nature,* **387**, 685–686.

Yu, Q-J., Tremaine, S., 1999, The dynamics of Plutinos, *Astron. J.*, **118**, 1873–1881.

Limited accuracy of asteroids track estimation at observations with CCD detectors

Biryukov Vadim, Rumyantsev Vasilij

Abstract. *Sometimes, «trail objects» were detected by CCD together with point-like ones during observations of minor planets. It is necessary to use the special methods of data processing to estimate parameters of such objects. The problem of accurate estimation of «fast» asteroids position has been considered from fundamental and applied points of view. First of all, the limited astrometric estimates of asteroid trails has been studying by means of Cramer-Rao information inequality. Cramer-Rao theorem about minimum variance bound fundamentally limit the accuracy of any estimate at a given signal-to-noise ratio. For many practical applications Maximum Likelihood Method gives asymptotically unbiased estimate closed to the «Cramer-Rao Lower Boundary». We have been investigating the properties of this method as applied to the problem of asteroid track astrometry. Moreover, the influence of the different observational conditions was considered. Numerous computer simulations show effectiveness of Maximum Likelihood Method for solution this problem.*

1 . Introduction

The problem of accurate estimation of astrometric properties of «fast» trail objects from single observation is important for predicting its positions at the next time of observation. For high precision forecast we need to know not only errors at current time, but also correlation properties of the estimate. Usage of Cramer-Rao theorem about minimum variance bound help us to investigate this problem.

2 . Image formation model

The probability function for observed Poisson image is :

$$f(\mathrm{y}|\mathrm{a}) = \prod_{k,l=1}^{N} e^{-q_{kl}(\mathrm{a})}[q_{kl}(\mathrm{a})]^{y_{kl}}/y_{kl}!$$

where $\mathrm{y} = y_{kl}$ – observed values of photoevents; $[q_{kl}(\mathrm{a})]$ - mean values of photoevents, which depends on the trail object **a**, *point spread function* (PSF) and some CCD properties. PSF is 2-D Gauss function $G(\sigma)$, where σ is a standart deviation. We take into account the finit size of the pixels, then calculating $q_{kl}(\mathrm{a})$ and integrated PSF inside of each pixel by analytical calculation. In that way

$$q_{kl}(\mathrm{a}) = b + f \cdot \int_{S} G_{kl}(\sigma, s) ds$$

where b – background, f – total trail flux, $\int_s (\ldots)ds$ – integral along segment $[(x_{begin}, y_{begin}),(x_{end}, y_{end})]$.

Hence, the problem is formulated as searching for the statistical estimate of parameters $a = (b, f, x_{begin}, y_{begin}, x_{end}, y_{end})$ of the trail object given the observed image **y** and the model $f(y|a)$.

3 . Cramer-Rao Lower Boundary

There are a lot of various methods for parameters estimation. The quality of the «ideal method» is defined by Cramer-Rao theorem about minimum variance bound [1]. This theorem states that difference between covariance matrix *C* of unbiased estimator and inverse *Fisher matrix* is a positive semi-defined matrix. Denote this as

$$C \geq inv(F(a))$$

where *Fisher matrix* is

$$F_{ij}(a) \equiv \langle -\frac{\partial^2}{\partial a_i \partial a_j} \ln f(y|a) \rangle, i, j = 1, \ldots, n$$

k,l = 1, ... , n; n – number parameters.

It is necessary to note that Cramer-Rao theorem assert only existence of minimum variance bound, but don't show the method to achieved it. Luckily, for many practical applications Maximum Likelihood Method gives asymptotically unbiased estimate closed to the Cramer-Rao Lower Boundary.

Table 1 : Model observation conditions

Telescope	
Aperture diameter	640 mm
Relative focal distance	1.4
Linear central obscuration	0.44
CCD	
Pixel	9x9 mkm
Quantum efficiency	0.4
Dark current	0.5 el/sec
Read-out noise(rms)	15 el
Sky	
Background	20^m/arcsec^2
FWHM	2 arcsec
Exposure Time	120 seconds

4 . Limiting precision of the trail object parameter estimate

Consider the properties of the trail object estimate corresponding to Cramer-Rao theorem. We used the diagonal of covariance matrix *C* as a liming variance estimate. As example, we chose observation model for the telescope T-64 of the Crimean Astrophysical Observatory [2].

Modeling was carried out for trail objects with magnitudes from 11^m to 16^m, and velocities from 2 arcsec/min to 40 arcsec/min. Some of sample images are represented in Fig.1.

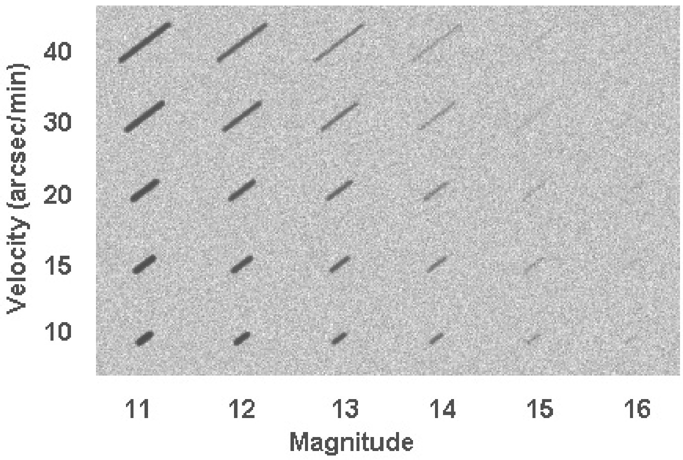

Figure 1 : Model images of trail for 2 min exposure on AT-64

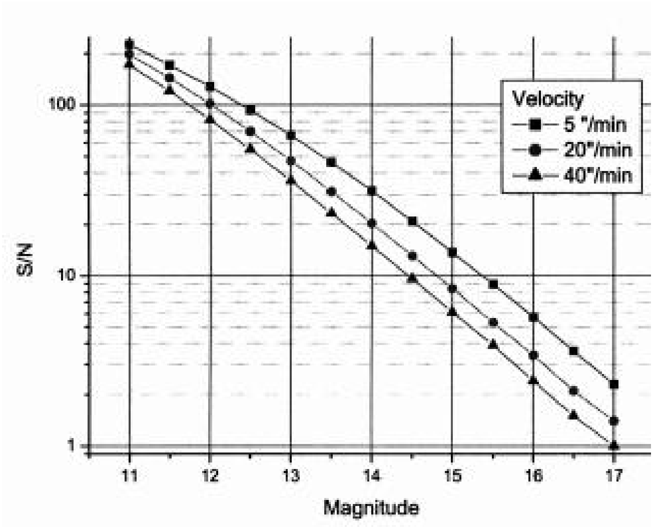

Figure 2 : Limiting signal-to-noise ratio for trail objects

Calculations shows that estimates of the trails beginning and ending coordinates are correlating with each other. More convenient parameters are vector velocity (absolute value and direction) of the trail object and its center coordinates. But for all that, last two parameters nevertheless highly correlating. Correlation coefficient changed from 0.5 to 0.94 for trail velocities 5 arcsec/min and 40 arcsec/min, correspondingly. That is why it's necessary to project errors of the trail position on sagittal and transversal directions (along and across motion). In the Fig.3 we can see corresponding errors versus trail magnitudes and velocities.

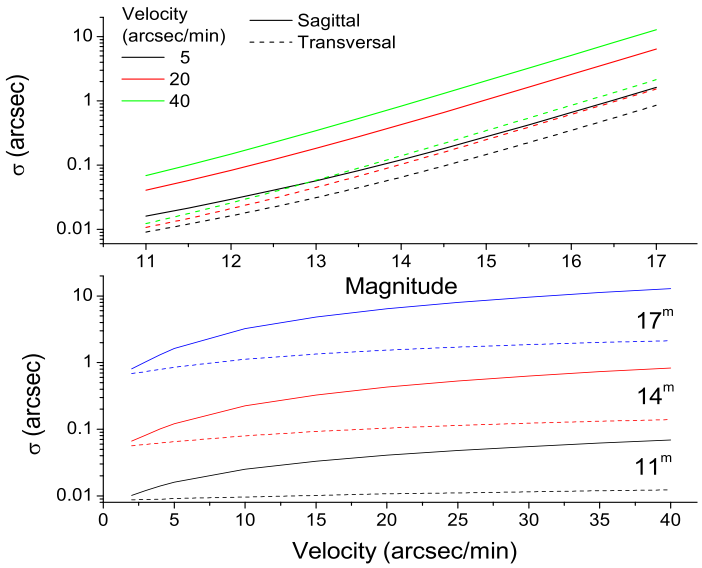

Figure 3 : Trail's position error

Estimates of object velocity and trail position angle is not correlating with estimates of other parameters.

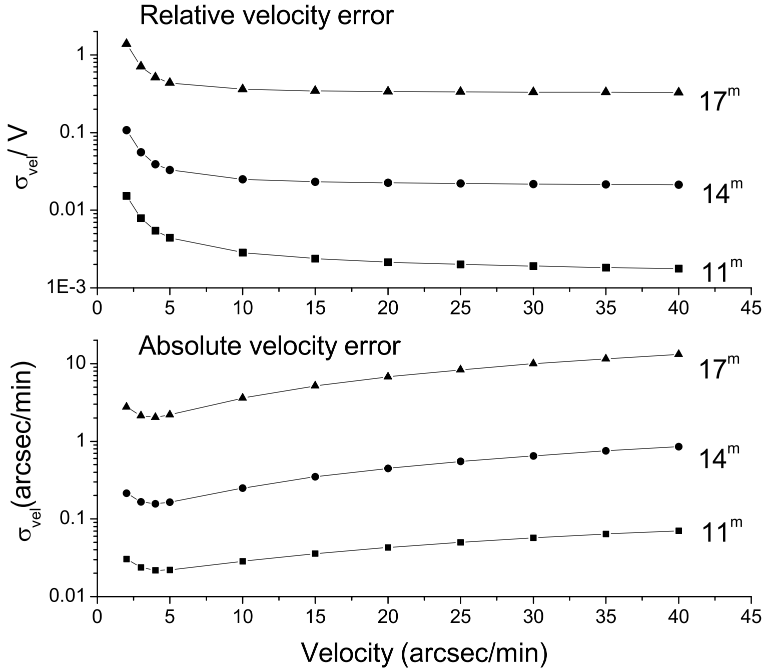

Figure 4 : Velocity estimates errors

Fig.4 shows dependence of absolute and relative velocities error versus velocity. One can see that for velocity more than 15-20 arcsec/min absolute error of the estimate is approximately proportional to the velocity. This is equivalent that relative error is constant. The angle error of the trail increased for velocities less then 5 arcsec/min (Fig.5). It means that the trail object practically does not differ from point-like ones for given observation conditions.

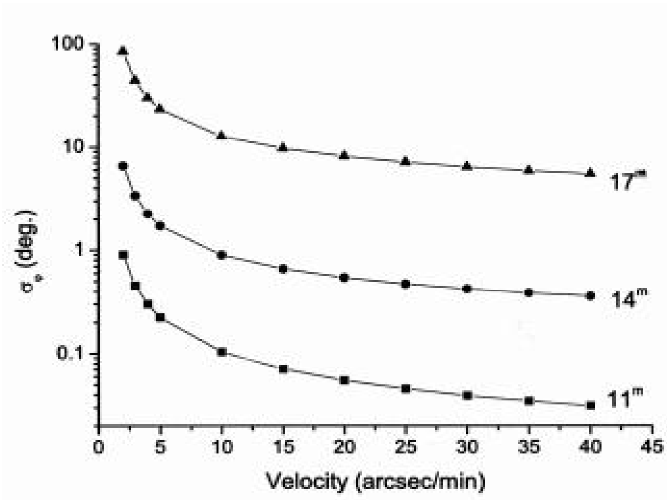

Figure 5 : Angle estimates errors

Consider 1-day **linear** position forecast of moving object from observing trail. Choose object coordinates in a day's time (linear extrapolation) as main parameters instead of trails center coordinates. Then we calculate Fisher matrix and limiting covariance matrix C, which fully characterized properties of our forecast. Correlation properties of the coordinates and velocity estimates were changed. First of all, correlations between estimates of velocity and positions appears. On the other side, correlation coefficient between x and y positions slightly decreased. For better visualization results of the forecast we simulated random samples with covariance matrix C. On the Fig.6 presented results of simulations for different velocities and magnitudes of trail objects. It shows that the size of error box of 1-day forecast is same as the size of field of view of telescope AT-64 equipment (35x53 arcmin). This fact allows successfully detecting «fast object» 1-day later of single trail observation.

As was mentioned earlier, Maximum Likelihood (ML) method often gives estimate closed to the Cramer-Rao Lower Boundary. In our case, numerous computer simulations shows that empirical covariance matrix of ML-estimates is in a good agreement with the limiting covariance matrix. Hence, if the model of image formation is adequate to observations then ML-estimates are useful and effective.

The authors are grateful to V.Yu.Terebizh, for valuable comments. This work was supported in part by the *Russian Foundation for Basic Research* under grant No 99–02–18040.

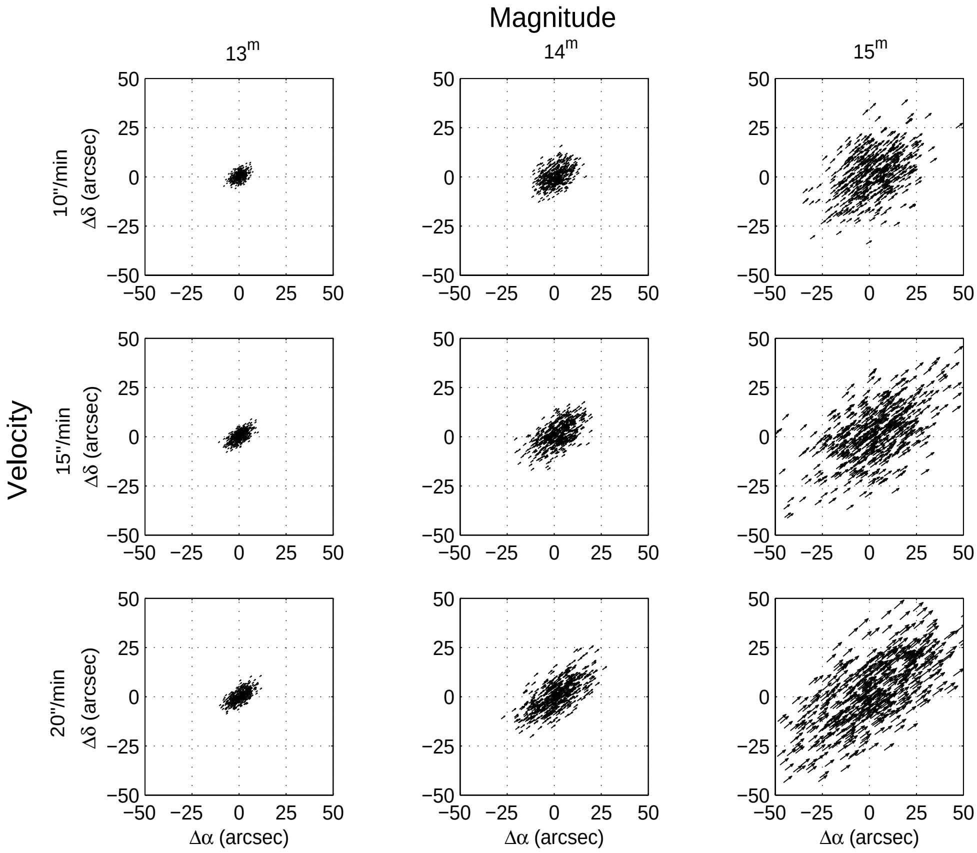

Figure 6 : 1-day forecast of the asteroid position

References

[1] John Wiley & Sons Ltd., 1984, «Handbook of Applicable Mathematics» (eds. by E. Lloyd & W. Ledermann), Volume VI: Statitics, PART A.

[2] The Crimean CCD telescope for the asteroid observations, *Ceres 2001 Workshop*, Paris, 2001, this volume.

New method for asteroid identification with the use of Pulkovo apparent motions parameters

Bykov O.P., Komarova N.O.

Abstract*. Authors take into considerations the first and the second derivatives of spherical coordinates of celestial body or the values of its angular velocity, acceleration, positional angle and curvature of trajectory as the additional Apparent Motion Parameters for an identification of the observed objects with the catalog's one.*

Modern CCD observations of asteroids give us several close accurate positions distributed along a short arc of celestial sphere. Usually such coordinate set contains 3–5 asteroid positions per night. It's sufficient for a calculation of the first derivatives of asteroid coordinates or the angular velocity and position angle of asteroid motion. Together with traditional data for an identification of the asteroids, i.e. the normal places, additional information about parameters of asteroid motion may be used in the process of the fast and reliable identification of the same object during a long time interval after the last its observation.

On the base of original Pulkovo EPOS Software [1] and Apparent Motion Parameters Method (the APM-method) developed by Dr.Kisselev and his colleagues [2–4] we had elaborated a new method for asteroid identification by means of the first and second derivatives of its spherical coordinates or with the use of anagular velocity and acceleration, positional angle and curvature of asteroid motion. We are sure that only a nearness of observed and calculated asteroid positions in a given moment of UT is not sufficient for a correct identification of observed celestial object with catalogue's one. We control also a coincidence of derivatives and Apparent Motion Parameters in procedure of an asteroid identification. It is obvious that preliminary orbital elements derived from limited short arc positional asteroid observations are not exact and can give large (O–C) residuals during several months after orbit determination. But an influence of the errors of orbital elements to the first and second derivatives of asteroid coordinates and also to the Parameters of its Apparent Motion is much smaller then to the its positions. This fact was established by our practice and may be confirmed theoretically. It's a basis of our method for an identification of observed celestial bodies with their orbital catalogue nominations.

Our method was tested with the vast examples and may be recommended to the real identifications as in the Minor Planet Center as also in the professional and amateur observatories.

An examples of our identifications are given in the Tables 1, 2.

Table 1 : Geocentric coordinates and their the first derivatives for celestial objects in sky area (9 23 < RA < 9 27, 19 00 < DEC < 20 21) at the moment 1999 02 18.9000 DT

Part 1. Identified pairs of asteroids

Num/Name	RA h m s	DEC ° ′ ″	dRA s	dDEC ′ ″	Mgn	Op	Obs	Cat
1	2	3	4	5	6	7	8	9
2000 JF66	9 23 19.99	19 23 59.6	– 50.32	+ 6 16.2	18.3	2	54	3
1999 CQ26	9 23 20.53	19 23 35.0	– 49.87	+ 6 07.0	17.8	1	12	13
1997 RR1	9 24 16.22	19 14 57.5	– 63.48	+ 4 44.3	17.7	2	31	13
NMP 15899	9 24 16.22	19 14 57.3	– 63.48	+ 4 44.3	18.4	6	51	2
1999 CR26	9 24 17.87	20 00 18.4	– 51.55	+ 3 49.1	18.1	1	10	13
2000 KW17	9 24 17.92	20 00 17.7	– 51.52	+ 3 48.8	17.9	4	44	3
1997 CR29	9 24 33.32	19 09 10.9	– 4.81	+ 25.7	23.4	3	29	13
NMP 15883	9 24 33.32	19 09 10.9	– 4.81	+ 25.7	23.4	3	29	2
1999 CP28	9 24 44.30	20 20 58.0	– 54.64	+ 2 07.2	18.0	1	10	13
2000 JC30	9 24 44.32	20 20 56.7	– 54.61	+ 2 06.6	18.1	2	28	8,9
1999 DS1	9 25 52.06	19 49 34.5	– 50.95	+ 3 44.8	17.5	3	99	8,9
NMP 27218	9 25 52.06	19 49 34.3	– 50.95	+ 3 44.8	18.1	4	125	2
1997 UY14	9 26 52.31	19 28 03.4	– 49.55	+ 3 37.4	17.5	2	45	13
NMP 14992	9 26 52.31	19 28 03.7	– 49.55	+ 3 37.4	17.6	19	113	2

Table 1 : Geocentric coordinates and their the first derivatives for celestial objects in sky area (9 23 < RA < 9 27, 19 00 < DEC < 20 21) at the moment 1999 02 18.9000 DT

Part 2. Unidentified asteroids

1	2	3	4	5	6	7	8	9
1997 WK5	9 22 40.42	20 19 07.0	– 66.26	+ 5 30.4	18.8	1	9	9,13
2000 HL52	9 22 47.30	19 55 34.1	– 50.79	+ 3 45.9	17.7	3	80	8,9
2000 KS41	9 23 05.28	19 15 22.9	– 52.97	+ 4 48.8	18.4	1	13	3-9
1999 BL10	9 23 16.02	19 17 29.1	– 48.15	+ 6 26.0	17.8	1	22	3,8
2000 QR117	9 23 24.27	20 18 01.2	– 99.43	– 6 47.5	19.1	1	21	3,8
1999 CO28	9 23 35.11	20 08 52.8	– 54.23	+ 3 19.4	18.0	1	12	3-13
2000 KV70	9 23 42.29	20 12 45.2	– 51.00	+ 7 18.1	18.1	1	15	3,8
1997 SC3	9 24 28.46	20 02 47.8	– 56.52	+ 2 46.1	19.9	3	26	3

Table 1 : Geocentric coordinates and their the first derivatives for celestial objects in sky area (9 23 < RA < 9 27, 19 00 < DEC < 20 21) at the moment 1999 02 18.9000 DT

Part 2. Unidentified asteroids

2000 LT16	9 24 34.09	20 16 07.7	– 51.13	+ 6 03.1	19.2	1	16	3-9
9066 P-L	9 24 39.43	19 59 12.7	– 65.38	+ 3 10.5	19.0	29	30	3,8
2000 EA139	9 24 39.37	19 04 57.9	– 43.75	+ 6 07.6	18.7	7	75	3
2000 KK75	9 24 53.08	19 37 31.7	– 52.14	+ 6 05.0	18.1	14	25	3-9
1999 CV6	9 25 05.98	19 59 23.4	– 94.46	– 12 38.8	18.4	1	16	3-13
1999 CR28	9 25 11.03	19 04 38.2	– 54.83	– 9.4	17.5	1	15	3-13
1999 DS1	9 25 52.06	19 49 34.3	– 51.00	+ 3 45.6	18.3	1	9	13
2000 JV69	9 26 42.51	19 16 28.6	– 51.52	+ 8 05.4	18.7	1	17	3-9
2000 KY13	9 26 45.11	20 07 08.1	– 50.99	+ 4 02.5	18.7	7	33	3
1999 DT1	9 26 49.37	19 42 16.0	– 67.25	– 2 41.9	18.0	1	15	3-13
1999 CE5	9 26 52.63	19 21 14.1	– 54.21	+ 3 11.0	18.6	4	40	3
NMP 739	9 26 59.13	19 01 24.9	– 47.75	+13 46.3	11.6	65	248	2
1994 AF10	9 27 06.02	19 23 43.4	– 50.86	+ 3 39.0	18.3	1	9	13

In the Table 1 all known celestial objects which might be seen in 1.5 × 1.5 square degrees field of view at moment 1999 Feb. 18.9000 DT are presented. The first column contains the nomination for the Unnumbered minor planet and number for the Numbered one. In column 2 and 3 the asteroid coordinates RA and DEC are given as they were calculated by EPOS Software on the base of several Bowell's orbital catalogues taken from Internet pages of the Lowell observatory. The next two columns give the first and second derivatives of coordinates (dRA/dt and dDEC/dt per day). Column 6 presents a magnitude of asteroid. Columns 7 and 8 show an observational basis (number of oppositions and positions) which were used for asteroid orbit determinations. The last column gives the number of orbital catalogue used. The 3d catalogue is a version from September 2001, the 13th catalogue is one of the old version (1998).

We can see a good agreement of old and poor systems of orbital elements with new and rich (in the sence of observational base) ones for the same asteroid. Also it is obvious the full coincidence of calculated and observed positions together with the first derivatives are the main indicator for correct identifications. With such Tables we can obtain a lot of new identifications immediately after carefull analysis of their content. For example, there are 1999 CP28 = 2000 JC30, 1999 CR26 = 2000 KW17, 1999 CQ26 = 2000 JF66, 1999 DS1 = NMP 27218, 1997 CR29 = NMP 15883 and others (see the first part of the Table 1). The second part of Table 1 shows the unidentified asteroid in selected sky field and illustrates how much asteroids with different velocities and magnitudes move in this celestial area.

First of all we pay attention on the asteroids which have old orbital systems based on the one opposition observations (6-12 positions only). Sometimes we identify them with new discovered object.

Table 2 : Geocentric positions and the Apparent Motion Parameters of the 1994 AF10 and 1999 DS1 for the Epoch 1994 01 05.0000

Num/Name	RA h m s	DEC ° ′ ″	Velocity arcsec	Accel. arcsec	Pos.ang. degree	Curvat.
1994 AF10	9 04 19.07	20 40 47.2	586.436	16.789	292.417	2.04382
NMP 26875	9 04 19.08	20 40 46.4	586.479	16.805	292.428	2.05055
1999 DS1	8 49 16.50	21 37 11.9	629.251	16.950	292.431	2.08258

In Table 1 an object 1994 AF10 might be identify with 1999 DS1 : its derivatives are close to the same values for 1999 DS1 and a large residuals (O–C) may be explaned by bad system of orbital elements for 1994 AF10 when they were used five years later after their determinations. But special investigation of this problem shows that 1994 AF10 is the NMP 26875 and in the Table 1 its appearence is uncorrect due to errors of its old orbit.

References

[1]. L'vov, V.N., Smekhacheva, R.I., Tsekmejster, S.D., 1999, EPOS - the Ephemeris Software Package for Solar System Bodies Research, *User's Guide*. Pulkovo, St. Petersburg.

[2]. Kiselev, A.A., Bykov, O.P., 1973, *Sov. Aston. J.*, **50**, 1298-1308.

[3]. Kiselev, A.A., Bykov, O.P., 1976, *Sov. Aston. J.*, **53**, 879-888.

[4]. Bykov, O.P., 1989, Problems of Universe investigations, **12**, 328-358, Leningrad, (in Russian).

Triumph of the Laplacean ideology for preliminary orbit determination in the CCD epoch *(abstract)*

Bykov Oleg

The epoch of supremacy of CCD technique allows us to elaborate the new approach to the problem of observations and identification of any celestial body moving on the background of stars. The fundamental base for such approach is the Classic Laplacean Method of initial orbit determination and its development.

Due to the accurate star catalogues and computers one can calculate several astrometric positions of any celestial object and its angular velocity by means of statistical processing of the set of object's coordinates almost in a real-time of CCD observations. These four parameters (namely RA, DEC, dRA/dt and dDEC/dt) are usually enough to determine its circular or parabolic preliminary orbit which may be useful for identification of observed object or for ephemeris service during several close nights or weeks. In this manner we can investigate each CCD frame for the search of small Solar system bodies.

The algorithms and software were developed in Pulkovo observatory for the fast analysis of any CCD frame where the moving celestial objects were detected. Due to this approach we can get new information as «by product» of dominating astrophysical CCD observations.

Asteroid photometric center determination *(abstract)*

Grynko Yevgen, Shkuratov Yu

Due to irregular shape of minor planets an error arises at precise measurements of asteroid position through astrometric observations. The photometric center of asteroid does not always coincide with the real position of asteroid geometric center. It is caused by the revolution of asteroid on its axis and by the variations of phase angle and rotation axis orientation. To investigate this error we used computer experiments. Our experiment simulates illumination and observation of asteroid revolving on its axis. At first we generate a model of a body with irregular shape and with adjusted degree of irregularity. It is represented in the computer memory as an arbitrary polyhedron, i.e. as the succession of triangular facets attached to each other. Then a beam of rays comes in the body surface at the known illumination/observation geometry. One can put a normal to each facet and determine local angles of incidence and emergence and to apply some indicatrix for surface element. Lommel-Seeliger light-scattering indicatrix was taken, but it should be emphasized that any other indicatrix could be involved in the analysis. Ray tracing procedure is realized to determine the part of the body which is illuminated and visible simultaneously, i.e. to derive the law of brightness distribution over asteroid. Our model allows derivation of brightness distribution law for a body with any shape and with any degree of deviation from spherical shape.

After that we can calculate photometric center at the given phase of rotation averaging out over visible elements taking into account the contribution of each element to the reflected flux. The coordinates of the real center of asteroid can also be easily determined. In this way it is possible to track how the photometric center moves about geometric one as model parameters change. Through modeling we obtained a number of time dependencies and diagrams of photometric center dispersal for a set of phase angles and for different values of irregularity parameter at arbitrary rotation axis orientation.

On the displacement of asteroid photocentre due to surface scattering *(abstract)*

Lupishko D.F., Tungalag N., Shevchenko V.G.

The recent increase of the accuracy of ground-based astrometric observations of asteroids due to the application of CCD-detectors and the use of highly accurate HIPPARCOS asteroid data make essential taking into account the asteroid displacement caused by nonuniform brightness distribution on asteroid apparent surface (limb-darkening, albedo distribution, etc). For this purpose, the numerical modelling of asteroid brightness distribution for different scattering laws (Lambert, Lommel-Seeliger, Hapke, theoretical and empirical Akimov laws) was carried out. The numerical photometric model of an asteroid which provides the arbitrary i) asteroid shape, ii) albedo distribution on the surface and iii) scattering law was used. The triaxial ellipsoid with semi-axis ratio a:b:c = 2:1.4:1 was chosen as a figure of the model. The calculations were carried out for the equatorial aspect of an asteroid. In this case, the point on the photometric equator of apparent asteroid disk, on the left and on the right of which the integral brightnesses are equal, determines the photocentre position.

It was shown that the photocentre displacement essentially depends on the asteroid shape, phase angle and light scattering. Its value can reach (0.3 - 0.4)R, where R is the asteroid angular radius. For the main-belt asteroids with angular sizes > 0.1" the displacements can reach the value of 0.02² and even more (up to 0.06-0.10" for the largest asteroids 1 Ceres, 2 Pallas, 4 Vesta and 324 Bamberga). For the NEAs the photocentre displacements can reach large values because of the large values of phase angles. For example, the Apollo-asteroid 4179 Toutatis in December of 1992 approached the Earth to 0.024 AU, and its angular size and phase angle were equal to 0.2" and 100&deg, respectively. In this case, the photocentre displacement was equal to 0.07". Such values exceed the accuracy of space-based astrometric measurements (0.015-0.020") and of the modern ground-based ones (or are compared with them) [1,2]. Therefore, taking them into account can noticeably improve the accuracy of asteroid position determination.

The practical recommendations on the determination of the asteroid photocentre displacements are given.

References

[1] Hestroffer, D., Viateau, B., Rapaport, M., 1998, *Astron. Astrophys.*, **331**, 1113-1118.

[2] Owen, Jr.W.M., Synnott, S.P., Null, G.W., Modern astrometry and astrodynamics, *Proceed. of Int. Conf. Vienna* (Austria), 25-26 May, 1998. R.Dvorak, H.F.Haupt, K.Wodnor (eds.), 1999, 89-101.

Observational programs for asteroid mass determination

Thuillot W., Bec-Borsenberger A., Rapaport M., Arlot J.-E., Bange, J.-F.

Résumé. *La détermination des masses des astéroïdes reste encore un problème difficile à résoudre, mais les questions concernées par ce problème sont fondamentales: elles concernent l'origine et l'évolution de ces objets. Parmi plusieurs méthodes applicables à ce problème, l'étude des déflexions gravitationnelles se produisant au cours de rapprochements a été utilisée avec succès. Nous donnons dans cette communication des informations sur ce type de résultats et sur des programmes d'observation actuellement menés d'une part sur le Méridien automatique de Bordeaux, d'autre part sur un télescope de l'Observatoire de Haute-Provence.*

Abstract. *The determination of the asteroidal masses is one of the difficult problems to solve in order to have a better knowledge of the asteroids, their origin and their evolution. Among several methods, the observation of close encounters between asteroids has been successfully applied for this purpose. We will give informations upon some previous results obtained and upon our observational programs performed both at the automatic meridian circles of the Bordeaux Observatory and at the Haute-Provence Observatory in France.*

1 . Introduction

In October 2001, more than 30 000 asteroids are numbered and many physical characteristics of these objects are studied and estimated thanks to photometric or spectroscopic methods. But despite several observational programs and the large availability of astrometric archives, the asteroid masses determination remains a difficult problem to solve. In recent papers, for example, Michalak (2000, 2001) gives a set of mass estimates deduced from different methods and it appears that only 21 asteroid masses are «accurately» known to this date. In this list, only 7 masse values are known at better than 10%. All the largest asteroids themselves have better determined masses since only the last years. Hilton (1999) shows the historic evolution of the mass of Ceres, Pallas and Vesta and it appears that these masses have now uncertainties of 1%, 3% and 7%, (respectively).

A better knowledge of the asteroid masses will induce improvements in several domains and in priority the following ones :

- First at all, assuming that the shapes and sizes of these objects is deduced from other observational data (stellar occultations, photometry), we can then get accurate values of the densities and therefore confirm or infirm several assumptions related to their origin and evolution. Taxonomic classes could then be investigated by means of the study of the dynamics families.

- Second, we will access to more accurate ephemerides of Mars and Moon-Earth barycenter only by a better knowledge of the asteroids masses. This is the main difficulty that forbid to have benefit of the full theoretical accuracy of the dynamical models. The actual ephemerides of Mars have uncertainties of several hundred of meters due to the uncertainties on the asteroid masses. Improved ephemerides will then allow to get accurate preparation and interpretation of the next space missions to Mars and to investigate the search of small relativistic effects.

In this paper we present several results obtained and projects to solve this problem of the asteroid mass determination by means of observational programs to survey close mutual encounters. This work is developed in France at Bordeaux Observatory, at the Institut de Mécanique Céleste (Paris) and at the Haute-Provence Observatory.

2 . The close encounters method

The astrometric measurements of asteroids involved in close encounters have been proved to be a powerful tool to get mass estimates. Positions of a target asteroid are observed before and after an encounter, and the mass of the perturbing object can be deduced from the orbital deflection observed (Fig. 1). In fact, two ways are possible to apply it :

- long term ground based observations (new accurate observations and use of archived observations), which imply to take into account only the more accurate data and to be aware of the mutual perturbing effects, eventually due to other asteroids, as explained below;
- very accurate short term observation by space probes. This has been possible from the data acquired during Hipparcos mission and this will be possible thanks to the next GAIA mission.

Several authors already published predictions of such events (Kuzmanoski and Knezevic 1993, Hilton et al. 1996, Viateau and Rapaport 1997, Hilton 2001, Galad 2001).

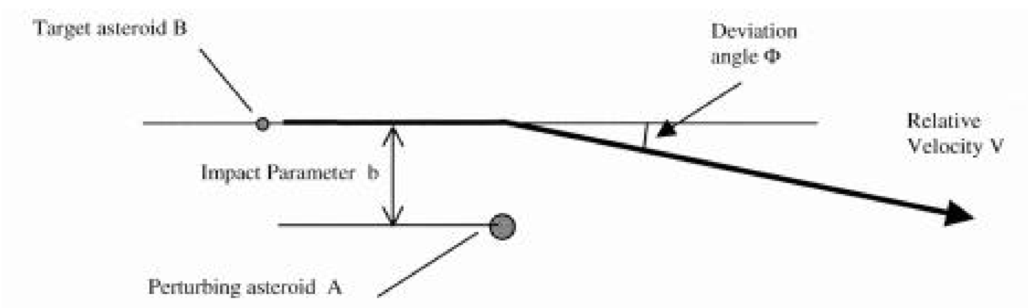

Figure 1 : Geometric conditions during close encounters of asteroids

3 . Observations and mass determination made at Bordeaux Observatory

Astrometric observations of asteroids with the meridian circle of Bordeaux began 15 years ago in the frame of the preparation of the Input Catalog of the astrometric satellite Hipparcos. During the period 1985-1991, 48 asteroids were intensively observed with the photoelectric meridian circle working at that time at Bordeaux Observatory. However from 1988 onwards, it was clearly demonstrated at Flagstaff (Stone et al.1996) that a CCD detector mounted at the focus of a meridian circle and working in drift scan mode could give a positional internal error of less than 50 mas up to V=15-16. A first 512x512 pixel CCD was built at Bordeaux Observatory in 1994. A second larger camera (1024x1024) was mounted in June 1996. Table 1 gives the main characteristics of the Bordeaux Meridian Circle. A more extensive description of the instrument and image processing can be found in Viateau et al (1999).

Table 1. Main characteristics of the Bordeaux Meridien circle

Diameter of front lens	202 mm
Focal length	2368 mm
Type of detector	Thomson 7896M
Number of pixels	1024x1024
Pixel size	19 μ
Pixel field	1.65 arsec
Declination field	28 arcmin
Magnitude range	8.5<V<16

Web site : http://www.observ.u-bordeaux.fr/

Since the beginning of our observation activity, many data concerning the astrometry of asteroids have been collected at Bordeaux; many of them are contained in the files of the Minor Planets Center. Using the data obtained in the various observatories, we searched to obtain masses using the perturbations of the bigger asteroids on well selected targets. The mains results obtained concern :

1 CERES : We used 9 asteroids in order to improve the mass of Ceres (Viateau & Rapaport, 1998).

11 PARTHENOPE and 4 VESTA : We succeeded (Viateau & Rapaport, 1997) to give the first determination of the mass of Parthenope, using a very close encounter with 17 Thetis. We later noticed that Thetis was also strongly pertubed by 4 Vesta and determined simultaneously the masses of Vesta and Parthenope with a determination of their coefficient of correlation.

16 PSYCHE and 121 HERMIONE : We determined a mass for these two asteroids from their perturbations on 94 Aurora and 278 Paulina respectively (Viateau 2000).

Our current program of observations with the CCD meridian circle concerns mainly asteroids which are targets (as May or Pompeja for Ceres) or which can perturb the targets.

4 . Mass determination made at IMCCE and observation program at Haute-Provence Observatory

Hipparcos data : At the Institut de Mécanique Céleste et de Calcul des éphémérides (IMCCE, formerly Service des calculs et de mécanique céleste du Bureau des longitudes), a determination of asteroid masses was performed after the Hipparcos mission. An estimate of the mass of Ceres thanks to an encounter with 63 Ausonia (Bange and Bec-Borsenberger 1998) and of 20 Massalia thanks to a close encounter with 44 Nysa were obtained (Bange 1998).

Uncertainties of 13% and 17% (respectively) were estimated but these results were issued from very accurate measurements on short time span : 52 observations spanning 4 years instead of 50 years currently necessary to other works using ground-based observations.

GAIA project for asteroid mass determination : A list of encounters occurring close or inside the time span mission GAIA has been computed (Bange and Bec-Borsenberger 1999). Asteroids with diameter greater than 50 km (targets) and 120 km (perturbing asteroids) were considered. A criterion involving the impact parameter, the relative velocity and the perturbing mass was used to select the most significative events on the 2004-2014 time span. 115 events involving 31 perturbing objects and 82 target asteroids are selected. In a further work (Fienga *et al*. 2002) a more complete list will be published.

Ground based observation Program at OHP: Starting from the end of 1998, we decide to include a selected list of GAIA asteroids in our observational programs with the CCD imaging system of Haute-Provence Observatory (OHP). The main characteristics of this sytem are given in **Table 2**. It allows us to get astrometric measurements by means of stellar calibration (mainly USNO-A2 or TYCHO2 catalog) in a 11.8 arcmin field. 65 asteroids are now concerned with this program. A first estimate of the accuracy was obtained in a peculiar study of 146 Lucina based on more than 600 measurements (Thuillot, Kikwaya and Rocher, 2001) where a preliminary rms of 90 mas was obtained. At this date, 3225 observations have been performed as given in **Fig. 2** (where data concerning 636 observations of 146 Lucina are not included).

Table 2. Main characteristics of the imaging system at Haute-Provence Observatory (T120)

Diameter	1.20 m
Focal length	7.2 m
Type of detector	Tektronix SITe
Number of pixels	1024x1024
Pixel size	24 µ
Pixel field	0.69 arsec
Field	11.8 arcmin
Magnitude range	V < 21

Web site : http://www.obs-hp.fr/

5 . Some problems occuring in the determination of masses from ground based observations

The importance of the problem of the dynamical model used in the problem of the determination of asteroids masses from ground based observations can be illustrated by the Bordeaux determination of the mass of 16 Psyche. The density of Psyche derived from the value of its mass deduced from the Bordeaux observations is smaller than expected. Michalak (private communication) gave us probably the good explanation of this result. He finds that the considered target, 94 Aurora, used for the determination of the mass of Psyche, is perturbed by another asteroid, 96 Aegle, not considered by Viateau and Rapaport; taking into account the perturbations of this object, he determines for the mass of Psyche a clearly better result. This example is a good illustration of the necessity to have a complete dynamical model taking into account the perturbations of several asteroids on the considered target and this is not always an easy task. This problem is all the more important with ground based observations because we need to consider the observations of the pertubed target on a long time interval due to the weakness of the perturbing effects. Another problem for the ground based observations is the determination of the mass of Pallas. Because of the high values of the inclination to the ecliptic (35°.7) and of the eccentricity of its orbit (0.18), close encounters of 2 Pallas with other asteroids are rare. The best encounters between Pallas and Ceres occured in the 19th century and the use of these data is not an easy task. After Michalak (2000), the best targets for the determination of the mass of Pallas are 9 Metis and 582 Olympia which have been included in our program.

6 . Conclusion

We have presented here a summary of results obtained in search of asteroid mass determination, both at Bordeaux Observatory and at Institut de Mécanique Céleste (IMCCE, Paris). Observational programs are pursuing both at the Automatic meridian and at the imaging system of Haute-Provence observatory (T120/OHP). The space mission GAIA will allow us to observe asteroids involved in close encounters and to determine accurate masses of around 100 asteroids. Ground-based observations will be certainly a precious help to analyze several of these events when GAIA could not observe both before and after the encounters and possibily to extend the number of measurable masses. The determination of asteroid masses appear to be a hard task since only a very few number of these objects have known masses until now (21 at this date). But these masses, combined with shape and size measurements, can lead to fundamental knowledge upon the origin and evolution of these solar system objects. Furthermore, this lack of mass values appear to lock the access to accurate dynamical model of Mars and of the Moon-Earth barycenter. Therefore several domain such as relativity tests, space missions preparation and analysis, and determination of dynamic reference frames will get benefit from this research.

.

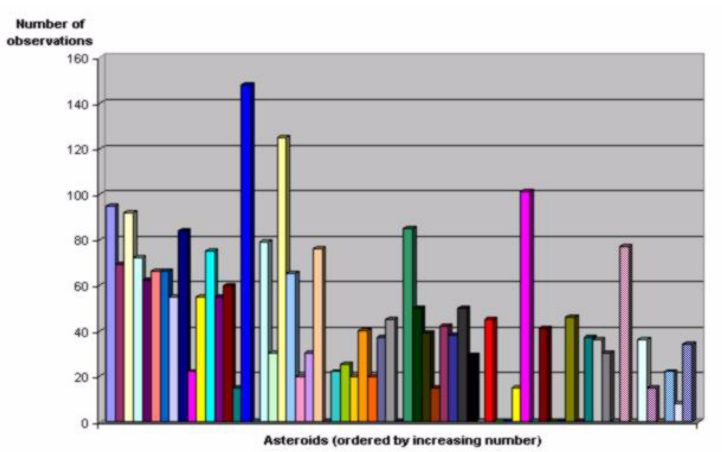

Figure 2 : Overview of astrometric observations of asteroids made at OHP (1999-2001)

References

Bange, J.-F., 1998, *A&A,* **340** L1-L4.

Bange, J.-F., Bec-Borsenberger, A., 1997, Determination of the masses of minor planets, *ESA Symp. Venice'97*, ESA **SP-402**, 169.

Bange, J.-F., Bec-Borsenberger A., 1998, Close encounters of large asteroids during the GAIA mission , GAIA Workshop, Torino Obs.

Fienga, A. Bange, J.-F., Bec-Borsenberger, A. , Thuillot, W., 2002, Close encounters of asteroids before and during the ESA GAIA Mission, *A&A* (*submitted).*

Galad, A, 2001, *A&A,* **370**, 311.

Hilton, J.L., 1999, *Astron. J.*, **117**, 1077.

Hilton, J.L., 2001, http://aa.usno.navy.mil/hilton/asteroid_masses.htm.

Hilton, J.L.., Seidelmann, P.K., Midour, J., 1996, *Astron. J.,* **112**, 2319.

Kuzmanoski, M., Knezevic, Z., 1993, *Icarus,* **103**, 93.

Michalak, G., 2000, *A&A,* **360** (Paper I).

Michalak, G., 2001, *A&A,* **374** (Paper II).

Stone, R.C., Monet, D.G., Monet, A.K., Walker, R.S, Ables, H.D., 1996, *Astron. J.,* **111,** 1721.

Thuillot, W., Kikwaya, J.-B. Rocher, P., 2001, Satellites of asteroids*, Note Sc. et Techn. de l'IMCCE* **S076**.

Viateau, B., 2000, *A&A,* **354**, 725.

Viateau, B., Rapaport, M., 1997, *A&A,* **320**, 652.

Viateau, B., Rapaport, M., 1998, *A&A,* **334**, 729.

Viateau, B., Rapaport, M., 2001, *A&A,* **370.**

Single nignt positional CCD observations of unknown celestial body : what's a problem?

Bykov O.P.

Mass positional CCD observations of celestial bodies moving against the background of reference stars are characterised by a high accuracy, a large efficiency and unlimited dencity of distribution of observed positions along a short arc of celestial sphere. Now these CCD-observations have a good star and orbital catalogues services. There are also various astronomical program systems for the fast processing of modern CCD asteroid observations. In Pulkovo observatory we use EPOS Software [1]. Only this Software can exactly calculate the first and second derivatives of coordinates for any celestial body having a known orbit and can also calculate the values of angular topocentric or geocentric velocities and position angle, angular acceleration and curvature of visible trajectory. The last four parameters were taken into consideration by Pulkovo astronomers as the Apparent Motion Parameters [2]. These parameters are an additional observational information on celestial object motion. They may be obtained by means of linear or square approximations of crowded coordinate sets obtained during single or several successive nights observations [3].

In these circumstances the observer himself can identify all known celestial objects which could be seen in his telescope field of view during a time of observations. It may be done by means of preliminary calculation of catalogue positions for all known objects at given UT moment. After this identification, initial circular, parabolic or sometimes elliptical orbits for the unknown asteroids having several positions per night may be calculated with the help of the Apparent Motion Parameters Method (the AMP-method) created by Dr.A.A.Kisselev and his colleagues in Pulkovo Observatory [3,4]. The AMP-method is a further development of the Classical Laplacean Method for preliminary orbit determination. One ought to remember that the AMP-method requares three or more observed positions distributed along a supershort arc. We would like to underline that Laplacean method have no developed alhorithms for circular, parabolic or conventional orbit determination. These new algorithms were elaborated in Pulkovo observatory [2-4].

The AMP-method was successfully applied by author for calculations of initial orbits of the Near Earth Asteroids, Kuiper Belt objects and Artificial Earth Satellites with the use of short arc positional observations when the Parameters of an Apparent Motion or spherical coordinates with their two derivatives were accurately obtained [5]. Our experience shows that an orbit calculated with the AMP-method is very close to the real object's orbit and it may be used for a searching unknown object in the first or second week after its discovery.

An example of determination of a circular orbit is given in the Tables 1–4. As «unknown» object the Numbered Minor Planet was specially celected. If a celestial body is a Near Earth Object or Asteroid with very fast angular motion we can calculate a parabolic orbit or Vajsala orbit with an assumption that the mean anomaly is equal zero. Observational data for these orbital determinations with help of Pulkovo AMP-method is the same, namely 3 or more single night positions.

Author believes that CCD observations of the unknown asteroid obtained by a single observatory during one night allow to observer himself to determine of asteroid orbit with the use of AMP-method for the continuation of its observations and finding out of this object in near future. Thus, a problem of «a single night close observations» may be solved by each asteroid's observer.

DETERMINATION OF CIRCULAR ORBIT BY MEANS OF THE AMP-METHOD

Table 1 : Geocentric positions of the Numbered Minor Planet 5257 and residuals (O–C) after linear approximation of α (gc) and δ (gc) – sets for two dates of CCD observations made at Steward Observatory
(Parallax corrections were obtained with topocentric circular orbits)

Scan number	DT	α (gc) h m s	(O–C) arcsec	δ (gc) ° ′ ″	(O–C) arcsec
9502241.133	C1995 02 24.33013	11 38 02.192	–0.23	4 58 40.66	–0.03
1.133	24.35162	11 38 01.668	0.46	4 58 44.96	0.06
1.133	24.37306	11 38 01.054	–0.23	4 58 49.06	–0.03
9503072.92	C1995 03 07.21771	11 32 58.808	–0.02	5 35 27.49	–0.02
2.92	7.23915	11 32 58.192	0.05	5 35 31.77	0.03
2.92	7.26063	11 32 57.565	–0.02	5 35 35.96	–0.02

COMMENT. In the first column «Scan number» means Year, Month, Date, Frame number and a Number of fixed object into Frame, i.e. «9502241.133» is 1995, Feb., 24, frame 1, object No 133.

Table 2: Parameters of geocentric motion of NMP 5257 and their comparison with EPOS ephemerides

moment DT 1995	Feb 24.35162	(O–C) s	Mar 07.23915	(O–C) arcsec
α	11 38 01.638	0.596	11 32 58.189	0.587
err.	+/– 0.022		+/– 0.002	
EPOS EPHEM.	11 38 01.042		11 32 57.602	
$\dot{\alpha}$, per day	– 26.507	0.237	– 28.961	0.072
err.	+/– 1.228		+/– 0.132	
EPOS EPHEM.	– 26.270		– 29.033	
δ	4 58 44.90	4.09	5 35 31.74	4.38
err.	+/– 0.04		+/– 0.02	
EPOS EPHEM.	4 58 48.99		5 35 36.12	
$\dot{\delta}$, per day	3 15.67	0.73	3 17.34	8.65
err.	+/– 2.56		+/– 1.32	
EPOS EPHEM.	3 16.40		3 25.99	
Angular velocity	0.122723		0.132015	
Positional angle	296.2882		294.5342	

The Earth’ coordinates and their derivatives are calculated by means of EPOS Software from LE200/DE200.

Table 3 : Elements of circular orbits obtained with the Pulkovo AMP-method and the real elliptical orbit elements of NMP 5257 calculated by EPOS

Epoch DT	1995 02 24.35162	1995 03 07.23915
r, a.e.	5.11251	5.19648
EPOS	5.21113	5.21106
i, deg.	2.68753	2.24362
EPOS	2.86564	2.86565
Ω, deg.	123.27792	108.22863
EPOS	126.94323	126.94344
u, deg.	46.37057	62.35791
EPOS *e*	0.03315	0.03315
EPOS ω, deg.	86.80318	86.83400
EPOS *M*, deg.	318.48499	319.35738

Table 4 : Prognosis with the use of Pulkovo circular orbits

direct : from 24 Feb. to 7 Mar.			revers : from 7 Mar. to 24 Feb.		
Positions	h m s	° ′ ″		h m s	° ′ ″
C 7.23915	11 32 55.84	5 35 22.5	24.35162	11 38 01.31	5 00 16.0
O 7.23915	11 32 58.19	5 35 31.7	24.35162	11 38 01.64	4 58 44.9
(O–C)	2.35	9.2		0.33	– 91.1
Derivatives					
C 7.23915	– 29.23	3 25.0	24.35162	– 26.29	3 08.4
O 7.23915	– 28.96	3 17.3	24.35162	– 26.51	3 15.7
(O–C)	0.27	– 7.7		– 0.22	7.3

References

[1] L'vov, V.N., Smekhacheva, R.I., Tsekmejster, S.D., 1999, EPOS - the Ephemeris Software Package for Solar System Bodies Research, *User's Guide*, Pulkovo, St. Petersburg.

[2] Kiselev, A.A., Bykov, O.P., 1973, *Sov. Aston. J.*, **50**, 1298-1308.

[3] Kiselev, A.A., Bykov, O.P., 1976, *Sov. Aston. J.*, **53**, 879-888.

[4] Bykov, O.P., 1989, Problems of Universe investigations, **12**, 328-358, (in Russian).

[5] Bykov, O.P., On the accuracy of CCD and photo observations of asteroids and their current orbit determinations, *Proceedings of IAU Symp*., **167** and **172**, The Hague, 1994, and Paris, 1995.

The Lowell asteroidal database and the future evolution (*abstract*)

Bowell E.L.G.

I maintain a suite of web URLs (see http://asteroid.lowell.edu) that mainly involve applications of orbit research conducted in collaboration with Karri Muininen and Jenni Virtanen of the University of Helsinki. The URLs, most of which are updated daily, fall into four groups, three of which are relevant to my presentation :

- **Target generation** URLs allow users to select asteroids that, for various reasons, are in need of astrometric observation. Prioritized lists may be generated, customized to users' observational resources and interests.
- **Observational aids** zero in on the observability of particular asteroids, as well as graphically displaying which regions of the sky the various NEO surveys have observed. Comprising this group of services are ephemeris generation, finder charts, observability plots, and a suggested observing strategy that will lead to an asteroid's numbering.
- There is **catalog access** to our asteroid orbital database *astorb.dat* (currently containing more than 140,000 sets of full-precision orbital elements and related data) and to the USNO-A2.0 star catalog.

Most of the anticipated work on the asteroid URLs will center around a new method of orbit computation that Virtanen, Muinonen and Bowell have been developing. (*Statistical Ranging of Asteroid Orbits (Icarus)*, in press) constitutes a completely general approach to orbit estimation that is particularly applicable to short orbital arcs, where orbit computation is almost always nonlinear. Orbits are selected in orbital-element phase space using Monte Carlo techniques, and the method can be applied to asteroids having only two observations. Among the applications we envisage presenting as web URLs are :

- **Classification of orbit type** (e.g., Aten, Apollo) will comprise a probabilistic assessment, with or without incorporating a priori information on the *(a,e,i)* distribution of the known or debiassed asteroid population.
- **Time dependence of ephemeris uncertainty**, already readily calculable using linear theory for most «long»-arc (>30 days, say) asteroid orbits, is particularly relevant for short-arc orbits.
- **Night-to-night linkage** will allow users to determine the probability that asteroids observed over short intervals on two different nights are the same object, and to see how the probability depends on the total arclength and on the surface density of asteroids observed.
- A **multi-dimensional all-sky map of moving objects** will allow users to examine sky-plane uncertainty domains of known asteroids, making two-dimensional cuts according to magnitude limit, asteroid type, sky-plane motion, etc., and allowing zooming in to a chosen region.

Observational network : the mutual events observations

Arlot J.E.

Some observations are interesting only because of the large number of independent data gathered by several observers or because of the simultaneous observations made of the same object. How to get them? The problem is to have a large number of observers ready to observe during the same period of time that is not easy to obtain because such a larger number of observers is, most of time, greater than the number of astronomers able to make the observations or interested by the observations. We have then to build a network of observers.

1 . What is an observational network?

An observational network is a tool allowing to get specific observations for a defined scientific goal at the same time during a specific period of time. In fact, a network is made in order to do what a single observatory is not able to do :

- to observe a specific phenomenon at a specific date. A single observatory may observe such an event only if several criteria are satisfied : the object of observation is above the horizon and the meteorological conditions are favorable. Then, a single observatory should be replaced by several observatories dispatched all around the world in order to be sure to catch the event.
- to accumulate a great number of data during a small period of time. A single observatory is not able to increase the duration of the visibility of any object and several instruments are necessary.

Then, an observational network consists in several observatories, well dispatched on the surface of the Earth, equipped with receptors adapted to the needed observations and ready to observe at any time when necessary for the purpose of the network. Let us see now how to build such an observational network.

2 . How to build an observational network

First, the problem is that the number of observers able to make specific observations for a specific campaign may be too small and not enough numerous to make a network. Second, the number of astronomers implied in the scientific development following the campaign of observations may also be smaller than the needed observers for the network.

The problem of the ability of observing specific events may be solved by a preparation several months before the campaign. Tests can be made and the efficiency of the observers may be improved in order to be ready at the beginning of the campaign. E-mails and web sites providing technical notes are of great help.

The problem of gathering observers even from scientific fields far from the one related to the planned campaign of observations may be solved if the observers have the ability to observe, sometimes better than the astronomers driving the network. However, the campaign of observation should not be too long and the results clearly useful and fastly published under the name of all the observers. Astronomers are not against using their observing abilities for observations even out of their scientific field if it appears to be useful. If the observations are not too difficult to make and, if they are interesting to make -mainly for rare events-, the building of the observational network will be more easy.

3 . The call to amateurs

Most of time, a coordinated campaign of observations needing a large number of observers does not need large telescopes (fifty or more 8-meters telescopes are not available on Earth!). The availability of sensitive receptors has increased the usefulness of small telescopes. The, amateur astronomers may be included in an observational network. As professional astronomers, they may not be familiar to the needed observations. However, amateur astronomers are, at first, observers, and may be trained before the campaign as stated above. Then, the call to amateur astronomers is able to increase greatly the number of observing sites. At the present time, numerous international networks gather professional and amateur astronomers and will not be able to work without the considerable supply of the amateurs.

4 . An example of a need of a network : the mutual events observations

Let now see an example. The Galilean satellites of Jupiter present eclipses by Jupiter regularly. They have been observed in the past through networks of observers : in that case, the campaigns of observations were endless and only observers interested in the analysis of the data made observations. In fact, it was sufficient because, in order to get more observations, it was just necessary to observe during a longer period of time. However, it has been proved that these observations were not enough accurate and it appears that an other type of events was much more interesting : the mutual phenomena of the satellites. In that case, the satellites are occulting and eclipsing each other and the observation of these events is easier to analyze because of the absence of atmosphere on the satellites. The difficulty comes from the fact that these events are occurring only during one year every six years when the Earth and the Sun pass through the orbital plane of the satellites. Then, a special effort has to be made in order to get as much events as possible during this small interval of time. A large network is necessary.

5 . The PHEMU network

In order to observe these rare events, all the astronomers interested by these observations are observing but their number is not sufficient to cover all the possible observations. A call was made, near the photometric observers observing variable stars or occultations of stars and having the receptors to be used for the observation of the Galilean satellites that is easy, these satellites being very bright. Now the participation of the observers of occultations of stars by asteroids is common since this type of event is close to mutual events The asked effort consists in observations to be made one or two times a week, each observation being made within one hour, most of time, and then, not disturbing the regular observing program. The Phemu network was then made working thanks to astronomers, professional and amateur, from several countries on all the continents.

6 . The past results

The table below provides the results of the former campaigns of observations. Our goal is to get the observation of as many events as possible, each event being observed two or three times in order to avoid ambiguities in the interpretation of the data (errors in the timing, in the photometric calibration,…). Note that the network must be developed mainly in the Northern hemisphere if the objects have a positive declination and Southern if negative.

Results of the past campaigns	1985	1991	1997
Number of sites	28	36	42
Number of observable events	218	251	242
Number of observed events	64	115	122
Number of observations made	166	401	255

7 . The Phemu03 campaign

In 2003, a new opportunity occurs during the transit of the Earth and the Sun in the equatorial plane of Jupiter. Then, observations should be made from October 2002 to June 2003. Since the declination of Jupiter is near +20°, the observations are easier to make in the Northern hemisphere. The table below provides the number of observable events for several observatories (valid for a large area around the observatory). The need of the network of observers appear clearly.

Observatory	number of events (1)	(2)
Alma-Ata (Kazakstan)	150	49
Nankin (China)	148	50
Moscow (Russia)	145	47
Pic du Midi (France)	140	43
Kiev (Ukraine)	138	41
Kavalur (India)	137	47
Bucarest (Romania)	137	47
Paris (France)	136	43
Canarian Islands (Spain)	136	40
Stuttgart (Germany)	134	40
Mc Donald (USA)	132	41
Torino (Italy)	132	38
Hawai (USA)	130	38
Itajuba (Brazil)	109	30
ESO (Chile)	97	32

(1): all events including the grazing ones

(2): only events easy to observe

Facilities of the Bulgarian National Observatory for astrometric and photometric observations of asteroids

Ivanova V., Shkodrov V., Apostolovska G., Borisov G., Bilkina B.

Abstract. *The equipement of the Bulgarian National Observatory Rozhen more suited to asteroids and comets observations are presented. Some astrometric and photometric results, their accuracy, and future developements are discussed.*

1 . Introduction

The Bulgarian National Astronomical Observatory Rozhen (BNAO) has been active for more than twenty years. Already at the beginning of its activity, positional observations of asteroids were obtained, receiving international resonance (Marsden 1983). This activity continued until 1990, when the astronomical community shifted to the use of CCD cameras, a technique far above the budget of the Institute of Astronomy. As a consequence, the activity of the observatory in this field had a restriction. In the meantime the reseach topics were extended to minor bodies photometry, needing a certain period of adaptation to obtain results. Recently the situation was deeply improved. In the following we present the observing facilities of BNAO and some photometric and astrometric results, in order to clarify our possible contribution to the observing network.

Table 1 : Telescopes in NAO – Rozhen

	2 m RCC telescope	50 cm/70 cm Schmidt telescope	60 \ cm telescope
1/f	8	3.44	12.5
Resolution	$12,89''$ / mm	$120''$ / mm	$27''$ / mm
FOV	$1° \times 1°$	$5° \times 5°$	$20'$
Detector	CCD Photometrics CE200A – SITe $1024 \times 1024 px^2$ $1px = 24 \mu m$	CCD SBIG ST–8E Kodak KAF–1602E $1536 \times 1024 px^2$ $1px = 9 \mu m$	Photomultiplier EMI-9789QA Pulse counting
Cooling	Liquid nitrogen	Thermoelectric	without cooling
FOV	$5' \times 5'$	$27,6' \times 18,4'$	
Filters	*UBVRI*	*UBVRI*	*UBV*

2 . The National Observatory Rozhen

The BNAO is the most important observing facility in south-east Europe. It is situated on the Rodope mountains (south-west Bulgaria) at coordinates $\lambda = 1^h 38^m 52^s$, $\phi = +41°43'$, 1750m above sea level, at 250 km from Sofia, where the Institute of Astronomy is located. During the year, astronomical darkness is granted for a total of 3050 hours, and the metereological efficiency is $\sim 40\%$. The average seeing is around $2''$.

The BNAO is equipped by 3 optical telescopes, whose parameters are presented in Table 1. The Ritchey-Chrétien telescope (2 m of aperture) can operate in two configurations of focus, the classical on-axis Ritchey-Chrétien and Coudé. The focal reducer «FoRoRo» has been expecially designed for comet observation, yeilding a field of $11,7'' \times 11,7''$ at $F = 7,2m$. At the Coudé focus a stellar spectrograph (havong 20 cm and 30 cm beams) is available, as well as three high-resolution cameras, allowing to reach scales of 4 A/mm, 9 A/mm, and 18 A/mm. The Institute of Astronomy of Belogradchik (NW Bulgaria) owns a 60 cm Cassegrain ($\lambda = 1^h 30^m 42^s$, $\phi = +43°37'$) equipped with a photoelectric photometer and a CCD camera SBIG ST-8. The main problem affecting the activity of the BNAO is the availability of CCD cameras, that does not really allow flexibility. For example, a $2K \times 2K$ sensor at the Schmidt telescope would be of great value.

3 . Astrometry

The first systematic observing program of the BNAO, mainly carried out by the Schmidt and the 2 m telescope, has concerned astrometry of Minor Bodies. As an example, the first photography of the comet P/Halley in Europe at the last comet return was obtained at the 2m telescope on Nov. 25, 1984, when the comet was at mag. ~ 22 (Shkodrov *et al.* 1986).

As a support to the the astrometric program, observational methods and software for data reduction were developed (Ivanonva 1977). The obtained measurements has shown to be consistent in their residuals to those normally published in MPCs. For CCD astrometric reduction, the programs «Astrometrica» (by H. Raab) and «Charon» (Project PLUTO) were employed.

The main observational programs were devoted to the discovery of new objects and to follow-up for the improvement of orbital elements. Following the visit of E.F. Helin, we participated to the first international program for searching of fast-moving objects (INAS) in collaboration with the Mount Palomar observatory and the Observatoire de la Côte d'Azur.

A fraction of 7 nights per month is granted to astrometric observations at the Schmidt telescope, used in cooperation with Macedonians collegues. Some statitics concerning the number of observations and the number of objects observed are presented in Fig. 1.

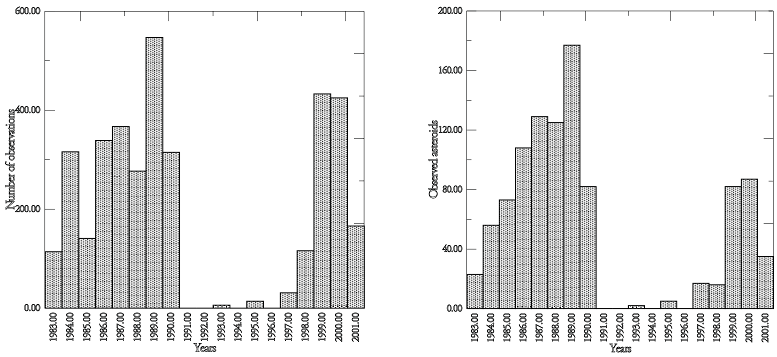

(a) (b)

Figure 1 : Statistic of astrometric observations

4 . Photometry

Regular photometric observations have been carried out starting in 1991 by the 60 cm Cassegrain telescope. The 2 m telescope was also used for faint objects, in particular for relative photometry during the international observing campaign of 1620 Geographos devoted to model the asteroid (Magnusson *et al.* 1996).

An effort was also made concerning the methods of observation and data reduction. On the basis of the existing software for photometric observations of stellar object (Kirov *et al*. 1991), a new tool specific to asteroid photometry was developed (Denchev 1996), according to the final requirements of this kind of study. We stress here some characteristics of our approach. First of all, the calculation of the first order extintion coefficients strictly follows the recommendations of A. Harris *et al.* (1989). Second order coefficients are taken into account as well. Finally, the errors resulting from each step of the data reduction are also computed.

At present, the photometry of 43 asteroids has been obtained by photoelectric techniques, while 14 objects were observed by CCD cameras (results concerning 27 objects published). In order to give some hints about the accuracy reached be our procedure we present here three light curves obtained at different telescopes (Fig. 2). Photometry has been performed also at the Schmidt telescope. Photometry has been possible in 18 nights over six months at the 2m and in 20 nights at the Cassegrain telescope.

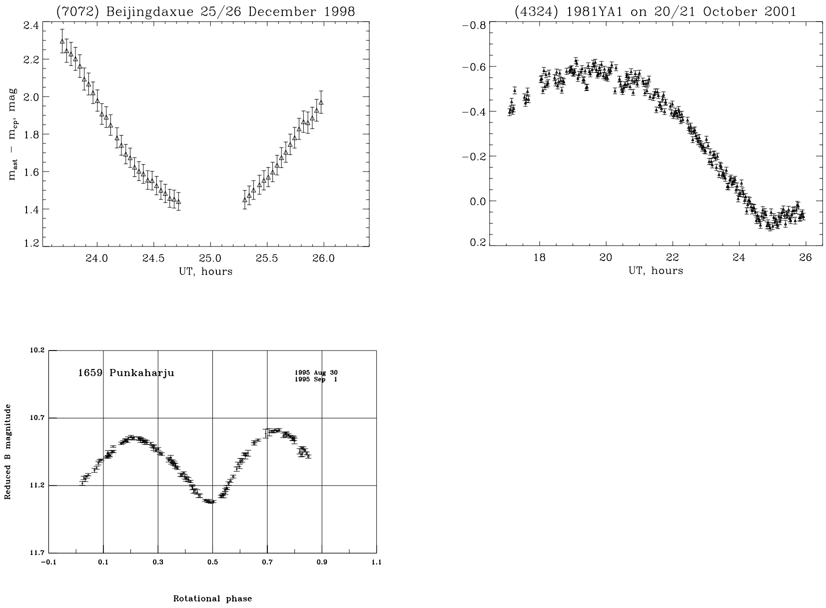

Figure 2 : Lightcurves of three asteroids obtained with 2m RCC, 50cm/70cm Schmidt and 60cm Cassegrain telescopes, respectively

5 . Conclusion

Fig. 1a shows that the rate of the astrometric observations recently obtained by CCD is similar to that of the old photographic technique. This fact encourage to continue following the present direction. However, due to the smaller field of view, the number of observed asteroids shows a slight decrease (Fig. 1b), thus suggesting a careful target selection that includes, in particular, NEOs needing follow-up astrometry.

The photometric observations will continue, with the aim of determining rotational and physical parameters. In particular, a special effort will be devoted to NEOs and distant minor bodies.

The current equipment of the observatory allows to observe the mutual events of the satellites of the giant planets (Arlot *et al.* 1997), and star occultations by asteroids.

In conclusion, it must be pointed out that international collaborations with collegues from other countries will be of great help in the exploitation of the BNAO instruments briefly descibed in this note.

References

Marsden, B., 1983, *Inf. Bull. IAU*, **54**,11.

Shkodrov, V.G., Bonev, T.R., Ivanova, V.G., 1986, *Comp. rend. Acad. bulg. Sci.*, **39**, 1, 11-13.

Ivanova, V.G., 1977, *NISZ*, **16**, 333.

Kirov, N.K., Antov, A.P., Genkov, V.V., 1991, *Comp. rend. Acad. bulg. Sci.*, **44**, 5-8.

Denchev, P., *PhD Thesis*.

Harris, A.W., Lupishko, D.F., 1989, in *Asteroids II*, 39-53.

Arlot, J.E., Shkodrov, V.G. *et al*., 1997, *A&ASS*, **125**, 399-405.

Magnusson, P., Ivanova, V., Komitov, B., Donchev, Z., Denchev, P., *et al*., 1996, *Icarus*, **123**, 227-244.

The natural satellites astrometric observations datbase NSDC *(abstract)*

Arlot J.E., Baron N.

The database of the astrometric observations of the natural planetary satellites is maintained under the auspices of the working group «Natural satellites» of the commission 20 of the IAU.

The data base gathers the observations under several forms :

- the raw data of the observations as published by their authors (see the web pages http://www.imcce.fr/nsdf/f.html),
- standard data reachable through a specific software (web address: http://digitale.bdl.fr/www/nsdb.html),
- bibliographic data regarding the natural planetary satellites reachable through specific key words (web address: http://www.imcce.fr/SFgate/nsdc_bibl.html).

Most of the planetary satellites systems are covered and most of the available observations are included in the database. We encourage observers to send their data as soon as possible in order to make them available for the fitting of the theoretical models and the making of ephemerides.

Agrupacio Astronomica de Sabadell : Our work in the field of the asteroids *(abstract)*

Casas Ricard

The Agrupacio Astronomica de Sabadell is Spanish amateur association with 800 members. Some members work in different field of asteroidal studies : occultations, approachs, astrometry, with the association's observatory, sited in Sabadell. In these studies, one goal was the discover of the asteroid 13260 Sabadell.

Physical investigations of asteroids in Shemakha Astrophysical Observatory (*abstract*)
Shestopalov Dmitry

Shemakha Astrophysical Observatory (ShAO AS of Azerbaijan) is situated 140 km from Baku city on the south foothills of the Great Caucasus Range, and is 1500 m above sea level. 2-m Zeiss reflector is the main observatory telescope which is in particular used for astrophysical observations of asteroids.

Physical studies of asteroids are the traditional direction of the observatory work. For the first time, the slight absorption band of pyroxene at 550 nm was found in Vesta spectrum in 1980 [1]. After that it was registrated in 3 Juno spectrum [2] and other S-asteroid spectra [3]. This absorption band was rediscovered in spectra of Vesta and near Earth asteroids [4]. Comparative investigations of properties of 505 nm band in asteroid, terrestrial pyroxene and meteorite spectra led to the following conclusion. Variations of S-asteroid spectra are connected with variations of chemical composition of pyroxene which, as we assume, is on S-asteroid surfaces in the greater quantity than in achondrites and ordinary chondrites [5]. The discovery of another slight absorption bands in the optical range of S-asteroid spectra, which may be assigned to Fe3+ cation (or Cr3+ cation) in pyroxene, led to a thought that asteroid minerals could be formed in the oxidative conditions [6]. Now this possibility is debated in connection with the discovery of aqueous alteration products in ordinary chondrite meteorites and OH absorption band in the spectrum of S-asteroid Hebe near 3000 nm [7].

Spectral properties of meteorites from the collection of Institute of Mines (St.-Petersburg, Russia) were also investigated and spectral classification of achondrites and ordinary chondrites has been devised [8]. The comparison of spectral characteristics of achondrites and ordinary chondrites on the one hand and main belt S-asteroids on the other hand showed their statistical significant differences. From here the conclusion was done on systematically different material compositions of these types of asteroids and meteorites [9]. The same result was also obtained for near Earth asteroid 433 Eros [10], what is now confirmed by data obtained with the help of spacecraft NEAR [11]. The comparison of reflectance spectra of C-asteroids and carbonaceous chondrites allowed to come to the following conclusion: the most ancient material of the Solar System presented by carbonaceous chondrites of CI group is practically absent on C-asteroid surface. Apparently, CI-material has been mainly removed with C-asteroid surfaces or reworked in the process of the formation of the present-day regolith covers on asteroids [12].

In order to investigate asteroid material composition the method of calculation of reflectance spectra of polymineral powder-like surface has been devised. Reflectance spectra of S-asteroids from various optical subtypes are simulated by this method. This permits approximately to determine the mineral surface composition that, as we obtained, one may attribute to basaltic type [13]. Besides, probable reflectance spectra of main rock-forming minerals on S-asteroid surfaces have been calculated [14]. Using the spectra it is possible approximately to determine the structural type and chemical composition of these minerals by remote sensed methods [15].

References

[1] Golubeva, L.F., Omarov, C.Z., Shestopalov, D.I., 1983, *Sov.Astron.J.*, **60**, 145.

[2] Golubeva, L.F., 1986, *Sov. Astron.J. Lett.*, **12**, 801.

[3] Shestopalov, D.I. *et al.*, 1990, *Astron. Vest.*, **24**, 232.

[4] Luu, J.X., Jevitt, D.C., 1990, *Astron.J.*, **99**, 1985.

[5] Shestopalov, D.I., Golubeva, L.F., 1991, *Sov. Astron.J. Lett.*, **17**, 453

[6] Shestopalov, D.I. *et al., 1991, Astron. Vest.*, **25**, 442.

[7] Rivkin, A.S., 2001, *32nd Lun.Plan.Sci.Conf.*, **1723**.

[8] Golubeva, L.F. *et al.*, 1986, *Astron. Vest.*, **20**, 116.

[9] Golubeva, L.F., 1988, *Astron. Vest.*, **22**, 49.

[10] Shestopalov, D.I., Golubeva, L.F., 1992, *Astron. Vest.*, **26**, 77.

[11] McCoy, T.J. *et al.*, 2001, *32nd Lun.Plan.Sci.Conf.*, **1556**.

[12] Shestopalov, D.I., *et al.*, 1998, *Astron. Vest.*, **32**, 58.

[13] Shestopalov, D.I., Golubeva, L.F., 2000, *Astron. Vest.*, **34**, 202.

[14] Golubeva, L.F., Shestopalov, D.I., 2001, *32nd Lun.Plan.Sci.Conf.*, **1004**.

[15] Shestopalov, D.I., Golubeva, L.F., 2001, *Astron. Vest.*, (submitted).

The recovery as an important part of NEA astrometric follow-up *(abstract)*

Ticha J., Tichy M., Kocer M.

The number of known Near-Earth Asteroids (NEAs) has rapidly increased in recent years due to LINEAR and other large surveys (Spacewatch, LONEOS, NEAT and CSS). This discovery process has to be folloved by follow-up observations to obtain a sufficient number of precise astrometric data needed for an accurate orbit determination of newly discovered bodies. About forty per cent of the known NEOs have been observed for more than one opposition.

This follow-up process starts by confirmatory observations and continues over a sufficient observing arc in the discovery apparition. Accurate orbit determination requires observations from at least two oppositions. If asteroids are not found in the next apparition, different from the discovery one, then they can be considered lost. This is particularly embarrassing for NEAs. Therefore NEA recovery is a very important part of NEA follow-up astrometry. If data for different apparitions are not find in the course of precovery surveys or in other achive data, then it is necessary to prepare targeted observations of a particular NEA in the second convenient apparition.

We discuss here methods, techniques and results of planned recoveries at the Klet Observatory using 0.57-meter telescope equipped with a CCD detector.

We also mention the overall work on NEA recoveries provided by several NEO follow-up programmes as well as a need for communication resources supporting astrometric observers.

Finnaly we present here a planned extension of Klet NEA recovery subprogramme to fainter objects by means of larger 1-m telescope, which is being built at Klet now.

Parameters of apparent motion of asteroids which collide with the Earth

Rumyantsev V.V.

Abstract*. This work is dedicated to the observable and dynamic features of Earth-crossing asteroids for the last several weeks before their impact. Orbits, bringing to such collision, were defined on the base of modeling from the position and velocity at a moment of collisions. From the received ensemble of orbits only elliptical orbits with direct motion were considered. Analysis of circumstances of approaching has show that velocity of visible motion of such asteroids for a week before the collision, does not exceed a value of 15 arcsec per hour, and even is vanishing little for some approach directions. It is two or more times slowly than visible velocities of main belt asteroids in opposition. For 300 m asteroid brightness for 2 months before the collision ranges from 13^m to 21^m, slowly increasing in last days before the impact, where the brightness is increasing very quick. Asteroids on the last revolution before the collision, for a month before the impact, have a horizontal parallax of some dozens of arcseconds. Wide-angle cameras can easy reveal such parallax. Observers who search for Near-Earth asteroids usually devote special attention to «quick asteroids», which leave long traces at the frames. The real «attacked» asteroids at their last 10 days are «slow» objects.*

1 . Introduction

There are more than 1200 near-Earth asteroids (NEA) registered now [1]. This objects have high velocities of visible motion (from several arcminutes to several dozens of arcminutes per hour and more). NEAs leave a long track on registered images. That is why they named «fast asteroids» but all of these asteroids are «going by». Hitherto was not received nor one observing an asteroid before it entering in Earth atmosphere. There are registration a bodies already fall into atmosphere of the Earth, fixed as ground-based observant stations [2] so and spacecraft's [3]. In this connection the determination of observed features of such asteroids (impactors) is actual for forthcoming and already acting programs of spying after the near-Earth space.

2 . Orbits of asteroids before collision with the Earth

We need to know orbits of impactors for determination the observational and dynamical properties of asteroids before collision with the Earth. There are no any real (observed) crossing Earth orbits at this moment. We got such orbits by Monte-Carlo modeling from the position and velocity at a moment of collision. Of course, distribution of the model orbits is different from real ones, which we do not know. But we will give all possible variants of the

Earth crossing orbits. We considered only elliptical orbits crossed the Earth in conducting calculations.

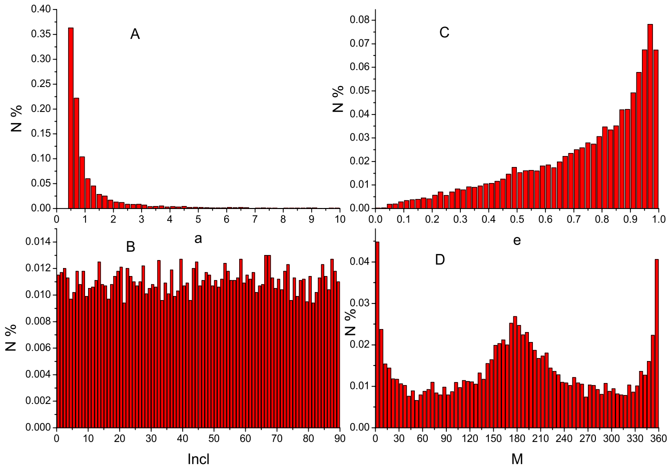

Figure 1 : The distribution of simulated orbital elements

2.1. Modeling of orbits

We calculate Earth crossing orbit from heliocentric coordinates X, Y, Z and velocities V_x , V_y , V_z of asteroid at the time T [4]. For the simplification of calculations we define orbits with head-on collision, i.e. orbits which go through the Earth center. Consequently we suppose $(X,Y,Z) = (X_\oplus, Y_\oplus, Z_\oplus)$ at the time T. We changed the velocity vector from –150 km/sec to +150 km/sec for getting the whole ensemble of «colliding with Earth orbits». Using known formulas of calculation of orbits from the position and velocity at an initial time [4] we received more 200.000 Earth crossing orbits. Hyperbolic orbits and orbits with the back motion were not consider.

2.2. Distribution the orbital elements

The distribution of simulated orbital elements are shown in fig. 1. Fig. 1(A) shows a distribution of the semimajor axis of Earth crossing asteroids by head-on collision. The distribution of the semimajor axis have maximum on 0.65 AU and the tail of this distribution extended up to 20.000 AU. Fig. 1(B) shows distribution of orbits inclination. Because of velocity vector has uniform distribution on the sphere, the distribution of inclination is uniform too. Fig. 1(C D) shows distribution of eccentricity and average anomaly. Fig. 1(D) shows that about 48% impactors at the moment of collisions are near the line of apses (25 degrees).

3 . Velocities of visible motion

Visible motion is a result of three moving : moving the Earth and asteroid on its own orbits and rotation of observer in consequence of the Earth rotating. All orbits were divided into 5 groups on eccentricity with the step 0.2 and each of them on 4 groups on the inclination : 0–10, 10–30, 30–60, 60–90. Calculated geocentric velocities of visible motion are shown on the fig.2. Each graph shows a dependence of visible motion velocity from time before the collision.

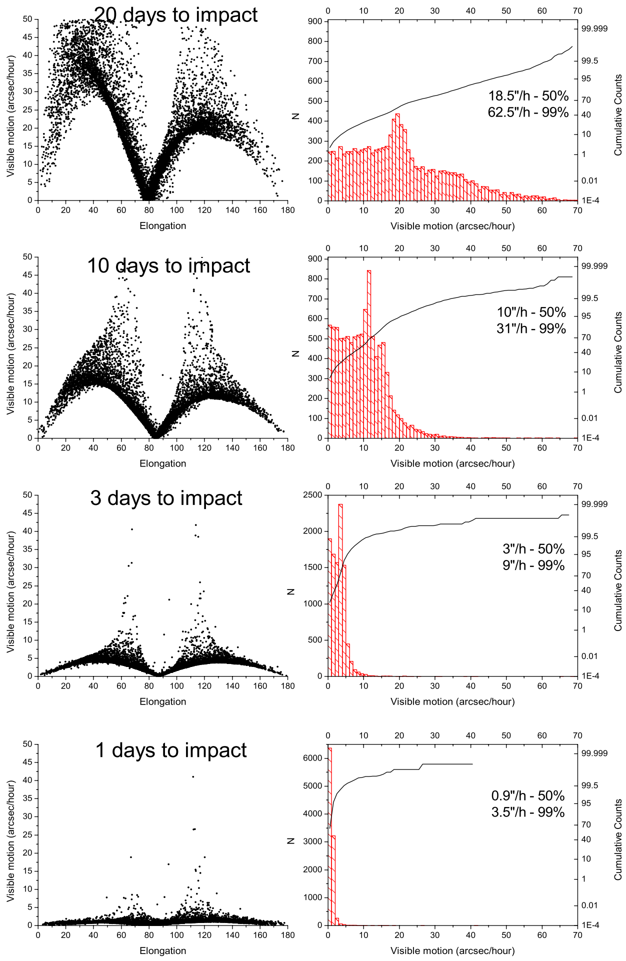

Figure 2

Most objects has a velocity of visible motion which does not exceed 50 arcsec/hour. Histograms of the velocities distribution for 20, 10, 3 and 1 day before the collision is shown on the fig.2. Velocity of visible motion is quickly decreased with approach a moment of collision. If for 20 days before the collision 50% objects had a velocity not exceed 18.5 arcsec/hour, for 3 days before the collision it does not exceed 3 arcsec/hour and 1 arcsec/hour for 1 day. Fig.2 shows a velocity of visible motion depending on the elongation for 20, 10, 3 and 1 day before the collision. We must note, that visible motion is small, especially for objects that approach to the Earth from the solar and antisolar directions, and also from the Earth apex and antiapex directions. Traditional method of searching of asteroids approaching the Earth using their high visible motion [5] will not effectively work on the last circuit before the collision. A group of asteroids with very small visible motion (< 1 arcsec/hour) always exists and its number increases to a moment of collisions. Even the most fast visible motion 60 arcsec/hour will not be detected for the typical CCD exposure.

It should be noted a several features on the graphics.

1) Geocentric velocity of visible motion decreases on the measure of approaching a moment of collision for any orbits.

2) There is a group of orbits, having visible motion which does not exceed 5 arcsec/hour for all bimonthly time lag before the collision.
3) Orbits with the small eccentricity and high inclination have a velocity of visible motion less 15 arcsec/hour for the fortnight before the collision.

4 . Changing brightness before collision

Brightness of asteroid depends on many parameters. This fact complicates its estimation. Fig.3 shows distribution of 300-meters asteroids magnitude depending on elongation for 20, 10, 3 and 1 days before the collision. Average value of brightness increases with approaching to the Earth and has value of 21.5^m for 20 days, 20.0^m for 10 days, 17.5^m for 3 days and 15^m for 1 day before the collision.

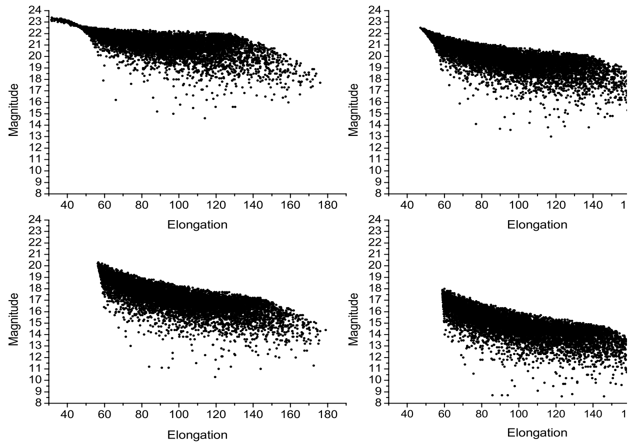

Figure 3

5 . Perturbation from the Earth

Most of the model bodies have impact velocities from 10 to 50 km/sec. Maximum of its distribution is about 27 km/sec. The impactors with such velocities pass the sphere of Earth gravitation actions for the time from 6 to 27 hours. It is sufficiently small time for feeling Earth influence on asteroid.

6 . Parallax

Changing the coordinates of asteroid due to parallactic displacing can be determined from equations :

$$\Delta\alpha = \rho \cdot \cos\varphi \cdot \sec\delta \cdot \cos t \cdot \Delta t / R$$
$$\Delta\delta = \rho \cdot \cos\varphi \cdot \sin\delta \cdot \sin t \cdot \Delta t / R$$

where φ - latitude of observatory,
Δ, t - declination and hour angle of object,
ρ, R - geocentric vector of observer and asteroid,
Δt - change of hour angle in the unit of time.

Fig.4 shows parallax changing with time before the collision. Parallax is calculated for the base in 1 $F_{\oplus}$. The distance of the impactor moving with the velocity 10 km/sec for 5 days before event is about 4.3×10^6 km or 0.029 AU. Its parallax is approximately 75 arcsec, that is easy detected by synchronous observations from two far observatories.

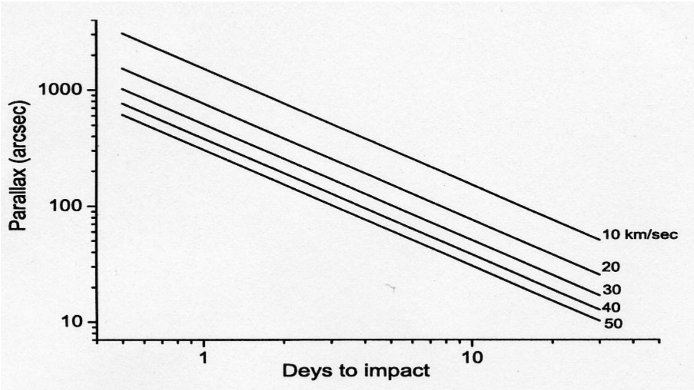

Figure 4

7 . Conclusion

How will be seen asteroids for certain time before its impact the Earth ?

1 month before collision

Visible moving velocities of the most asteroids will be from 0 to 50 arcsec/hour (maximum in distribution is 30 arcsec/hour). Brightness during a month almost will not change. Telescope of type Spacewatch can detect almost all asteroids with eccentricity < 0.6. For two exposures through the half an hour part of objects will be seen as asteroids of main belt, but there will be «slow objects» as well. Impactors will be seen as main belt asteroids on the two images obtained with 30 minutes delay. Moreover, some of this asteroids will be even more slow objects.

10 days before collision

Geocentric velocity of visible motion for all approach paths will be from 0 to 25 arcsec/hour. The shift of observer due to the Earth rotation begins to influence to the topocentric visible velocity of asteroids. Visible magnitude of 300 m asteroid will be in the interval $17\text{-}23^m$.

3 days before collision

Geocentric velocity of visible motion for all approach paths will be from 0 to 10 arcsec/hour. Influence of the shift of observer due to the Earth rotation will be more considerable for the topocentric visible velocity of asteroids. Visible magnitude of 300 m asteroid will be in the interval $14\text{-}20^m$. Brightness of the asteroid will be sharply increased to the time of collisions.

Most of impactors can be detected as objects more slow than asteroids of main belt. They do not appear on CCD frame as a long tracks, which are attracting our attention.

References

[1] IAU : Minor Planet Center, MPC Orbit Database, ftp://cfa-ftp.harvard.edu/pub/MPCORB/.

[2] Ceplecha, Z., 1994, Impacts of meteoroids larger than 1 m into the Earth's atmosphere, *Astron. Astrophys*., **286**, 967-970.

[3] Satellites detect record meteor, June 1994*, Sky and telescope*.

[4] Subotin, M.F., 1968, *Introduction to the theoretical astronomy*, (in Russian).

[5] Pravdo, S.H., *et al*., 1999, *AJ*, **117**.

On sky scanner-telescope efficiency *(abstract)*

Shestopalov Dmitry

Two regimes of work of scanner-telescope intended for detection of the moving objects near Earth are considered. In the first regime, that one may call «stopped», sky survey is realized due to diurnal rotation of the sky sphere. In the second regime («step by step») telescope exposes one and the same sky area several times, and each exposition differs from other by a very small displacement along coordinate «declination». Then telescope turns on angle equivalent to own field angle along the coordinate «right ascension» and again several «quasimotionless» exposures of next sky area are carried out and so on. The formula describing efficiency of telescope-scanner work in these regimes was obtained. It is shown that other things being equal efficiency of the second regime is approximately in 6 times as much as the first.

The Crimean CCD telescope for the asteroid observations

Chernykh N.S., Rumyantsev V.V.

Abstract. *Old 64-cm Richter-Slefogt telescope (F=90 cm) of the Crimean Astrophysical Observatory was reconstructed and equipped with the SBIG ST-8 CCD camera received from the Planetary Society for the Eugene Shoemaker Near Earth Object Grant. First observations of minor planets and comets were made with it. The CCD matrix of St-8 camera in the focus of our telescope covers field of 52' .7 × 35' .1. The 120 - second exposure yields stars up to limiting magnitude of 20.5 for S/N=3. According to preliminary estimations it is possible to cover during the year the sky area of 550 sq. deg. with threefold overlapping and to open up to 3500 main belt asteroids and 2 Near-Earth Asteroids (NEA). An automation of the telescope can increase the productivity up to 20000 sq. deg. per year. The software for object localization, image parameters determination, stars identification, astrometric reduction, identification and catalogue of asteroids is worked up. The first results obtained with the Crimean CCD 64-cm telescope are discussed.*

Crimean program of observing Near Earth Asteroids is a logical continuing a photographic review of minor planets conduct in the CrAO with 1963 on 1997 [1]. In 1993 the work was started according to the initiative of A.G. Sokolsky and N.S. Chernykh on the reconstruction of old 64-cm telescope in order to use it for observing of the asteroids, approaching to the Earth. 64-cm telescope of Richter-Slefogt system [Fig.1] was designed and build by the German company Carl Zeiss Jena during the Second World War. Telescope has a spherical mirror of diameter of D = 675 mm and focal length 905 mm. Correction system consists of two lenses of diameter 643 mm.

Flat surface of second lens has an aluminum covering of diameter 285 mm and serves a secondary mirror, shortening an optical system. Focal length of the whole system is 894 mm. Field of view is 80 mm and has a radius of curvature 90 cm. Flat field correction lens, installed before focal surface, ensures a flat field of diameter 60 mm (4 degrees) and shortens an equivalent system focal length to F = 822 mm. Focal surface is inside the tube, on the distance of 35 cm from back edge of the cassette tube.

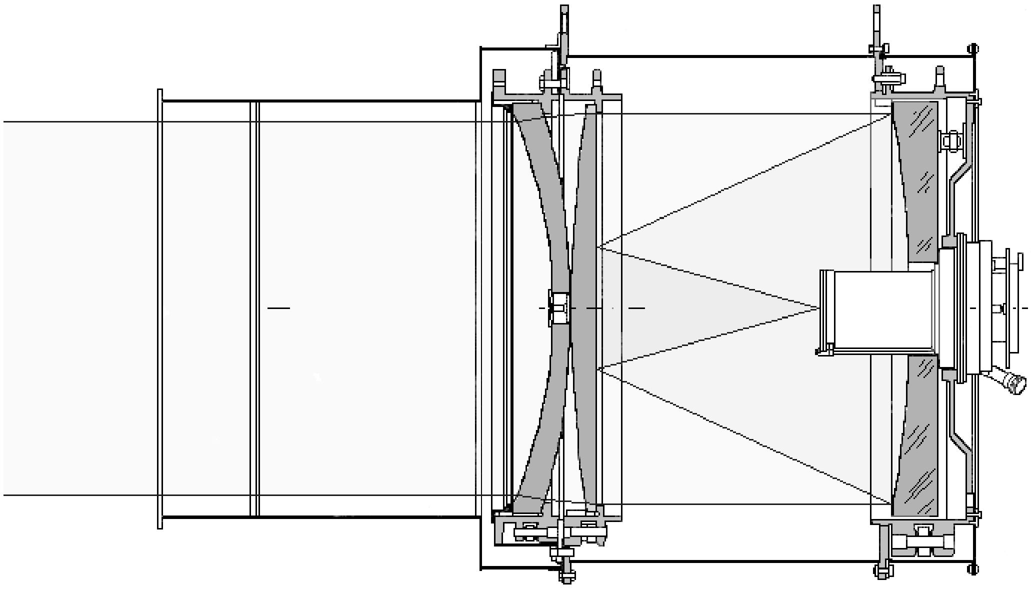

Figure 1 : Optical scheme of the 64-cm telescope

In March 1999 we have get CCD camera SBIG St-8 for a grant of the American Planetary Society, given to us in October 1997 for the developing of the ITA-CrAO observing program. Its main features are presented in the table.

Table 1 : Main features of ST-8

CCD size	1530×1020
Area	13.8×9.2 mm
Field of view	$52'.7 \times 35'.1$
Pixel size	9 mkm
Well Depth	80Ke
Quantum efficiency	40% in 6000-8000 Å
Digital resolution	16 bit
Dark signal	36 e/min*pix @ 0 C
Read noise	$15\ e^{-1}$

Limiting magnitude registered by CCD telescope, depends on acting area of telescope, technical features of CCD matrixes, time of accumulations and background of the sky and it can be determined by following expression :

$$m = 7.1 + 0.5\mu + 2.5\lg\left(\frac{\sqrt{S \cdot \eta \cdot T}}{k \cdot \Delta}\right)$$

where S - effective area of telescope in sq. cm.,
η - quantum efficiency of CCD matrix,
T - exposure in seconds,
Δ - side of square of number of elements, covered by image of the star on matrix in arcsecond,
k - signal to noise ratio,
μ - brightness of the sky background in stellar magnitudes for square arcsecond.

Considering constructive particularities optical system of our telescope and take values $\mu = 21^m.0$ /sq. arcsec., $\eta = 0.4$, $k = 5$, $\Delta = 4$, one find the following values of limiting magnitude depending on exposures.

Table 2 : Limiting magnitude with CCD

64-cm telescope, S=1700 cm^2				
T, sec	10	30	60	120
m	19.1	19.7	20.1	20.5

In the May of 1999 we had began the first test observations with the matrix ST-8, installed in the primary focus of the telescope. We found that limit magnitude for stars is 20.5^m with for exposure of 2 minutes, that is in well agreement with theoretical evaluations. Limit magnitude was estimated from observations of selected areas SA 51 and SA 57 [2].

Table 3 : Accuracy of astrometric observations of the sample objects

Object	No	Period of observation	$\sigma\alpha$ (arcsec)	$\sigma\delta$ (arcsec)
C/1999 H1	6	1999 11 08 - 1999 11 10	0.4	0.2
C/1999 J2	6	2000 07 16	0.4	0.4
2000 NM (Motion=10/min)	64	2000 07 04 - 2000 07 28	0.1	0.3
1999 KW4 (Motion=45/min)	36	2001 05 24	0.4	0.4

Evaluation of an overexposed stars shows that stars brighter 11.7^m cause an overflow of charge in pixels. Amount of an overexposed stars in the frame can be several dozens.

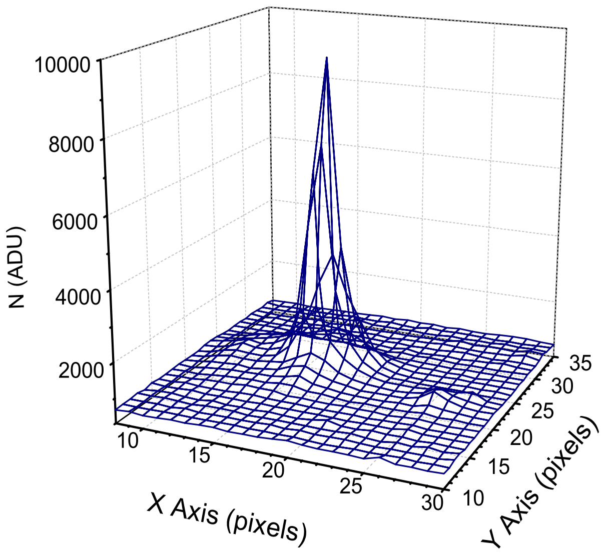

Figure 2 : Fragment of frame $3' \times 4'$

Telescope gives image of the stars of the diameter 2σ =18 mkm, that corresponds to an area of 2 x 2 pixels. Fragment of frame $3' \times 4'$ with the stars of different brightness is shown on the figure 2.

V.V. Rumyantsev had develope a software AstroMet ver.1.2 that allows to make a preliminary image preprocessing, localization of the registered stars, determination of parameters of image of stars and astrometric and photometric reduction. Profiles of star are presented by the fixed Gauss model functions [3].

$$D_{x_i, y_i} = a_1 + a_2 \cdot e^{-\frac{1}{2}\left(\frac{1}{1-a_7^2} \cdot (q_x^2 + q_y^2 - 2 \cdot a_7 \cdot q_x \cdot q_y)\right)}$$

where

$$q_x = \frac{x_i - a_3}{a_4} \quad , \quad q_y = \frac{y_i - a_5}{a_6}$$

Here a_1 is refer to local background density, a_2 describes peak density in image, a_3 and a_5 describe image center coordinates and a_4 , a_6 and a_7 describe the axis and orientation of general elliptical figure of star image.

From June 2000 to May 2001 first working observations of several asteroids (including and NEO 2000 NM and 1999 KW4) and comets were carried out. Simultaneously the work on the improving of the software and developing of the methods of observation was made. Altogether about 1000 frames was received. At present the work on automations of telescope and the improvement of programs of image processing are continued.

Accuracy of astrometric observations of some objects is present in table 3.

Telescope productive capacity, i.e. area of the sky covered by the observations for unit of time for the fixed limiting magnitude, much depends on degrees of automation of telescope. At present our telescope is not automated, pointing of it to the observed area is made manually, and besides, the coordinate circles of it have low accuracy. In these conditions a time between exposures («dead time») reaches 7-10 minutes. Therefore, for average 6-hours night it possible to get 30-35 frames, or 3000-3500 frames per year. It corresponds to 500-600 square degrees per year for the triple overlapping of observed areas. For the automated telescope dead time may be shortened to 1 minute and therefore, productivity will increase to 100-120 frames for a night, or to 1600-2000 square degrees per year for the triple overlapping. Probability of discovery of the NEAs in such area of the sky during a year is evaluated according to the results of E. Helin and R. Dunbar [4]. Possible number of Near Earth Asteroids of corresponding limiting magnitude is presented by the table 4.

Table 4

Magnitude	Number of asteroids	
V_{lim}	NEO	Main Belt
15	-	200
16	0.2	430
17	0.5	1030
18	1.2	2500
19	3.1	6000
20	7.8	14000
21	15	60000

An estimation of probable number of asteroids of main belt is based on the statistics by van Houten C. G and others [5].

For the comparison let we to note that known program with the Spacewatch telescope of the Observatory Kitt Peak, using a method of scan when observing, gets at the average 1250 square degrees per year under the triple overlapping of observed areas and registers near 20000 asteroids to 21^m.

We understand, that automation necessary not only for the achievement of high velocity and accuracy pointing on the selected areas of the sky. It needs as well for ensuring of quick and exact returning to the preceding areas, since a workspace for the triple overlapping is a crossing of all three frames. More exact knowledge of coordinates of observed area will allow to shorten a time for the identification of catalogue stars. All this will do a telescope more efficient instrument in the work of study of small bodies of the Solar system.

References

[1] Chernykh, N. S., 1999, Crimean minor planet survey, *Dissertation for Dr. Sc. Degree*, St-Petersburg (in Russian).

[2]Everhart, E., 1984, Finding Your Telescope's Magnitude Limit, *Sky & Telescope*, **77**, 1.

[3] Sanders, W.L., Schroder, R., 1980, Membership in the cluster NGC 6494, *Astron. Astrophis.*, **88**, 1/2, 102-107.

[4] Helin, E., Dunbar, R., 1990, Search techniques for near-Earth asteroids, *Vistas in astronomy*, **33**, 21-37.

[5] Van Houten, C.J., van Houten-Groeneveld, I., Herget, P., Gehrels, T., 1970, The Palomar-Leiden survey of faint minor planets, *Astr. and Aph. Suppl.*, **2**, 5, 339-448.

Near-Earth Asteroids and Their Interest *(abstract)*

Binzel Richard

Near-Earth objects (NEOs) are of intense scientific interest because this population contains asteroids, active and extinct comets, and also meteorite source bodies. Thus an understanding of near-Earth objects is essential for resolving the relationships between asteroids, comets, and meteorites. Because of their proximity to Earth, NEOs are also the smallest solar system bodies that can be observed. As such, they display an array of physical properties (unusual shapes, configurations, rotations) that have been previously unobserved in physical studies of larger main-belt asteroids.

The use of radar observations of Near-Earth Asteroids for different astrometrical purposes

Yagudina Eleonora I.

Abstract. *Beginning 1968 radar observations for more than 130 asteroids, mainly Near-Earth Asteroids (NEAs), have been obtained. In this paper available radar observations of 30 NEAs and 4 main belt minor planets (345 radar observations) together with optical ones about 17000 observations) have been used to obtain precise asteroid orbits, catalogue orientation parameters and motion of the dynamical equinox in the Hipparcos system. The problem of the use of radar observations with optical ones for asteroid masses determination is discussed.*

1 . Introduction

The exact relations between different systems in astronomy (dynamical, ICRS, Hipparcos, FK5, FK6, etc) are still of much importance. It was shown firstly in (Yeomans et al., 1991) that even a few radar NEA observations, when added to optical ones, can significantly improve the precision of asteroid's ephemeris and reduce the standard deviations of the orbital elements, and in (Shuygina and Yagudina, 1996) that the catalogue orientation parameters can be determined more successfully from combined radar and optical NEA observations, than in the case of the use of only optical ones. Among the catalogue orientation parameters (correction to the mean longitude of the Earth, dL, the FK5 equinox correction, dA, the FK5 equator correction, dD, the secular variation of the equinox correction, $d\dot{A}$), $d\dot{A}$ is known as non-precessional motion of the equinox. It is unknown till now whether this mysterious phenomenon is a really existing kinematic effect or it is nothing else but the accumulation of the systematic errors in the old observations. When Hipparcos catalogue was introduced in astronomical practice it became possible to use Hipparcos as a reference frame for further study of this phenomenon.

The asteroid mass determination problem now is very important for the improvement the of the existing modern ephemerides of major planets. The use of radar observations of asteroids in combined solution with optical ones for the asteroid mass determination is also discussed.

2 . The FK5 Catalogue Orientation Parameters from Optical and Radar NEAs Data

Previously 8 (Yagudina, 1996), then 24 (Yagudina, 2001) asteroids with available radar data in combined solution with optical ones have been used for catalogue orientation parameters determination and for the analysis of equinox motion. Now we collected the observations of 34 minor planets with available radar data. Most of them, 30, are NEAs. The interval covered by optical observations for some objects is about 100 years, radar measurements are available after 1968. All optical observations were taken from MPC catalogue, radar observations (Doppler and delay) from JPL database «Small-body astrometric radar observations». The accuracy of optical observations are of the order of $1''$ for old observations and better than $0.5''$ for observations made after 1960. The precision of Doppler observations varies from 30.0 Hz till 0.1 Hz for the frequency, and from 140 till 0.1 μs for delay.

Several versions of the global solution have been considered: the solution with all available observations of 34 asteroids, the solution with all asteroids with long optical history (earlier of 1950 till 2000, 11 asteroids), solution with all asteroids with optical history after 1950 (23 asteroids) and last version, where we used all asteroids with optical history after 1960 (17 asteroids). The solution with all observations of optical and radar (34 asteroids) was considered as the main result : $dA = 0.063'' \pm 0.040''$, the equinox correction; $dD = 0.047'' \pm 0.008''$, the FK5 equator correction; the secular variation of the equinox correction, $d\dot{A} = -0.009''/cy \pm 0.001''/cy$; the correction of longitude of the Earth $dL = 0.085'' \pm 0.015''$. All calculations have been performed within the framework of ERA system (Krasinsky and Vasiliev, 1996). The DE200/LE200 ephemerides were used for calculations of the coordinates of perturbing planets and the Moon.

Table 1: The dynamical motion for different intervals of time

epoch	Time interval	$d\dot{A}$ $''/cy$	number of observations	Accuracy of optical obs.
2001.8	11 asteroids 1900–2000	– 1.034 ±0.079	10252 opt 107 rad	$1''$
	23 asteroids 1950–2000	– 0.004 ±0.001	6398 opt 238 rad	$< 1''$ $> 0.5''$
	17 asteroids 1965–2000	– 0.003 ±0.000	3150 opt 181 rad	$< 0.5''$
	34 asteroids 1900–2000	– 0.009 ±0.001	16660 opt 345 rad	$0.5'' - 1''$

The new solution gives us a rather small value of the equinox motion with very small error and confirms previous values of other parameters with small errors. Our previous determinations $d\dot{A} = -0.60''$ per century and $d\dot{A} = -0.203''$ per century were obtained by using optical and radar data of only 8 NEAs and 24 ones respectively. The present paper results in the value of $d\dot{A} = -0.009''$ per century with small uncertainty $\pm 0.001''$ per century.

In (Duma and Kozel, 1998) the analysis of different determinations of $d\dot{A}$ was made and the possible reasons of their big scatter were discussed. It is resumed in the paper that the effect is real, but the possible relations with some physical phenomenon or particular motion of celestial bodies are not proved. It can be seen from the table that the main reason of large value of $d\dot{A}$ obtained from old observations, can be ascribed to the poor quality of observations fulfilled before 1950. When we added the observations of asteroids with optical history after 1950 the value of $d\dot{A}$ became rather small. The value of $d\dot{A}$ obtained for asteroids at the time interval 1965–2000 is smaller than that obtained for asteroids at the other intervals and the uncertainty is insignificant.

To study the equinox motion from observations the corrections to the equinox position whatever obtained, as it was made by Blackwell (1977), have been gathered. Blackwell collected and reduced to homogeneous system all meridian observations of the Sun during 250 years interval, 1755–1973, and lunar occultations of stars at the end of this interval. He approximated in the FK4 system the equinox motion by parabola with statistically significant coefficients. The present investigation adds the new determinations not used by Blackwell. In so doing, both the old and new ones were transformed firstly to FK5 and then to the Hipparcos system, using the matrix given in (Mignard and Froeschle, 1997). The resulting curve in Hipparcos system is presented at figure. It is clear from figure that after 1950 all determinations made with better accuracy are distributed near the zero line. It is reasonable to believe that the poor quality of old observations is the source of the effect of the non-precessional equinox motion, but so far we can not exclude other possible causes.

Recently in (Vityazev and Yagudina, 2000) have been given explanation that the motion of the equinox may be caused by neglect of transition from UT to ET in treating the observed (not computed) declinations of the Sun. It was showed that corrections to the Newcomb's equinox were well correlated with the curve $\Delta T = ET - UT$ on the time interval near 170 years. In this way it may be stated that the fictitious motion of the equinox discovered about 100 years ago, was the first evidence of the irregular rotation of the Earth. But problem requires further study at the new level of accuracy (with use of the new modern observations as radar and CCD ones) and until it is not done this explanation should be considered as a guiding hypothesis.

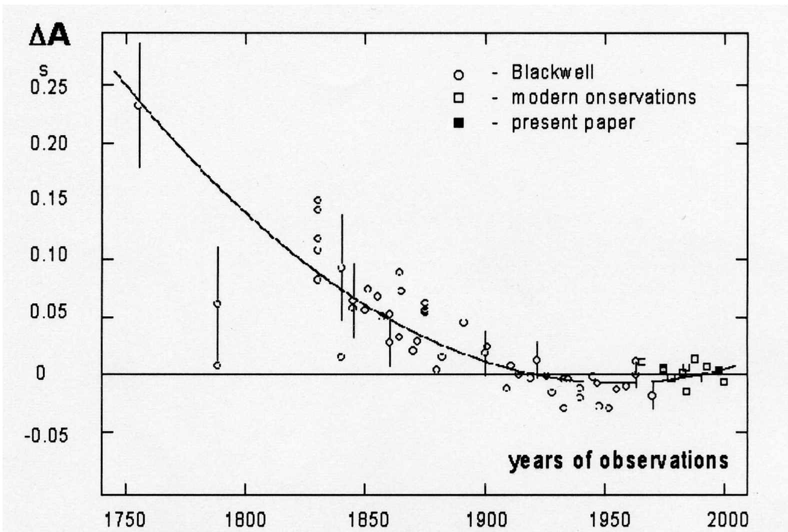

Figure 1 : Approximation of the changing of the equinox position (the equinox motion) at 1750–2000 interval by parabola. Blackwell and modern determinations in the Hipparcos system.

3 . The problem of asteroid mass determination

At present the problem of asteroid mass determination is the most important due to the necessity to take into account the perturbations caused by the minor planets in construction of planetary ephemerides. As it is shown by different researchers (Krasinsky et al., this issue) for further progress of fundamental planetary ephemerides it is necessary to have got the most reliable values of masses of perturbing asteroids. Now the main methods of the asteroid mass determination are two: the astrophysical, based on the measurements of the flux of radiation from asteroid and spectral observations which provide its spectral class, and dynamical, where the mass of asteroid has to be estimated from its perturbations upon the motion of other celestial bodies. In dynamical method the main results are based on photographic observations from MPC catalogue.

In (Hilton J. L., 1997) was demonstrated that the main changes during close approaches of asteroids are in mean motion and eccentricity of main asteroid. That means that very important for mass determination are radar observations of perturbed asteroid. Besides, as it was mentioned earlier, the combined solution of radar and optical observations gives the position of perturbing asteroid with rather good precision than in the case only optical ones, if even only few radar observations are available. In the same paper for the first time has been shown that the uncertainty of the mass value (15) Eunomia, with including only one simulated radar observation for asteroid Berna, which has encounter with Eunomia, was reduced two times, that is one radar observation is equivalent to 150 photographic ones. We repeated this simulation for asteroid Latvia which had the encounter with Eunomia also, and obtained uncertainty 2-2.5 times better (in the case of two ideal radar observations of Latvia). At present radar observations of these asteroids are not available. We hope that the number of asteroids with radar observations will arise during 1-2 years and this fact will help to determine asteroid masses with rather good precision by dynamical method.

4 . Conclusion

- The processing of radar and positional observations of 34 NEAs and main belt minor planets shows that the combined solution with modern radar and refined optical observations gives more precise catalogue orientation parameters.
- At the present stage of the problem, modern radar observations with refined sets of positional ground-based observations of NEAs and the main belt minor planets covering long interval of time can be quite useful to relate the Hipparcos system with dynamical one.
- Nowadays modern radar observations with refined sets of positional ground-based observations of NEAs and the main belt minor planets can be successfully used for the problems asteroid mass determination by dynamical method.

References

Blackwell, R. L., 1977, Equinox – position and motion during 250 years, *Month. Not. Roy. Astron. Soc.*, **180**(2), 65P.

Duma, D. P., Kozel, O.V., 1998, If nonprecessional equinox motion is real?, *J Kinemat Phys Celest Bodies*, Kiev, (in Russian).

Hilton, G.S., 1997, The mass of the asteroid 15 Eunomia from observations of 1313 Berna and

1284 Latvia, *Astr. Journal*., **179**, 402.

Krasinsky, G.A., Vasiliev, M.V., 1996, ERA : knowledge base for ephemeris and dynamical astronomy, *Proceedings of IAU Colloquium 165, Poznan, Poland*, July 1-5, 239–244, Wytrzyszczak I.M., Lieske J.H. and Feldman R.A., (eds).

Krasinsky, G.A, Pitjeva E.V., Vasiliev, M.V.,Yagudina, E.I., 2001, Estimating Masses of Asteroids, *Proceedings of Ceres 2001*, Paris, France, October 9-12, this issue.

Mignard, F., Froeschle, M., 1997, Comparison of the FK5 frame to Hipparcos, *Proceedings of the ESA Symposium «Hipparcos-Venice 97»*, Venice, Italy, May 13-16 1997. ESA SP-402, 57.

Shuygina, N.V., Yagudina, E.I., 1996, The FK5 equinox and equator from combined radar and optical data of near-Earth asteroids, *Proceedings of the 172nd Symposium of the IAU*, Paris, France, July, 3-8, 469–474, Ferraz-Mello S. *et al*., (eds).

Vityazev, V.V., Yagudina, E.I., 2000, The non-precessional motion of the equinox: a phantom or a phenomenon?, *Proceedings of Journees 2000*, Paris, in press.

Yagudina, E.I., 1996, The FK5 zero point corrections by radar and optical data of near-Earth asteroids, *Proceedings of Fourth International Workshop on positional astronomy and celestial mechanics*, Penyscola, October 7-11, 59–64, Lopez Garcia A. *et al*.(eds).

Yagudina, E.I., 2001, The use of radar observations of Near-Earth Asteroids in the determination of the dynamical equinox, *Cel.Mech.*, **80**(3/4), 195-203.

Yeomans, D.K. *et al*., 1991, Asteroid and comet orbits using radar data, *Astron.J.*, **103**(10), 303–317.

Kuiper Belt Objects photometry and position measurements with BTA - 6m telescope
(abstract)

Bykov Oleg, Maslennikov K. L., Gnedin Yu. N.

We have carried out BVRI photometry and positional measurements for 16 transneptunian (Kuiper belt) asteroids (KBOs) with BTA-6m telescope (Special Astrophysical Observatory, North Caucasus, Russia). Two color types for the asteroids were revealed according to their reflectance spectra at red wavelengths. In particular, a group of KBOs with a pronounced maximum of normalized reflectance near 7000 A was noticed. In this group, asteroids display on average smaller eccentricities and inclinations, compared to those with "flat" normalized reflectance. Suggestions are made concerning the possible reasons for these color differences. Astrometic positions of these KBOs were calculated also with good accuracy. In addition, several unknown Main belt asteroids were detected in the course of the observations and their colors were directly compared with those of the KBOs.

Photometric Study of Outer Solar System Bodies

Peixinho Nuno, Doressoundiram A., Barucci M.A.

Abstract. *Trans-Neptunian Objects (or Edgeworth-Kuiper Belt Objects) and Centaurs are very faint and elusive objects, and a careful data reduction has to be performed. Growthcurve correction is the most common technique applied in order to optimise data extraction. At Paris-Meudon Observatory a multicolour photometric survey is being dedicated to these objects which might contain important clues on the formation of the Solar System. A large colour diversity is shown raising questions on their nature, formation processes and physical and chemical evolution. Some results of this survey are presented and discussed.*

1 . Historical Introduction

Edgeworth (1943; 1949) and Kuiper (1951) speculate on the existence of planetary material beyond the orbit of Pluto – the sow called Edgeworth-Kuiper Belt (EKB). However, at that time not much attention was payed to these ideas. Only after a review on the solar system by Cameron (1962), in which these ideas were repeated, some astronomers started to gain interest on this subject. By the time, due to Oort's work on the long-period comets (Oort 1950), all comets were believed to have their origin in the Oort Cloud. The short-period comets were later considered as a result of Jupiter's gravity on a subset of objects in the Oort Cloud (Everhart 1972), even though Joss' demonstration that this model could not explain the excess of short-period comets (Joss 1973). But, in 1977, Kowal (1977) discovered an object with a short-living orbit (10^6 – 10^7 years) between Saturn and Uranus, Chiron – the first Centaur. Soon after, Fernandez (1980) explicitly advanced a trans-Neptunian comet belt (and not only trans-Plutonian) as source of short period comets, supported by numerical simulations. Duncan *et al.* (1988), explicitly showed that Chiron could be a member of the parent comet population in transition from the EKB, and made quite precise estimations on the magnitude of the Trans-Neptunian Objects (or Kuiper Belt Objects).

The advent of the high quantum efficiency CCD detector made the turning point for this research. After several negative attempts from various groups, in 1992, finally, Jewit & Luu (1993) observe the first TNO, 1992QB_1, at R = 41.2 AU, making the Edgeworth-Kuiper Belt (EKB) an observational reality.

2 . The Objects

Centaurs and TNOs, as parents of the short-period comets, are believed to possess interiors rich in molecular ices (*i.e.*, H_2O, CO_2, CO, NH_3 and CH_4). Presently (December 2001), about 500 TNOs and 30 Centaurs are known, and these numbers are growing at a great rate due to wide-field CCD surveys. There are no strict definitions for their classification and sub-classification, but generally :

1. Centaurs have semi-major axis and perihelia between the orbits of Jupiter and Neptune;
2. Trans-Neptunian Objects are subdivided in 3 groups :
   (a) Plutinos, are the objects in the resonance 3:2 with Neptune (representing about $\sim 20\,\%$ of the observed objects) – few objects are also trapped in other resonances, like 4:3, 5:3 and 2:1 –;

   (b) Classical Objects, have almost circular and low inclination orbits between 40 and 48 AU (being about $\sim 70\,\%$ of the observed objects);

   (c) Scattered Disk Objects (SDOs), are the objects with highly eccentric orbits beyond Neptune, being potentially the biggest subclass but under-sampled due to their faintness (representing, for the moment, $\sim 10\,\%$ of the TNOs).

The total mass of the EKB is estimated to be $\sim 0.1 M_{\oplus}$. The number of TNOs with diameter above 1 km is $\sim 10^{10}$, and above 100 km should be $\sim 10^{5}$ (Duncan *et al.*1995). Analogously, there are $\sim 10^{7}$ Centaurs bigger than 1 km, and only ~ 100 with diameters above 50 km (Sheppard *et al*. 2000).

3 . Observational Measurements

Only the brightest objects are accessible to high quality spectroscopic study and even those only with 8–10 m class telescopes. The available spectra already have shown the presence of water ice and methanol in some of them. For the moment, only broadband photometry allows a compositional survey relevant for statistical work. With the colors we may built a very low resolution reflectivity spectra and from here look for characteristics and correlations.

Size determination of these bodies are made with the knowledge of their geometrical albedo p_V and distance (Russel, 1916). However simultaneous measurements of optical and thermal radiation, to determine p_V, are difficult to accomplish due to their faintness. When unknown, the average geometrical albedo from comet nuclei and Centaurs of $p_V = 0.04$ is used. The uncertainty on this value has a consequent uncertainty on the estimated sizes presenting us a possible false picture of the size distribution. As an example, Chariklo, the biggest Centaur (D = 303 km), has a $p_V = 0.045$ – very close to the average value –, but Varuna, one of the biggest TNOs (D=900 km) has $p_V = 0.070$.

4 . Observations and Data Reduction

Centaurs and TNOs are inherently faint and difficult to detect, with typical V-magnitudes above 17 and 20, respectively. They are slow moving objects, trailing typically a few arcsec/hour, allowing us to observe them at sidereal tracking rate. Due to possible magnitude variations from a rotational lightcurve or albedo changes, photometry is performed with the filter sequence: V-B-V-R-V-I-V an then each color (B-V, V-R, V-I) is determined with an interpolation between two consecutive V measurements and the other corresponding filter. Exposures have to be limited to ~ 10 min to avoid both contamination of the signal by cosmic rays events and excessive trailing. In addition, we aim at S/N of about 30.

The photometric measurements have to be carefully performed. Typically an aperture with radius bigger than 3 times the full-width at half maximum (FWHM) of the objects is needed to collect all its flux. But, increasing the aperture will make the number of «pure» sky pixels be dominant over the measured area. This makes the sky estimation very critical for faint objects. For instance, a small error on the sky estimation will may introduce a big error on the estimated magnitude and the probability of contaminations by faint unseen background sources rises (*i.e.*, a «hidden» 26 magnitude source gives a 0.07 error on a 23 magnitude object). To escape from this problem we measure the flux with apertures where the S/N is maximized and the sky estimation is, consequently, less critical – typically the S/N is maximum for an aperture radius approximately equal to the FWHM. A correction for the flux loss is done by the analysis of the growth of the collected flux versus the aperture increase (growthcurve) of the bright stars in the field (Howell 1989; Barucci *et al*. 2000).

5 . Our Results

Our group, at the Observatory of Paris-Meudon (France), is carrying out a multicolor survey of TNOs, presently with about 60 objects, using mainly the 4 m class telescopes : NTT, TNG, WHT and CFHT.

The extension of our TNOs and Centaurs' color dataset is motivated by the controversy about bimodality on TNOs color distribution (presently solved!), the search for genetic links between the TNOs and the presumably associated populations, and the need of an homogeneous set of high quality observations.

5.1. Color–Color Relations

From our dataset, published by Doressoundiram *et al*. (2001), we may see that there is a great spread of colors among the TNOs, ranging continuously from neutral until very red colors (figure 1). Long term irradiation by energetic particles is known to cause surface darkening and chemical modification (Moore *et al*., 1983). A very red and very dark carbon rich «Irradiation Mantle» is therefore expected to cover the TNOs. How to explain such a large color diversity? Several hypothesis have been advanced:

1. Collision resurfacing : impacts on the objects excavate fresh material from the interior (unaffected by the irradiation and therefore more neutral) and the instantaneous color of the surface will be the result of the competition between progressive reddening by irradiation and the stochastic resurfacing from these less red collisional debris (Luu & Jewitt, 1996).

2. Intrinsic differences : objects may have intrinsic different surface compositions due to their formation circumstances – nevertheless this is a less favoured scenario since the temperature gradient between 30 and 50 AU during their formation was only of ~ 10 K, not enough to generate significantly different chemical compositions.

3. Grain sizes : it has been shown that the size of the grain on a surface layer has a significant effect on the measured color, even for the same composition (Moroz *et al*., 1998) – even though this effect is unlikely to explain the large color differences, it may play an important role.

5.2. Color–Size–Orbital Relations

The main results of the analysis of our data are here summarized. We find no correlation between size, color, or heliocentric distance. Nevertheless, there is an excess of very red objects with perihelion distance greater than 40 AU, that may indicate that resurfacing mechanisms may be inefficient in reworking objects beyond 40 AU. More interestingly, we found objects with high eccentricity and inclination are always neutral/slightly red, suggesting that collisions are efficient processes rejuvenating the surfaces in that region of the Edgeworth-Kuiper Belt. For more details see (Doressoundiram *et al.*, 2001).

6 . Conclusion

The most clear, and undeniable, conclusion is that there is a large diversity of colors. No significant differences with the associated populations are detected. A more «efficient» sampling of the subpopulations is needed, in order to demonstrate, or refute, any correlations. We need an extension of the data to the infrared, in order to better characterise these objects. Actually, the most important spectral information is concealed in the infrared bands. Error bars need, still, to be reduced for a better significant statistical work, hence improved data reduction techniques should be developed.

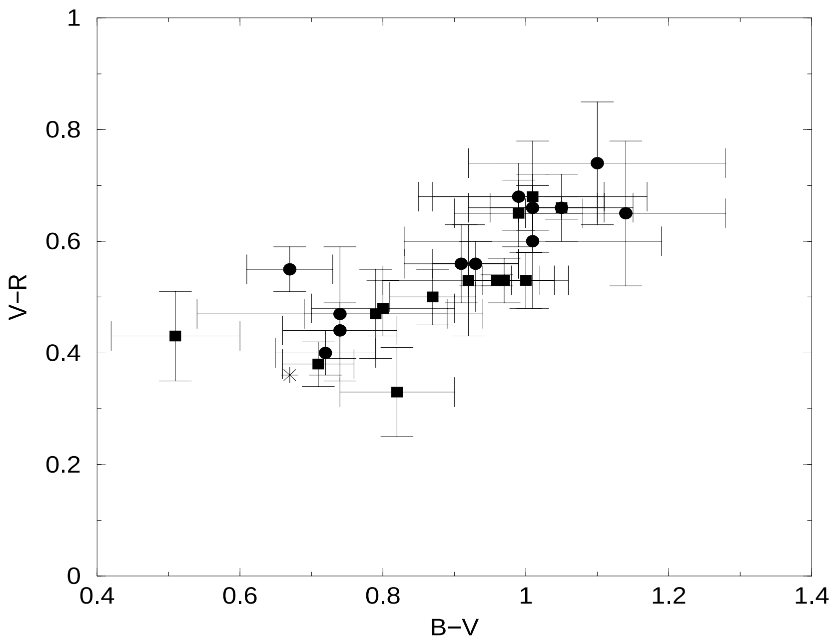

Figure 1 : B-V versus V-R color plot of TNOs from Doressoundiram *et al*. (2001).The star represents the color of the Sun. There is a continuous spread of colors ranging from the neutral (solar like) to the very red.

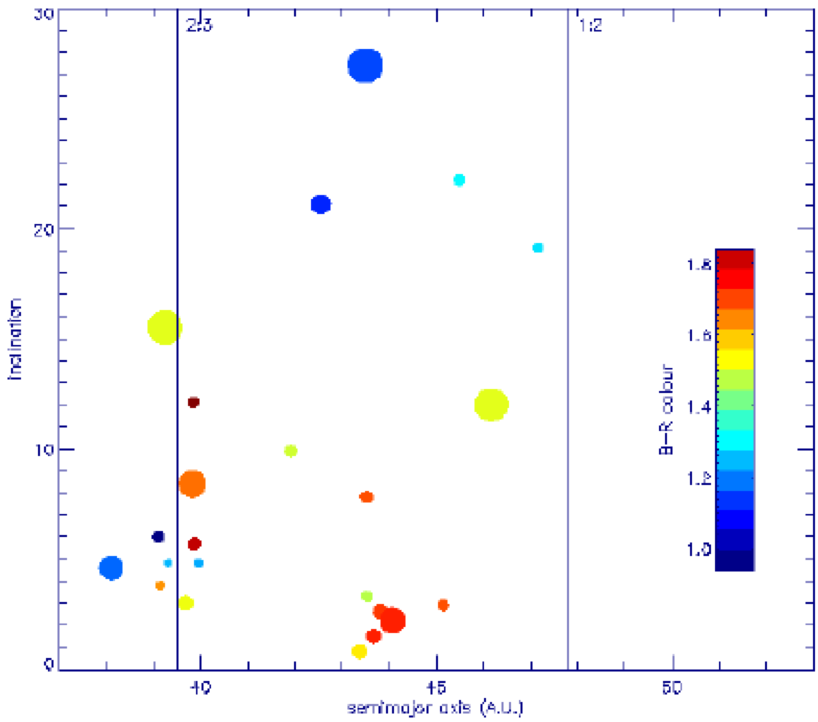

Figure 2 : B-R colors in the orbital inclination versus semmimajor axis plane from Doressoundiram *et al*. (2001). The size of the symbols are proposrtional to the corresponding object's diameter. Alack of red objects with high inclination orbits is apparent.

References

Barucci, M. A., Romon, J., Doressoundiram, A., Tholen, D. J., 2000, *AJ*, **120**, 496.

Cameron, A., 1962, *Icarus*, **1**, 13.

Doressoundiram, A., Barucci, M. A., Romon, J., Veillet, C., 2001, *Icarus*, in press.

Duncan, M. J., Quinn, T., Tremaine, S., 1988, *ApJ*, **328**, L69.

Duncan, M. J., Levison, H. F., Budd, S. M., 1995, *AJ*, **110**, 373

Edgeworth, K., 1943, *J. Br. Astron. Soc.*, **53**, 181.

Edgeworth, K., 1949, *MNRAS*, **109**, 600.

Everhart, E., 1972, *ApL*, **10**, 131.

Fernandez, J., 1980, *MNRAS*, **192**, 481.

Howell, S. B., 1989, *PASP*, **101**, 616.

Jewitt, D., Luu, J., 1993, *Nature*, **362**, 730.

Joss, P. C., 1973, *A&A*, **25**, 271.

Kowal, C., 1977, *IAU Circ. No. 3129*.

Kuiper, G., 1951, On the Origin of the System, *Astrophysics*, J. A. Hynek ed., 357.

Luu, J., Jewitt, D., 1996, *AJ*, **112**, 2310

Moore, M. H., Donn, B., Khanna, R., A'Hearn, M. F., 1983, *Icarus*, **54**, 388.

Moroz, L., Arnold, G., Korochantsev, A., Wasch, R., 1998, *Icarus*, **134**, 253.

Oort, J., 1950, *Bull. Astr. Inst. Netherlands*, **11**, 91.

Russel, H. N., 1916, *ApJ*, **43**, 173.

Sheppard, S. S., Jewitt, D., Trujillo, C., Brown, M., Ashley, M. C., 2000, *AJ*, **120**, 2687.

Perturbations of Mars by the asteroids *(abstract)*

Bretagnon Pierre

The most perturbations of the planet Mars by the asteroids reach amplitudes of about 13 km (with a 300 year period) and 5 km (with a 50 year period). The uncertainties of the masses of the asteroids limit the quality of the ephemerides of Mars at several hundred of meters.

Pierre BRETAGNON

Pierre Bretagnon, astronomer at the Institut de Mécanique Céleste et de Calcul des Ephémérides (IMCCE), passed away on November 17, 2002. We wish here to pay homage to him.

Since 1969 Pierre Bretagnon was astronomer at the «Service des calculs et de mécanique céleste du Bureau des longitudes» (become, in 1998, the Institut de mécanique céleste et de calcul des éphémérides).

He initially devoted himself to the construction of the planetary theories. He built as well «general» theories as «secular variations» theories. The general planetary theory built by Pierre Bretagnon in 1972 made a considerable improvement to the existing theories. With this theory, one can say that the celestial mechanics provided a clock to planetology. Pierre Bretagnon, throughout his career, continued to be interested in the general theories. His work was used, in particular, in the study of the paleoclimates of Mars and in that of resonances between asteroids and Jupiter.

Pierre Bretagnon was the first to build a theory of the eight main planets with secular variations. In 1984 the ephemerides drawn from its solution VSOP82 (Variations Séculaires des Orbites Planétaires) replaced, in the French national almanac «La Connaissance des temps», the ephemerides drawn from the theories of Le Verrier and Gaillot. Solutions VSOP, constantly improved, became world references as regards ephemerides. They were used, for example, in the reduction of the data of the European satellite Hipparcos.

During these last years Pierre Bretagnon had undertaken the development of planetary theories within the framework of general relativity, in collaboration with Victor Brumberg (from Intitute of Applied Astronomy, Moscow). He had become one of the world specialists in the relativistic celestial mechanics.

Pierre Bretagnon was also interested in the rotation of the Earth. He was at the head of the small team of researchers of IMCCE which built an outstanding theory of the rotation of the solid Earth, SMART97 (Solution du Mouvement de l'Axe de Rotation de la Terre) which became a reference among the specialists of this domain.

Parallel to his research activities, Pierre Bretagnon implied himself also much in the diffusion of information at the astronomical community. With a great rigour and a remarkable effectiveness, he was from 1988 to its death, the person in charge for the service of information of the IMCCE.

In the difficult field of Celestial mechanics directly applied to the movements of the celestial bodies, Pierre Bretagnon has been one of the most brilliant researchers of his generation.

Impact of the dynamical perturbations of the main belt asteroids on planetary ephemerides : why is it important to have accurate determination of the main belt asteroids size and shape *(abstract)*

Fienga A.

In this presentation, I will present new results obtained at JPL on testing how the main belt asteroids could perturb the ephemerides of Mars and the Earth and at what level. A survey of several masses, sizes and shapes estimations was done and the impact of these severel determinations on the ephemerides was computed. Monte Carlo simulations was also performed to estimated the sensiblity of the DE405 ephemerides to the change of asteroids masses. I will conclued in stressing the fact that in the future, we will need more and more accurate ephemerides of Mars due to a huge number of spacecraft missions and the improvement of these ephemerides are closely correlated to improvement of our knowledge of the shape and size of more and more asteroids.

Finding Small Bodies by Their Luminescence Properties

Simonia Irakli, Simonia Tsitsino

Finding unknown small bodies (comets, asteroids) of the solar system still remains a challenging task of observational astronomy. Various instrumants are applied to search and detect those bodies. Basic methods used for it consist in recording The sunlight reflected by the surfaces of the small bodies moving on the background of the stars.

It is common knowledge that the solar system's bodies are also irradiated by the solar UV emission. The UV photons may couse photoluminescence of surfaces of atmosphereless bodies, asteroids, planet companions, as well as the cometary dust. Photoluminescence may be exhitited as fluorescence or phosphorescence, depending on the chemico-mineralogic properties and temperatures of the cosmic luminophors. However, luminescence exhibited by the cosmic dust is less intensive, and the intensity level of luminescent emission is below the level of the reflected solar continuum. This type of photoluminescence can be detected by the method of division of the spectra [Churyumov *et al*., 1999]. It is essential to study photoluminescence of the solid cosmic matter. Photoluminescence provides us with information on the chemicomineralogic composition of the matter, its temperature, crystal lattice, etc. However, owing to the low intensity of photoluminescence of small bodies, it cannot be recorded by the method of detecting unknown bodies. The solar system's bodies are also exposed to intensive corpuscular solar radiation, solar wind and solar plasma clouds. As it was shown in literature [Dodson-Prince, 1977] the most powerful solar flares of cosmic rays with proton energies over 500 Mev are rare events. The proton flares give out protons of energies 10MeV=E<100MeV. These events are more frequent. Proton flares are accompanied by emission of nonrelativistic electrons with energies over 4 KeV and fluxes of up to 5000 electron/cm2.sec.sterad. The flares with electrone eruption characterized by fluxes of under 100 electron/cm2.sec.sterad are also frequent. Among particularly curious events [Tandberg-Hanssen, 1977] one should consider prominences of the surge and spray type, fast eruptions with over 1000 km/sec speed, that frequently escape from the observer's ege and fail to be recorded due to a great Doppler whift. The surge matter frequently moves away from the Sun, and the spray substance, a plasmoid connected with the flare event, also may have velocities higher than the velocity of escape. It is now believed that the solar wind's basic component is a high-speed flux escaping at 380 km/sec to 800 km/sec. The spread of the Solar wind is limited by the heliosphere's dimensions which do not exceed 100 a.u. in the conditional radius, according to different researchers. The above said proves clearly the effect of the Solar corpuscular radiation upon the Solar System's bodies.

The Solar electron and ion fluxes, plama clouds collide with small bodies to give rise to an intensive cathodo and ionoluminescence of the solid matter on the surface of those bodies.

During the electron bombardment most part of the kenetic enery of the electrons decetera-ting in the matter is spent for heating that matter, while its minor part is spent to excite cathodoluminescence and to cause a secondary electron emission. Electrons of 10 KeV energy penetrate into the luminophor dawn to 2.5 • 10^{-4} cm depth. During cathodoluminescence the incoming energy is absorbed by all the crystal lattice nodes and then transferred to the glow centres. In our poinion, when a small body gets into the field, of solar electron flux the body may surface start luminescing (with its side facing the Sun) with an intensity of cathodoluminescence :

$$I = k \bullet r \bullet p \int_{E_1}^{E_2} z de \qquad (1)$$

where k is a constant coefficient equal to 1.6 • 10^{12}, r is the body's radius, p is the bundle current density, z is the electron energy (in erg) at $E_2>Z>E_1$. The cathodoluminescence duration of a small body will be $T = t + \tau$ (2), where t is the duration of the small body's bombardment with electrons, τ is the duration of possible afterglow. The cathodoluminescence duration of a small body will vary from some seconds to several hundreds of seconds. Too long exposure of cosmic luminophors to high-energy electrons may couse the luminophor's destruction resulting in the full or partial loss of their luminescence properties. If the small body surface is rich in the crystals of ZnO, CaO, SrO (pure), in low-temperature conditions the crystals will exhibit a specific cathodoluminescence spectre in the 3600-4000 A range. Cathodoluminescence of chondrites is discussed by Dehart *et al.*, 1989. Their data may serve as a comparative material in the study of cathodoluminescence of asteroids and comets. Bombardment of the small bodies with ion fluxes will cause ionoluminescence of those bodies surface hard matter. Ions of several KeV will be sufficient to induce luminescence, the depths of the ion penetration being about several A. The time duration of bright ionoluminescence of the small body surface can hardly be of any significance due to the fast aging of the ionoluminophors treated with bombarding ions. (The conclusion is based on the laboratory results for terretrial ionoluminophors). For the practical search of unknown bodies by their cathodo and ionoluminescence we suggest using :

1. The method of an after flare electronic-graphic search.
2. The method of an afterflare spectral search.

The first method implies :

a) Obtaining a betescopic and CCD-camera image of a particular area of the sky at a certain moment t1 before the solar flare (a control frame).

b) Obtaining a series of images of the same area of the sky X days after the solar flare. The value X will be defined considering the velocity of the sun particles and the heliocentric distance of the search area. X may be 3,5,7 or more days.

c) Comparing each image from the obtained series with the contror frame, using a computer.

The exposure time of the control frame must be absolutely equal to that of the series frames, Varying from some tens of seconds to several minutes. The equipment used throughout the experiment must be the same. The following criteria will indicate to an unknown small luminescent body : I. A starlike obfect appearing in one or several images in the afterflare series at a place (spot) where no object is seen in the control frame. II. A starlike object appearing only in one or several frames of the series (1 to 10). So, one or several frames in the afterflare image series show a starlike object that is absent in the control frame.

The sun particles have excited a short-term cathodo or ionoluminescence of the body, its surface «flashing up» and quickly going out. The process is recorded in several frames of the afterflare series. All the known variable objects in the sky area under observation must be properly considered.

The second method implies using on objective prism with small dispersion, in addition to the telescope and CCD camera. Items a, b, c are to be observed, as well. A third criteria indicating to the presence of a small body is added to the above mentioned : III. Not a star spectrum but a cathodo or ionoluminescence spectrum of solid bodies exhibited by the object. The second method may help to reveal on unknown body by its unusual spectrum. If after a certain period of time and after a second, third... N-th solar flare the same sky area shows an object with close coordinates, one may suppose that the detected body is not an asteroid or comet, but a so far unknown planet moving at a long distance from the Sun and having quite a low albedo. It seems reasonable to use the above mentioned methods for the heliocentrie distances of r = 4 a.u. The question is : Why weren't these events, if they are really taking place, observed earlier? Taking into account the nature of interaction between charged particles and solid matter, the question can be answered: the reason is the short duration of the events. An observer working alone can hardly detect unknown objects. A network of observation points, each responsible for a certain part of the sky, would be a reasonable arrangement. The above offered methods can ensure detection and observation of unknown asteroids, comets, Kuiper objects, planets and their companions. The method may be successfully used for early detection of low-albedo bodies approaching the sircumterrestrial space.

References

[1] Cheryumov, K.I., Kleshchonok, V.V., 1999, Parameters of Luminescence Cometary Continuum in Spectra of Comets Schaumasse (24P) Scoritchenko-George (c/1981 y1) and Hale-Bopp (c/1995 01). *American Astronomical Society*, DPS meeting 13.

[2] Dodson-Prince, H.V., Bruzek, A., 1977, Illustrated glossary for Solar and Solar-Terrestrial Physics, A. Bruzek and C. J. Durrant eds., Dordrecht Holland / Boston - USA.

[3] Tandberg-Hanssen, E., 1977, Ilustrated glossary for Solar and Solar-Terrestrial Physics, A. Brizek and C.J. Durrant eds., Dordrecht-Holland/ Boston - USA.

[4] Dehart, I.M., Lofgren, G.E., Sears, D.W.G., 1989, The Composition and Luminescence Properties of Chondrule Olivines and Pyroxenes in the Type 3 Ordinary Chondrites, LPSC XX.

Observations of Mimas to determine the eccentricity of Tethys and understand the Mimas-Tethys commensurability

Vienne A.

***Abstract**. Tethys' eccentricity induces secondary resonances inside the present main resonance between Mimas and Tethys. It is why this eccentricity has a deciding influence upon the evolution, under tidal effects, of the dynamics of this system. In past studies, the orbit of Tethys was always supposed to be circular. With the new dynamical model TASS, the value of the eccentricity of Tethys is still badly known. We find that the ellipticity of the orbit of Tethys is more influent on the position of Mimas. With the help of the recent reduction of precise CCD observations of Mimas, we present a new determination of this eccentricity.*

***Keywords**: satellites, resonances, observations, astrometry.*

1 . The eccentricity of Tethys

Several years ago, we have built a theory of motion of the eight major satellites of Saturn. The physical model takes into account the Saturn's oblateness, the mutual interactions, the solar perturbation and the given mean mean motions. It was constructed in a dynamically consistent way, in which the satellites are considered all together; its only parameters are explicitly the initials conditions, the masses of the satellites and the oblateness coefficients of Saturn. Its internal precision is a few tens of kilometers. This theory is based on the set of the Earth-based observations, from 1874 to 1985 (TASS1.7, Vienne & Duriez 1995, Duriez & Vienne 1997).

This study has shown some new terms in the mean longitude of Mimas which upset the vision of the dynamics of the Mimas-Tethys system (Table 1).

The ancient descriptions of this dynamics were limited to the primary 2:4 mean motion resonance : the argument $\varphi = 2\lambda - 4\lambda' + \Omega + \Omega'$ librates, so the conjunction line oscillates between $-48°$ to $+48°$ around the mean point $(\Omega + \Omega')/2$ of the nodes, with the frequency ω (period 70 years). In these descriptions, the orbit of Tethys is supposed to be circular. But, considering a non-circular orbit for Tethys, TASS shows new terms near the resonance corresponding to the argument $\sigma = (\Omega - 3\Omega')/2 + \varpi'$ (with period 200 years, ϖ' is the longitude of the perisaturn of Tethys). These terms are proportional to the eccentricity e' of Tethys, but the value of e' is badly known (between 0 and 0.001).

Table 1 : Mean longitude of Mimas and eccentricity of Tethys. Only terms greater than, respectively, 500 km and 50 km are given. These series are given for a value of the eccentricity of Tethys equal to 0.001.

Mean longitude of Mimas : λ expressed in sinus				ecc. of Tethys : $e' \exp(\sqrt{-1}\,\varpi')$ expressed in exponential			
amp. (km)	period (years)	arg.	frequency (rad/year)	amp. (km)	period (years)	arg.	frequency (rad/year)
141197.	70.6	ω	0.0889514				
2304.	23.5	3ω	0.2668535	251.	4.97	ϖ'	1.263056
1218.	109.5	$\omega - \sigma$	0.0573619	114.	5.35	$\varpi' - \omega$	1.174011
840.	52.1	$\omega + \sigma$	0.1205358	114.	4.65	$\varpi' + \omega$	1.352101
628.	198.9	σ	0.0315910				

Because of tidal effects due to dissipation in Saturn, the mean angular velocity of the arguments φ and σ are variables. Then, the system can enter in one or several secondary resonance. Champenois and Vienne (1999 a and b) have shown that the system may have been trapped in a secondary resonance or may have behaved in a chaotic way on capture in the present ii' resonance. At the epoch of the capture in the main resonance (about two hundred millions years ago), the inclination of Mimas may have been higher, or lower than derived by Allan (1969). Moreover, the eccentricity of Tethys have been higher (up to 0.008). The probability of capture into the present resonance, extremely depends upon the value of e', may be much higher (up to 1) than 0.04 found by Sinclair (1972).

The Table 1 shows that the value of the eccentricity of Tethys is more influent in the position of Mimas than in the position of Tethys. The terms with the argument $\sigma = (\Omega - 3\Omega')/2 + \varpi'$ (period 200 years) was never been taken into account before. The Earth-based observations of the satellites of Saturn allow to reach the precision of about 500 to 1000 km. It is why the orbit of Tethys was, until now, supposed to be circular. So, if we want to determine the eccentricity of the orbit of Tethys, we have to analyze the orbit of Mimas. And more particular, we have to analyze the mean longitude of Mimas.

Note that it is possible that some observers have made a confusion between these terms and a eventual acceleration in the longitude of Mimas (see Vienne *et al.* 1992).

2 . Analysis of recent observations

TASS is based on Earth-based observations which cover more than one century, from 1874 to 1985. Nevertheless, the eccentricity of Tethys is not well determined with this set of observations. After 1990, only few observations of the satellites of Saturn are available. It is only recently that we begin to find some more observations. This gap (roughly 1985-1995) is due to the transition between the use of photographic plates and the CCD receptors. These recent reductions of the CCD observations are given in Table 2.

Table 2 : Comparison between different reductions of CCD observations

Observers	nb of observations		precision	
	S1 to S8	Mimas (S1)	S3 to S6	Mimas
CCD:				
Beurle, Harper *et al*. 1993	249	16	$0.''101$	-
Harper, Murray *et al*. 1997	1206	73	$0.''080$	-
Harper, Beurle *et al*. 1999	1514	15	$0.''090$	-
Qiao, Shen *et al*. 1999	381	15	$0.''080$	$0.''141$
Vienne, Thuillot *et al*. 2001	6006	216	$0.''068$	$0.''081$
Peng, Vienne *et al*. 2001	913	54	$0.''039$	$0.''052$

The large set of observations of (Vienne, Thuillot *et al*. 2001) are from international campaign in 1995 of observations mutual occultations and eclipses, and more precisely from Laboratório Nacional de Astrofísica at Itajubá in Brazil. Many CCD frames were then obtained without any detection of events because of the difficulty to measure a faint magnitude drop closely to the planet. But astrometric data have been extracted from these observations.

We have tried to determined again the eccentricity of Tethys with these recent observations. The method is the following one :

- for each observation of Mimas, we compute a value of the longitude of Mimas for which the o-c is minimum : λ_{obs}

- for each observation of Mimas, we compute a value of the longitude with TASS and without the terms of the argument σ (that is with $e' = 0$) : λ_c

- So we suppose that

$$\lambda_{obs} - \lambda_c = f \times e' \times [1218 \sin(\sigma + \omega) + 850 \sin(\sigma - \omega) + 628 \sin(\sigma) + \ldots]$$

where f is a factor which takes into account the nominal value of e' and transforms the units of the expression (km to rad). In this expression, all the parameters are know except e' and ϖ' (in σ). Furthermore, in ϖ', only its phase is unknown and its frequency is easily well computed by TASS.

- We then obtained an equation of condition for each observation. We resolve the whole set by a least square procedure.

The first computations done give the following result : $e' = 0.00021 \pm 0.00008$.

The uncertainty is still large, so we have to investigate more the analysis of the longitude of Mimas.

3 . Conclusion

The orbit of Tethys was, in the past, always supposed to be circular because it is difficult to measure its value on the orbit of Tethys. In fact, the ellipticity of this orbit is more influent on the position of Mimas. Some recent precise observations of Mimas and an analysis of the mean longitude of Mimas allow to determine a value to the eccentricity of Tethys. Nevertheless, the present uncertainty is large, and then, more investigations are necessary. This determination is important because the eccentricity of Tethys has deciding action upon the evolution of the resonance Mimas-Tethys.

References

[1] Allan, R.R., 1969, Evolution of the Mimas-Tethys commensurability, *Astrom. J.*, **74**, 497-506.

[2] Beurle, K., Harper, D., Jones, D.H.P., Murray, C.D., Taylor, D.B., Williams, I.P., 1993, Preliminary analysis of CCD observations of Saturn's satellites, *Astron. Astrophys*., **269**, 564-567.

[3] Champenois, S., Vienne, A., 1999a, Chaos and secondary resonances in the Mimas-Tethys system, *Celest. Mech. & Dynam. Astr*., **74**, 111-146.

[4] Champenois, S., Vienne, A., 1999b, The role of secondary resonances in the evolution of the Mimas-Tethys system, *Icarus*, **140**, 106-121.

[5] Duriez, L., Vienne, A., 1997, Theory of motion and ephemerides of Hyperion, *Astron. Astrophys*., **324**, 366-380.

[6] Harper, D., Murray, C.D., Beurle, K., Williams, I.P., Jones, D.H.P., Taylor, D.B., Greaves, S.C., 1997, CCD astrometry of Saturn's satellites 1990-1994, *Astron. Astrophys. Suppl. Ser*., **121**, 65-69.

[7] Harper, D., Beurle, K., Williams, I.P., Murray, C.D., Taylor, D.B., Fitzimmons, A., Cartwright, I.M., 1999, CCD astrometry of Saturn's satellites in 1995 and 1997, *Astron. Astrophys. Suppl. Ser*., **136**, 257-259.

[8] Peng, Q., Vienne, A., Shen, K. X., 2001, Positional Measuring Procedure and CCD Observations for Saturnian Satellites, accepted for publication in *Astron. Astrophys*.

[9] Qiao, R. C., Shen, K.X., Liu, J.R., Harper, D., 1999, 1994-1996 CCD astrometric observations of Saturn's satellites and comparison with theories, *Astron. Astrophys. Suppl. Ser*., **137**, 1-5.

[10] Sinclair, A. T., 1972, On the origin of the commensurabilities amongst the satellites of Saturn, *Mon. Not. R. Astrom. Soc*., **160**, 169-187.

[11] Vienne, A., Sarlat, J.M., Duriez, L., 1992, About the secular acceleration of Mimas, in Proceedings of *Chaos, Resonance and Collective Phenomena in the Solar System,* S. Ferraz-Mello (ed.), 1992, IAU Symposium 152, 219.

[12] Vienne, A., Duriez, L., 1995, TASS1.6 : Ephemerides of the major Saturnian satellites, *Astron. Astrophys*., **297**, 588-605.

[13] Vienne, A., Thuillot, W., Veiga, C.H., Arlot, J.-E., Vieira Martins, R., 2001, Saturnian satellites observations made in Brazil during the 1995 opposition with an astrometric analysis, *Astron. Astrophys*., **380**, 727-733.

Detection of Asteroid Companions by Astrometric Methods *(abstract)*

Monet Alice K.B., Monet David G.

Three years ago, we reported on results of a study of the detectability of astrometric «wobble» in the orbits of binary asteroids (A. Monet and D. Monet, 1998, BAAS, 30, 3, 1144.) At that time, only one asteroid companion had been detected. In the ensuing years, several more asteroid companions have been directly imaged, primarily from the ground using large telescopes with adaptive optics. Although the numbers are still small, these detections have led to better physical models of asteroid structure, evolution, and collisional histories. The simple fact that asteroid companions are being identified every few months, now that sufficiently high optical resolution is widely available, suggests that duplicity is rather common. The question addressed in this poster is how to design an astrometric survey to detect asteroid companions, using smaller aperature (< 2-meter) telescopes, such as the automated, 1.3-meter telescope, just now nearing completion at the USNO Flagstaff Station.

Precession of the satellite of oblate asteroid

Portyankina G., Aleksandrov Yu. V.

To describe the motion of a satellite (both artificial and natural [1]) of asteroid it is desirable to take into account the fact that asteroids in most cases have irregular shape with large oblateness (especially in comparison with planets).

In this paper we approximate the shape of asteroid by the triaxial ellipsoid with the ratio of semiaxes $a:b:c = 2:\sqrt{2}:1$ [2, 3] and in addition consider asteroids (except for the largest ones) as homogeneous bodies.

In the light of mentioned above the problem of two fixed centers appears to be a good approximation to describe the dynamics of binary asteroid. In this case the primary is represented by two point masses m_1 and m_2 fixed on complex distances d_1 and d_2. The complex distances allow us to take into account the oblateness of the primary. For description of the primary oblateness we use so called doublet parameter d (if the body is symmetrical relatively to the equator $d_1 = di$, $d_2 = -di$; $d = \sqrt{J_2}R$, R - typical size of the primary, in the case of ellipsoid $R = a_1$, i.e. major semiaxis).

To investigate the satellite precession motion of non-spherical body the description given by the following well-known equations for secular perturbations of the orbit elements under the influence of the second harmonic of gravitational potential is used most of all.

$$\frac{dp}{dt} = 0 , \frac{de}{dt} = 0 , \frac{di}{dt} = 0 , \tag{1}$$

$$\frac{d\Omega}{dt} = \frac{3}{2} \cdot n \cdot J_2 \cdot \left(\frac{a}{p}\right)^2 \cos i, \frac{d\omega}{dt} = \frac{3}{4} \cdot n \cdot J_2 \cdot \left(\frac{a}{p}\right)^2 (1 - 5 \cdot \cos^2 i) \tag{2}$$

The goal is to compare description (1) - (2) of the satellite motion in the field of oblate planet and the problem of two fixed centers under the condition that primary can have big oblateness.

General solution of the problem of two fixed centers is evaluated in the elliptical coordinates by the inversion of elliptical integrals. The method of this inversion (and so the sort of the solution that is evaluated through Jacobi elliptic functions) essentially depends on initial conditions [4].

Employing solution for the problem of two fixed centers the satellite orbit was computed under chosen initial conditions. That is, elliptical and then rectangular coordinates of the satellite were found. It was made in the reference frame that is connected with equatorial plane of the primary under the following normalization requirement : $fm = 1$, $a_1 = 1$, $\mathrm{T} = 1$ (m -

asteroid mass; a_1 - its major semiaxis; T - period of unperturbed keplerian motion under the same initial conditions).

Using rectangular coordinates the osculating keplerian orbit elements Ω, ω, a, i, e were calculated and values of node longitude Ω and pericentric distance ω were compared with the same values obtained from equations (2) for the same moments of time. It must be noticed that in the case of problem of two fixed centers all keplerian elements of orbit are changing.

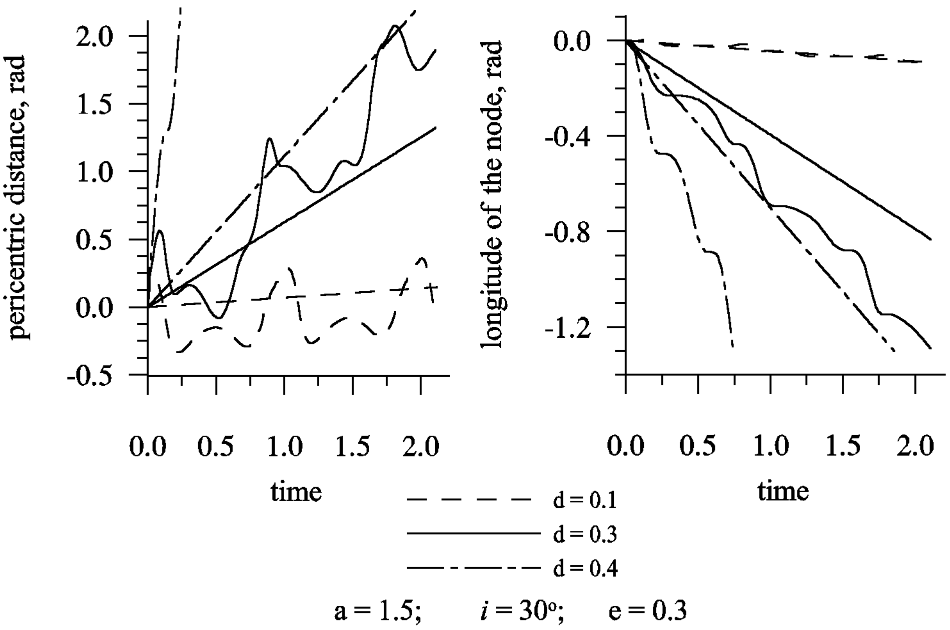

Figure 1 : The influence of the primary oblateness on precession of asteroid satellite

Figure 1 represents the changes of node longitude Ω and pericentric distance ω with time computed under chosen initial conditions and different oblateness of the primary. The curves represent values of Ω or ω calculated in the problem of two fixed centers and straight lines are the same values obtained using equations (2). In the last case periodical changes of longitude of the node Ω and pericentric distance ω are lost, but in the problem of two fixed centers the information about periodical perturbations remains.

Time is measured in the units of unperturbed period, distance - in the units of characteristic size of the central body (in the case of triaxial ellipsoid it is its major semiaxis).

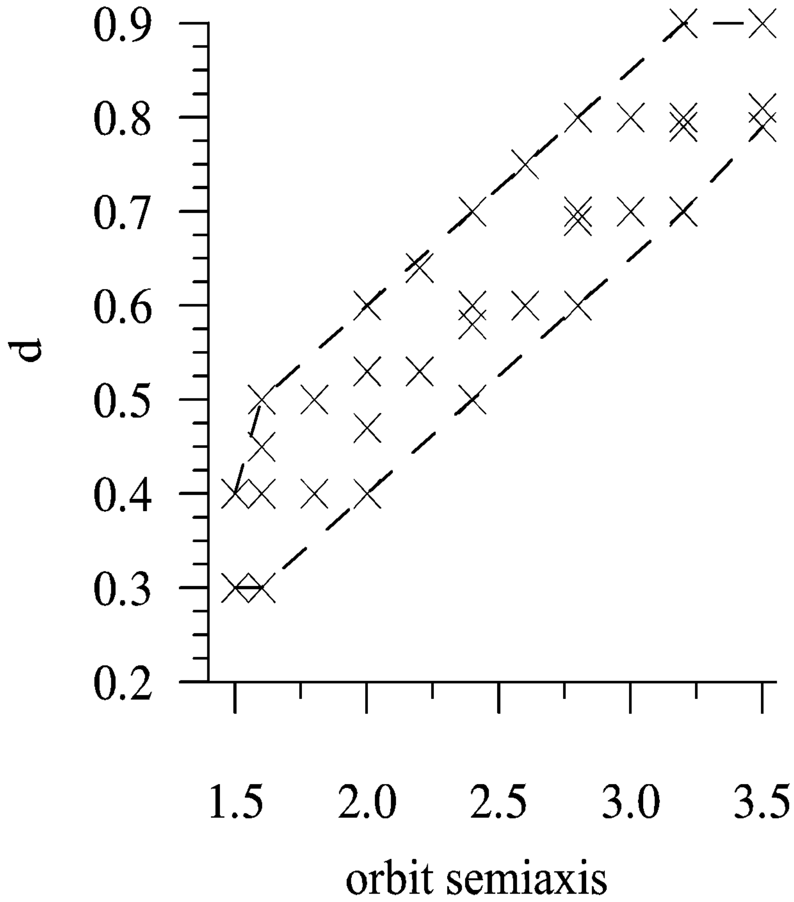

Figure 2 : Critical values of the primary oblateness

The calculations have been made for the orbits with initial value of major semiaxis in the range from $1.5a_1$ to $3.5a_1$. The smaller distance from the primary surface, the bigger perturbation, the more chaos in the motion. Comparison between two considered above approaches shows that at the distances ≥ 3.5 the values of Ω and ω, obtained from equations (2), coincide with the ones of the problem with two fixed centers with acceptable accuracy for all primary oblatenesses. For smaller distances there is a value of oblateness (critical value) at which the difference between two descriptions becomes much bigger than amplitudes of Ω and ω (fig.1). For the values of oblateness larger than critical it is impossible to represent perturbed motion as expansion by the precession of line of apsides and precession of line of nodes. Such critical values of oblateness are represented at fig.2, their family divides plane on two regions: region 1, where it is possible to use equations (2), because they are applicable, and region 2, where the problem of two fixed centers gives more accurate description.

References

[1] Chapman, C. R. *et al.*, 1995, *Nature*, **374**, 783 - 785.

[2] Fujwara, A., Cerront, P., Davis, D.R. *et al.*, 1989, Asteroids II, Binzel R. ed., Gehrels T., Mattews M. (Tuson : Univ. Arizona Press), 240-265.

[3] Lupishko, D.F., Di Martino, M., 1997, *Planetary and Space science*, **45**, 11.

[4] Grebennikov, E.A., Demin, V.G., Aksenov, E.P., 1961, *Artificial satellites of the Earth*, **8**, 64-72, in Russian.

Asteroid satellites formation as a natural outcome of collisions *(abstract)*

Tanga P., Michel P., Benz W., Richardson D.

Numerical simulations ot the collisional fragmentation of asteroids have been performed by an SPH code. The gravitational evolution of fragments has been simulated by an N-body code. Results clearly show the possibility to form satellites and binary bodies such ads those observed in recent years by high resolution techniques.

Astrometry applied to the search for asteroid satellites

Thuillot W.

Abstract. *In this work I propose to apply astrometric measurements to the search for satellites of asteroids or to the measurement of their orbital characteristics. The data already acquired and characterizing these systems allow us to assume that asteroids satellites are currently orbiting the primary object within a few days, at a distance from several hundred kilometers to thousand kilometers. Therefore the search of an astrometric signature due to the wobble motion of the primary object around the center of masses appears to be possible, for some cases, thanks to a spectral analysis of astrometric measurements spanning several consecutive days or weeks.*

Since the direct observation of Ida and Dactyl by the Galileo space probe, the status of satellites of asteroids has been shifted from controversial objects to robust reality. The previous indices of their existence were founded on several observational techniques. Since the beginning of international surveys of stellar occultations (starting from the 1970's), short and unexpected occultations, called secondary events, during close apulses have sometime been observed, unfortunately only by visual observers most of the time. The recording of such secondary events by some detectors remains very rare, first of them were performed with a photometer (Taylor *et al*., 1978) and by a SIT VIDICON camera (Arlot *et al*., 1985). The existence of satellites was suggested by these observations and also by the shape of some light curves of rotation or from theoretical considerations.

The recent advent of high resolution imaging, mainly thanks to adaptive optics but also thanks to radar imaging, made recently a real break in our knowledge of such binary systems. Radar imaging of Near Earth Asteroids and OA observations lead to assume that 16% of these objects are binaries (Margot *et al*., 2002). Main belt binary objects could also be numerous. Systematic surveys for the detection of such systems are performed from large telescopes, nevertheless it appears that the measurements of the orbital periods, and more generally the characterization of the orbits remain a difficult task which would require observations on the long term.

In this context, it is important to apply several observational methods in order to get complementary measurements. Small telescopes may then be very useful tools in order to complete the measurements done with the large ones, eventually they can also permit the detection : for example their photometric measurements can give access to the observation of mutual occultations between the primary and secondary objects (Pravec *et al*., 2000,). Here we propose to apply an astrometric method from small telescopes in order to detect satellites of asteroids.

1 . Astrometric signatures

At the end of 2001, we know more than 16 binary systems (table 1), among them 8 have been detected thanks to the adaptive optics, 5 by detecting mutual events in the light curves, 2 by radar observations and 1 from space. Furthermore several theoretical considerations and several observational reports allow us to build a much longer list by adding the suspected satellites of asteroids to the list of the detected ones.

Table 1 : Parameters for the main known binary systems

asteroid		**satellite**				
name	diameter (km)	designation	period (days)	diameter (km)	separation minimum (km)	method
(243) Ida	31	S/1993 (243) 1	0.8	1.2x1.4x1.6	90	S
		Dactyl				
1994 AW1	-	-	0.9	-	-	MO
1991 VH	-	-	1.4	-	-	MO
(3671) Dionysus	1.7x3.7	S/1997 (3671) 1	1.2	1.5	1000	MO
(45) Eugénia	215	S/1998 (45) 1	4.7	13	1200	AO
		Petit-Prince				
1996 FG3	-	-	0.7	0.4	-	MO
(90) Antiope	85	-	0.7	85	170	AO
(762) Pulcova	137	-	4	20	800	AO
2000 DP107	0.8	-	1.8	0.3	5	R/MO
2000 UG11	0.2	-	0.8	0.1	-	R
1999 KW4	-	-	0.7	-	2	R
(87) Sylvia	261	S/2001 (87) 1	4	13	1200	AO
(107) Camilla	223	S/2001 (107) 1	-	9	996	AO
(22) Kalliope	181	S/2001 (22) 1	-	36	1000	AO
(617) Patroclus	141	S/2001 (617) 1	-	-	700	AO
(3749) Balam	7	S/2002 (3749) 1	80	1.5	352	AO

S : space observation, AO : adative optics, R : radar, MO : mutual occultations

Several assumptions are made upon the orbital characteristics of these objects and it is then possible to compute the possible wobble effects which is induced by the motion of the binary system around its center of gravity. Monet and Monet (1998) proposed to detect this motion for the Near Earth Asteroids when their distance to the Earth is close enough. But in these conditions we would have to perform astrometric measurements of fast objects and accuracy would probably be not sufficient. Starting from this idea, we looked at the amplitude of such effect for a list of detected or suspected satellites of asteroids.

The figure 1 shows the amplitudes of the wobble effect for several asteroids. Knowing the minimum and maximum of distance from the Earth, we can compute the maximum and minimum effects by means of circular orbits of the satellite, assuming that we also know the distance to the primary and the mass (or radius) ratio. This graph gives such quantities in milliarcseconds (mas) for each asteroid (labeled thanks to their number) in ordinate versus the diameters ratio in abscisse. The objects easiest to be measured would be preferably affected with high wobble effect but low diameter ratio in order to keep the primary object photometrically distinct from the secondary. This figure shows that 9 Metis and 18 Melpomene would then be good candidates for this kind of measurement since a wobble effect up to 60 mas could be detected. This figure also gives a close view for the objects with low diameters ratio where we see that several asteroids could exhibit wobble effect up to 10 mas.

2 . Method of detection

Detecting the wobble effect thanks to direct astrometric measurements of the primary object would certainly be possible only for a few objects, mainly for the Near Earth Asteroids when their geocentric distance becomes to be small enough, although the radar observations seems to be more efficient in this configuration for the detection and measurements of binary asteroids. We can however probably detect this wobble motion by a statistical method applied to a larger number of asteroids. Indeed when we model the apparent motion of the binary asteroid thanks to a numerical integration, this apparent motion represents the orbital motion of the center of mass of the binary system. However the observations give the position of the primary object, assuming that the ratio in diameters/magnitude is large enough. The idea is then to try a detection of the periodic wobble effect thanks to a spectral analysis of the O-C residuals where periodical motion of the primary around the center of mass would appear as an astrometric signature of a second composant. Several encouraging attempts using this method have been made (Thuillot *et al*., 2000) and campaigns of observations from several sites are organized in order to apply it.

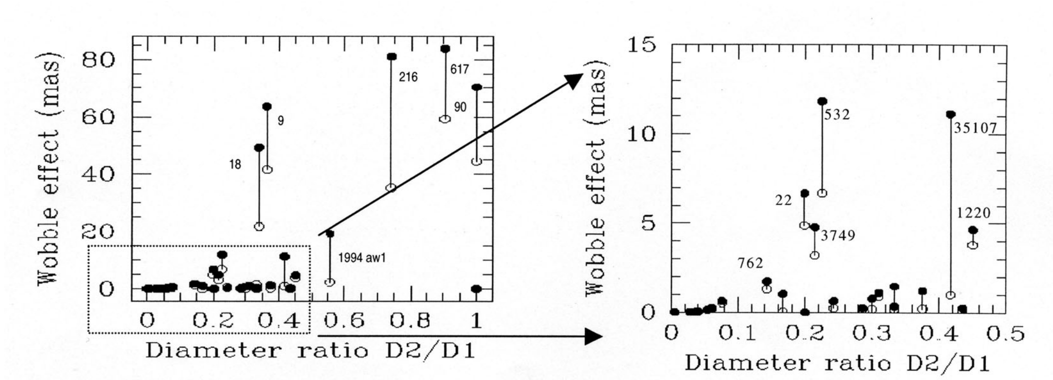

Figure 1 : Maximum (dark disks) and minimum (empty disks) values of the astrometric displacement in mas due to the motion of the primary around the center of mass of observed or suspected binary systems versus the diameters ratio. Asteroid numbers are indicated. The figure on right gives details of the square zone of the left one

3 . Conclusion

Several dynamical problems relating to the binary systems require observational data in order to validate theoretical models: the stability is the major question which has long divided the astronomical community on the existence itself of the binary asteroids. Now several observational programs involving adaptive optics and radar observations are performed and are detecting new binary asteroids. Beyond this detection, measurements of the orbital characteristics must be done and it is important to mix different observational methods for that. In addition to the determination of fundamental dynamical and physical parameters such as the density of the asteroids, the improvement of our knowledge of these objects will contribute to answer to the question on their origin and evolution, and it will contribute to a better understanding of collision processes and of their role in the formation of the Solar System.

References

Arlot, J.-E., Lecacheux, J., Richardson, Ch., Thuillot, W., 1985, A possible satellite of 145 Lucina, *Icarus,* **61**, 224.

Margot, J.-L. *et al*., 2002, Binary asteroids in the Near-Earth Objects population, *Science,* **296**, 1445.

Monet K. B., Monet D. G., 1998, *BAAS, **30***, 1144.

Mottola, S. Lahulla, F., 2000, Mutual Eclipse Events in Asteroidal Binary System 1996 FG_3: Observations and a Numerical Model, *Icarus*, **146**, 556.

Pravec, P., Kusnirak, P., Hicks, M., Holliday, B., Warner, B., 2000, 2000 DP_107, *IAUC,* **7504**.

Taylor, G. E., Dunham, D. W., Bowell, E., A'Hearn, M., McMahon, J., Horne, K., 1978, 1978 (532) 1, *IAUC,* **3241**.

Thuillot, W, Kikwaya, J.-B., Rocher, P., 2000, Satellites d'astéroides, *Journées Scientifiques 2000 de l´Institut de Mécanique céleste*, *Note Scientifique et Technique **S076***, IMCCE.

Research of binary asteroid 1996 FG3

Zheleznov Nikolaj

Asteroid 1996 FG3 belongs to the type of Near-Earth Asteroids. During the discovery 1996 opposition it was observed by Mottola [2]. When this asteroid approached the Earth in 1998 its photometric observations were carried out by Pravec *et al*. [1] and by Lahulla [2]. For the first time the conjecture as to dual nature of 1996 FG3 was made in the paper [3]. The papers [1,2] contain convincing evidences for this supposition.

The lightcurves of binary asteroids can reveal features which obviously specify duality of this object. Besides short-period brightness variation, these curves have variations of long period ($16^h.135$ for 1996 FG3) which can be explained only by the mutual occultations and eclipses occurring in the binary system. The short-period variations of the lightcurve ($3^h.594$ for 1996 FG3) are explained by rotation of the main non-spherical component (primary).

In Fig.1 the lightcurve represented by dots has the feature with the greatest amplitude of brightness variation which is connected with mutual phenomenon. This variation is explained by the satellite passage over the disk of the primary («primary minimum»). The feature in Fig.2 is explained by occultation of the satellite by the primary («secondary minimum»). Thin continuous curve on these pictures is the best fit of the short-period variations by the 5-th order Fourier series derived by Pravec *et al*. Obviously, the character of these variations explained by the asymmetrical form of the primary.

The long-period component of 1996 FG3 lightcurves is shown in Fig.3 at several epochs. It was obtained by subtraction of the short-period variation from the full lightcurve [1].

Pravec *et al*. and Mottola & Lahulla have obtained the effective diameters, the elements of the satellite orbit, and the density of the components. They considered the primary to be triaxial ellipsoid and its semiaxes have been found. Besides, Mottola & Lahulla have been determined the satellite form as an ellipsoid with two equal short axes.

However, the authors of both papers use a simple model of the system : the relative orbit of the satellite is considered to be circular and motion along it is executed according to the Kepler laws; the satellite moves around the primary in the equatorial plane of the latter. The rotation axes of the components are perpendicular to the satellite orbital plane.

However, this model of the binary asteroid is not quite correct. Indeed, the binary asteroid is a system in which mutual distance between components exceeds their own sizes by several times only. The gravitational interaction of the components in such system is rather complex when these have non-spherical form. In such a case the gravitation force depends not only on distance between the bodies centers, but on their mutual orientation as well. On this account, the study of motion of binary asteroid components can not be separated from study of their rotation. It is impossible to estimate correctly the variation of brightness which depends on orientation of bodies and their mutual positions not knowing reliably the motion of the components.

As distinct from papers [1,2] we consider determination of orbital and physical parameters of the asteroid having regard to complex motion of its components. The components are approximated by homogeneous triaxial ellipsoids moving under the influence of the Sun and mutual gravitation.

In order to solve this problem two programs were developed by author.

The first program is concerned with numerical integrations of the equations of the prograde-rotational motion of two triaxial ellipsoids [4]. The perturbation function of gravitational interaction of components is presented in the form of series in terms of spherical functions up to 4-th harmonic [5]. The equations of motion are integrated by the Everhart's method. The computed values of the component's coordinates and the Euler's angles of their orientation are used for simulation of the lightcurves of binary system.

Basing on the well known method of approximation of ellipsoid surface by great number of small plane facets the program of lightcurve simulation taking into account the mutual eclipses and occultations of components has been developed [6]. The essence of the method consists in summing up the illuminations being created by facets on the Earth with exception for those which are eclipsed or occulted by the other component. Further, the integral value of illumination transfers into the magnitude scale.

In order to approximate the observed lightcurves of 1996 FG3 the following model of the binary asteroid have been used. The components are approximated by triaxial ellipsoids rotating around the shortest axis being perpendicular to satellite orbital plane.

Using the least-squares method (LSM) the long-period component of lightcurve obtained by Pravec *et al*. was approximated for all epochs. As a result the elements of satellite orbit and the effective diameters of bodies have been determined.

Further, the full lightcurve of the asteroid was examined. By the LSM the semiaxes of the components, as well as their common density were derived. Albedo was accepted to be equal to 0.06 for both components.

As a result all the parameters of the binary asteroid have been obtained. The most important parameters are given below :

- ratio of primary semiaxes – 1 : 0.96 : 0.92,
- effective primary diameter – d_p = 1.48 km,
- ratio of satellite semiaxes : 1 : 0.86 : 0.86,
- effective satellite diameter – d_s = 0.47 km,
- d_s / d_p = 0.32,
- density – ρ = 1.03 g/sm^3,
- excentricity of satellite orbit – e = 0.07,
- major semiaxis of satellite orbit – $a = 1.46 d_p$ = 2.19 km,
- longitude of satellite orbit pole – $\lambda = 348°$,
- latitude of satellite orbit pole – $\beta = -22°$;

It deserves attention that found density of the components is very low, slightly larger than that of water. It seems that the components of 1996 FG3 are to be a «rubble pile».

Using these parameters the model lightcurves can be simulated. In Fig.1 and Fig.2 the approximation of full lightcurve is shown (fat curve) and in Fig.3 the approximation of long-period component of lightcurve is given at the epoch 1998 Dec. 23.1 (continued curve).

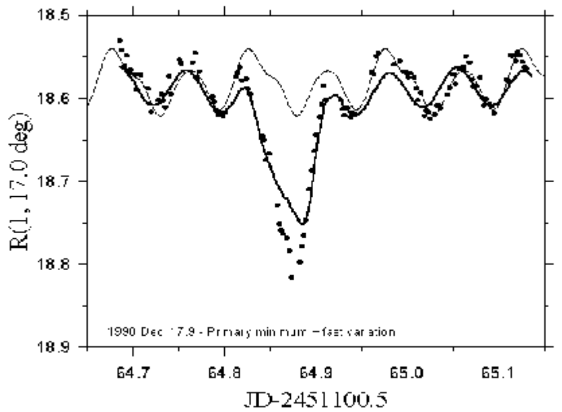

Figure 1 : Approximation of the primary minimum of the lightcurve obtained by Pravec *et al.*

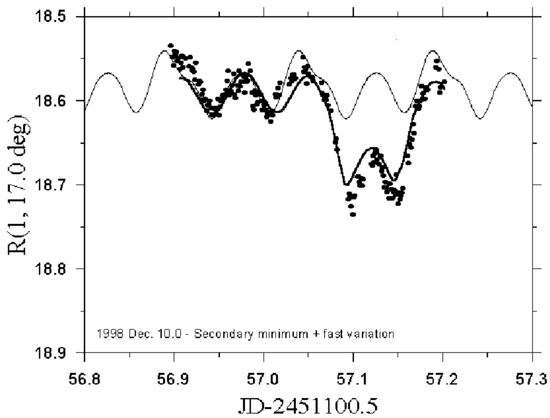

Figure 2 : Approximation of the secondary minimum of the lightcurve obtained by Pravec *et al.*

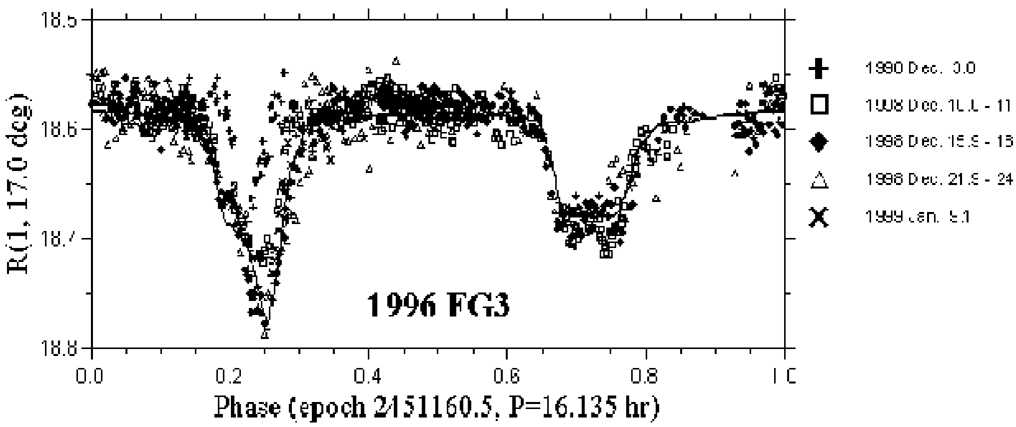

Figure 3 : Approximation of the long-period component of the lightcurve of 1996 FG3 at the epoch 1998 Dec. 23.1 (triangles)

As can be seen in these figures, the real lightcurves are on the whole in good agreement with simulated ones. However, the model lightcurves for some epochs approximate the real ones not very correctly.

In author opinion, this can be explained by use of inadequate model of the binary asteroid. Indeed, more good approximation can be obtained if the longitude of node and the inclination of the satellite orbit to primary equator are supposed to be variable during the time interval of observations. The variation can be caused by nonzero inclination of the satellite orbital plane to the equator of non-spherical primary. The initial conditions can be selected so as to discribe the real motion and the same time lightcurve variations in the best way.

We have made several attempts to follow the motions in a binary system with parameters like those found for 1996 FG3 during the long time interval. In so doing we have considered the systems with zero inclination of the satellite orbital plane to the equator of the primary as well as the systems with satellite moving in inclined orbit. For both types of motion we did not reveal any secular changes except of trivial precession of the satellite orbit in the case of non-zero inclination. Quasi-periodical oscillations of the satellite orbital plane seems to be stable during the time interval of several thousand revolutions. It is interesting to note that synchronization of satellite rotation with its orbital motion was broken up in all cases after about one thousand revolutions and satellite became to rotate chaoticaly. In case of non-zero inclination the satellite motion seems to be somewhat more stable.

Acknowledgments : the author would like to thank Dr. Petr Pravec for placing the results published in [1] at my disposure in electronic form and for attention to my work.The author thanks Viktor A.Shor for constructive remarks and help in preparation of this paper.

References

[1] Pravec, P., Sarounová, L., Rabinowitz, D., Hicks, M., Wolf, M., Krugly, Yu., Velichko, F., Shevchenko, V., Chiorny, V., Gaftonyuk, N., Genevier., G., 2000, Two-Period Lightcurves of 1996 FG_3, 1998 PG, and (5407) 1992 AX : One probable and two possible binary asteroids, *Icarus*, **146**, 1, 190–203.

[2] Mottola, S., Lahulla, F., 2000, Mutual eclipse events in asteroidal binary system 1996 FG_3 : Observations and numerical model, **146**, 2, 556–567.

[3] Pravec, P., Sarounová, L., Wolf, M., 1998, 1996 FG_3, *IAUC Circ.*, **7074**.

[4] Zheleznov, N. B., 1999, Numerical integration of the equations of prograde-rotational motion of a binary asteroid, *Trudy IPA*, **4**, 273–290 (in Russian).

[5] Zheleznov, N. B., 1999, Calculation of the fifth order member of the inverce power series of mutual distance between two ellipsoidal bodies, *Trudy IPA*, **4**, 261–272 (in Russian).

[6] Zheleznov, N. B., 1999, The method of calculations of occultations and eclipses in binary asteroid system for solution of photometric problems, *Preprint of Institute of Applied Astronomy*, **131** (in Russian).

List of participants / Liste des participants

Alderweireldt Tom, Observatory code 145, Schilde (Belgium)

Apostolovska Gordana, Institute of Physics, Faculty of Natural Sciences, Skopje (Repubic of Macedonia)

Arlot J.-E., Institut de mécanique céleste, IMCCE Paris Observatory (France)

Banchi Adnan, IMCCE Paris Observatory (France)

Barucci Antonella, DESPA Paris Observatory (France)

Bec-Borsenberger Annick, Institut de mécanique céleste, IMCCE Paris Observatory (France)

de Bergh Catherine, DESPA, Observatoire de Paris (France)

Berthier Jérôme, Institut de mécanique céleste, IMCCE Paris Observatory (France)

Binzel Richard, MIT (USA)/ Paris Observatory (France)

Birlan Mirel, DESPA, Paris Observatory (France)

Biryukov Vadim, Crimean laboratory of Sternberg Astronomical of Moscow, Nauchny, (Crimea)

Blanco Carlo, Dipartimento di Fisica e Astronomia dell'Universita` di Catania (Italy)

Borisov Galin, Institute of Astronomy, Bulgarian Academy of Sciences, Sofia (Bulgaria)

Bowell E.L.G., Lowell Observatory, Flagstaff (USA)

Bratsolis Emmanuel, Ecole Nationale Superieure des Telecommunications, Departement Traitement de Signal et des Images Paris (France)

Bretagnon Pierre, Institut de mécanique céleste, IMCCE Paris Observatory (France)

Bykov Oleg, Pulkovo Astronomical Observatory, St Petersburg (Russia)

Calvani M., Astronomical Obervatory of Padova (Italy)

Carpino Mario, Osservatorio Astronomico di Brera (Italy)

Casas Ricard, Agrupacio Astronomica de Sabadell (Spain)

Cavagna Marco, Osservatorio di Sormano, Sesto S. Giovanni (Italy)

Christophe Bernard, Paris (France)

Christou Apostolos, Armagh Observatory, Northern Ireland (United Kingdom)

Colas François, Institut de mécanique céleste, IMCCE Paris Observatory (France)

Dawson Matt, Roeser Observatory, Luxembourg (Luxembourg)

Decoene Astrid, IMCCE Paris Observatory (France)

Descamps Pascal, Institut de mécanique céleste, IMCCE Paris Observatory (France)

Doressoundiram Alain, DESPA Paris Observatory (France)

Dunckel Nick, Los Altos, CA (USA)

Elliot Andrew, Reading (United Kingdom)

Elst Eric W., Royal Observtory, Uccle (Belgium)

Eltumi Ali M., University of Garyounis, Benghazi (Libya)

Fauvaud Stéphane, Sarrebourg (France)

Fienga Agnès, Institut de mécanique céleste, IMCCE Paris Observatory (France) and Jet Propulsion Laboratory (USA)

Fodera Giorgia, Faculty of Sciences of Palermo University, Palermo (Italy)

Fornasier Sonia, Laboratory: Astronomy Dep. - Padova University, Padova (Italy)

Fulchignoni Marcello, Paris Observatory (France)

Goffin Edwin, Hoboken (Belgium)

Grynko Yevgen, Kharkov Astronomical Observatory (Ukraine),

Gudkova Ludmila, Nikolaev Astronomical Observatory (Ukraine)

Hestroffer Daniel, Institut de mécanique céleste, IMCCE Paris Observatory (France)

Ivanova Violeta, Institute of Astronomy, Bulgarian Academy of Sciences, Sofia (Bulgaria)

Jaumann Ralf, German Aerospace Center (DLR), Institute of Space Sensor Technology and Planetary Exploration

Kaasalainen, M., Observatory, Univ. Helsinki (Finland)

Kikwaya Eluo Jean-Baptiste, Institut de mécanique céleste, IMCCE Paris Observatory (France) and Vatican observatory.

Kocer Michal, Klet Observatory, Ceske Budejovice (Czech republic)

Kryszczynska Agnieszka, Astronomical Observatory of A. Mickiewicz University, Poznan (Poland)

Lecacheux Jean, DESPA Paris Observatory (France)

Lopez Garcia Alvaro, Astronomical Observatory, Valencia (Spain)

Manara Alessandro, Observatorio astronomico di Brera, Milano (Italy)

Manca Francesco, Sormano astronomical Observatory, Bosisio Parini (Italy)

McFarland John, Armagh Observatory (Northern Ireland, UK),

Michalowski Tadeusz, Poznan Astronomical Observatory (Poland)

Normand Jonathan, IMCCE Paris Observatory (France)

Pauwels Th., Koninklijke Sterrenwacht van België Brussel (Belgium)

Peixinho Nuno, Observatoire de Paris / Centro de Astronomia e Astrofisica da Universidade de Lisboa

Pitjeva Elena V., Institute of Applied Astronomy, Russian Academy of Sciences (IAA RAS), St. Petersburg (Russia)

Portyankina G., Kharkov Natonal University, Department of Astronomy (Ukraine)

Rapaport M., Observatoire de Bordeaux (France)

Renaudineau Jacky, Institut de mécanique céleste, IMCCE Paris Observatory (France)

Ruatti Christian, Institut de mécanique céleste, IMCCE Paris Observatory (France)

Rumyantsev V., Crimean Astrophysical Observatory,

Sicoli Piero, Sormano astronomical Observatory, Garbagnate Monastero (Italy)

Simon Dominique, Institut de mécanique céleste, IMCCE Paris Observatory (France)

Simon Jean-Louis, Institut de mécanique céleste, IMCCE Paris Observatory (France)

Simonia Irakli, Abastumani Observatory (Republic of Georgia)

Simonia Tsitsino, Abastumani Observatory (Republic of Georgia)

Tanga Paolo, Observatoire de la Côte d'Azur, Nice (France) and Osservatorio Astronomico di Torino (Italy)

Thizy Olivier, Crolles (France)

Thuillot W., Institut de mécanique céleste, IMCCE Paris Observatory (France)

Vargas Santiago, Oldury WestMidlands (UK)

Vaubaillon Jérémie, Institut de mécanique céleste, IMCCE Paris Observatory (France)

Velichko Fiodor, Astronomical observatory Kharkiv (Ukraine)

Vienne Alain, Institut de mécanique céleste and Laboratoire d'Astronomie, IMCCE Paris Observatory (France) and Etudes des Systèmes Dynamiques, Université des sciences et technologies de Lille (France)

Yagudina Eleonora I., Institute of Applied Astronomy, Russian Academy of Sciences (IAA RAS), St. Petersburg (Russia)

Zheleznov Nikolaj, Laboratory of Small Bodies of the Solar System, Institute of Applied Astronomy, Russian Academy of Sciences (IAA RAS), St. Petersburg (Russia)

Index of authors / Index des auteurs